

APPLICATIONS OF CAPILLARY ELECTROPHORESIS AND TANDEM MASS  
SPECTROMETRY FOR THE SEPARATION OF SULFATED GLYCOSAMINOGLYCAN  
MIXTURES FROM BIOLOGICAL SAMPLES

by

PATIENCE SANDERSON

(Under the Direction of I. Jonathan Amster)

ABSTRACT

Sulfated glycosaminoglycan (GAG) carbohydrates are linear, acidic polysaccharide chains abundant on the surface of mammalian cells that affect several biological processes through protein-binding interactions. Structural characterization of sulfated GAGs is challenging due to their non-template biosynthesis resulting in the production of heterogeneous mixtures with different chain lengths and varying modification patterns. Tandem mass spectrometry methods have been developed for the structural analysis of purified oligomers to determine sites of sulfomodification involved in these binding relationships, but the analysis of mixtures remains a significant challenge. Using capillary zone electrophoresis tandem mass spectrometry (CZE-MS/MS), GAG mixtures were separated to reduce analyte heterogeneity before online tandem MS sequencing. This advance enables the determination of binding motifs responsible for the interaction of GAG chains with proteins, as these sequences typically range from at least tetrasaccharides to octasaccharides and greater in length.

For this work, GAG mixtures varying in extent and position of sulfation have been separated using reverse polarity CZE and detected in negative ion mode MS. Purified standards

and various biological samples were analyzed using this platform. Compositional analysis was performed to determine the various components using accurate mass measurement, and the most intense species were analyzed using tandem mass spectrometry to sequence the GAG chains. Collision induced dissociation/high-energy collision dissociation (CID/HCD) and negative electron transfer dissociation (NETD) were utilized to fragment the isolated GAG precursors which enabled determination of sulfate position on GAGs post separation. To demonstrate the effectiveness of this platform, GAGs extracted from healthy human urine and GAG chains released from the proteoglycan bikunin were examined.

INDEX WORDS: Sulfated glycosaminoglycans, carbohydrates, capillary electrophoresis, high resolution mass spectrometry, separations, mixtures, collision induced dissociation, higher energy collision induced dissociation, negative electron transfer dissociation, urine, proteoglycan

APPLICATIONS OF CAPILLARY ELECTROPHORESIS AND TANDEM MASS  
SPECTROMETRY FOR THE SEPARATION OF SULFATED GLYCOSAMINOGLYCAN  
MIXTURES FROM BIOLOGICAL SAMPLES

by

PATIENCE SANDERSON

B.S., Spring Hill College, 2013

A Dissertation Submitted to the Graduate Faculty of The University of Georgia in Partial  
Fulfillment of the Requirements for the Degree

DOCTOR OF PHILOSOPHY

ATHENS, GEORGIA

2019

© 2019

PATIENCE SANDERSON

All Rights Reserved

APPLICATIONS OF CAPILLARY ELECTROPHORESIS AND TANDEM MASS  
SPECTROMETRY FOR THE SEPARATION OF SULFATED GLYCOSAMINOGLYCAN  
MIXTURES FROM BIOLOGICAL SAMPLES

by

PATIENCE SANDERSON

Major Professor: I. Jonathan Amster

Committee: Ron Orlando  
Lance Wells

Electronic Version Approved:

Ron Walcott  
Interim Dean of the Graduate School  
The University of Georgia  
December 2019

## DEDICATION

This dissertation is dedicated to my husband Tim, my family, and my friends for their unconditional support and encouragement.

## ACKNOWLEDGEMENTS

To begin, I would like to express my appreciation for the guidance and support from my advisor Dr. I. Jonathan Amster throughout my time at the University of Georgia. I want to acknowledge my committee members, Dr. Ron Orlando and Dr. Lance Wells, for their contribution in shaping the work presented in this dissertation. Furthermore, this work would not be possible without the aid of collaborators from the labs of Dr. Robert J. Linhardt at Rensselaer Polytechnic Institute and Dr. Geert-Jan Boons at the Complex Carbohydrate Research Center at the University of Georgia.

During my time at the University of Georgia, I had the pleasure of working with a multitude of people who shaped my scientific journey. Dr. Franklin E. Leach III, Dr. Dennis Phillips, and Dr. Chau-wen Chou played an essential part in helping me grow as a mass spectrometrists and scientist. To the former and current Amster group members, thank you for fruitful discussions about carbohydrates and mass spectrometry. I will forever be grateful for the knowledge and support I received while working at UGA. Finally, I would like to thank my friends and family for their unwavering support during this journey.

## TABLE OF CONTENTS

	Page
ACKNOWLEDGEMENTS.....	v
LIST OF TABLES.....	ix
LIST OF FIGURES .....	xi
 CHAPTER	
1 INTRODUCTION AND LITERATURE REVIEW .....	1
Sequencing Glycosaminoglycans .....	4
Separations of Complex Mixtures .....	8
Applications.....	13
References .....	17
2 EXPERIMENTAL METHODS .....	30
Preparation of Glycosaminoglycans .....	30
Capillary Coatings .....	34
Capillary Zone Electrophoresis Mass Spectrometry of Oligosaccharides.....	35
References .....	37
3 HEPARIN/HEPARAN SULFATE ANALYSIS BY COVALENTLY MODIFIED REVERSE POLARITY CAPILLARY ZONE ELECTROPHORESIS-MASS SPECTROMETRY.....	39
Abstract .....	40
Introduction .....	41



Materials and Methods .....	44
Results and Discussion.....	48
Conclusions .....	65
Acknowledgements.....	66
References .....	67
 4 STRUCTURAL ANALYSIS OF URINARY GLYCOSAMINOGLYCANS FROM HEALTHY HUMAN SUBJECTS .....	 75
Abstract .....	76
Introduction .....	77
Experimental.....	80
Results and Discussion.....	84
Conclusions .....	98
Acknowledgements.....	99
References .....	100
 5 CAPILLARY ZONE ELECTROPHORESIS AND MASS SPECTROMETRY FOR THE ANALYSIS OF CHONDROITIN SULFATE GLYCOSAMINOGLYCANS RELEASED FROM BIKUNIN .....	 108
Abstract .....	109
Introduction .....	110
Materials and Methods.....	113
Results and Discussion.....	116
Conclusions .....	126
Acknowledgements.....	127

References .....	128
6 CONCLUSIONS .....	135
References .....	140
APPENDICES	
A Supplementary Data for Chapter 3 .....	143
B Supplementary Data for Chapter 4 .....	146
C Supplementary Data for Chapter 5 .....	152

## LIST OF TABLES

	Page
Table 3.1: .....	46
Table 3.2: .....	63
Table 4.1: .....	88
Table 5.1: .....	119
Table A.1: .....	143
Table B.1:.....	146
Table B.2:.....	147
Table B.3:.....	148
Table B.4:.....	149
Table C.1:.....	152
Table C.2:.....	153
Table C.3:.....	153
Table C.4:.....	154
Table C.5:.....	154
Table C.6:.....	155
Table C.7:.....	155
Table C.8:.....	156
Table C.9:.....	163
Table C.10:.....	165

Table C.11:.....	168
Table C.12:.....	170
Table C.13:.....	172
Table C.14:.....	174
Table C.15:.....	176
Table C.16:.....	178
Table C.17:.....	181
Table C.18:.....	183
Table C.19:.....	185

## LIST OF FIGURES

	Page
Figure 1.1: .....	3
Figure 1.2: .....	9
Figure 1.3: .....	15
Figure 3.1: .....	50
Figure 3.2: .....	52
Figure 3.3: .....	54
Figure 3.4: .....	55
Figure 3.5: .....	57
Figure 3.6: .....	58
Figure 3.7: .....	61
Figure 3.8: .....	65
Figure 4.1: .....	86
Figure 4.2: .....	90
Figure 4.3: .....	92
Figure 4.4: .....	94
Figure 4.5: .....	97
Figure 5.1: .....	118
Figure 5.2: .....	121
Figure 5.3: .....	123

Figure 5.4: ..... 125

Figure C.1: ..... 157

Figure C.2: ..... 158

Figure C.3: ..... 159

Figure C.4: ..... 160

Figure C.5: ..... 161

Figure C.6: ..... 162

## CHAPTER 1

### INTRODUCTION AND LITERATURE REVIEW

The work presented in this dissertation focuses on the separation and sequencing of sulfated glycosaminoglycans (GAGs) mixtures using capillary zone electrophoresis (CZE) coupled with tandem mass spectrometry. Sulfated GAGs are linear polysaccharides found on the surface of mammalian cells [1]. As a large component of the cellular surface, carbohydrates frequently interact with proteins for cell signaling, adhesion, and communication. Thus, a variety of biochemical pathways are affected by GAG-protein binding interactions, which has the potential to up- or down-regulate biological processes leading to developmental and disease progression [2-4]. In order to understand the significance of sulfated GAG-protein binding, GAG chains need to be structurally characterized. However, their non-template biosynthetic production leads to an assortment of compositions resulting in a heterogenous mixture within a biological species. As a result, a combination of separation and characterization are necessary to examine biological samples.

There are multiple classes of sulfated glycosaminoglycans: chondroitin/dermatan sulfate (CS/DS), heparin/heparan sulfate (Hp/HS), and keratan sulfate (KS). Each GAG class is defined by its residue composition as well as the sulfation and linkage pattern. Chondroitin/dermatan sulfate (CS/DS) and heparin/heparan sulfate (Hp/HS) are two of the most complicated and sulfated glycosaminoglycan classes and will be the focus of this work. These carbohydrates are composed of a repeating disaccharide building block containing a hexuronic acid and hexosamine residue. Figure 1.1 depicts the basic structure of these two classes of GAGs and their

various modifications. For chondroitin and dermatan sulfate, the hexosamine sugar, galactosamine, is linked  $\beta(1,3)$  to a hexuronic acid residue; whereas, the linkage is  $\alpha(1,4)$  for heparin/heparan sulfate (Hp/HS) with glucosamine rather than galactosamine. The hexosamine sugar is most commonly produced with either an N-acetyl or N-sulfo modification; N-acetylation is typically uniform in CS/DS, but a mix of N-acetyl and N-sulfo is present in Hp/HS. Modifications of the carbohydrate chain occur in a non-uniform manner. Chain length, uronic acid stereochemistry, sulfation, and de-acetylation are dictated by several enzymatic steps that do not go to completion. Sulfates can be placed in a variety of positions on CS/DS and Hp/HS based on the activity of different sulfotransferases. Additionally, epimerases can change the stereochemistry of the C-5 carbon in a hexuronic sugar, switching it from glucuronic acid (GlcA) to iduronic acid (IdoA). Due to these enzymatic processes, a heterogeneous mixture is created making analysis difficult. Previous research has shown there are regions with an abundance of sulfation or very little modification present, and these subtle differences strongly impact activity and protein binding.



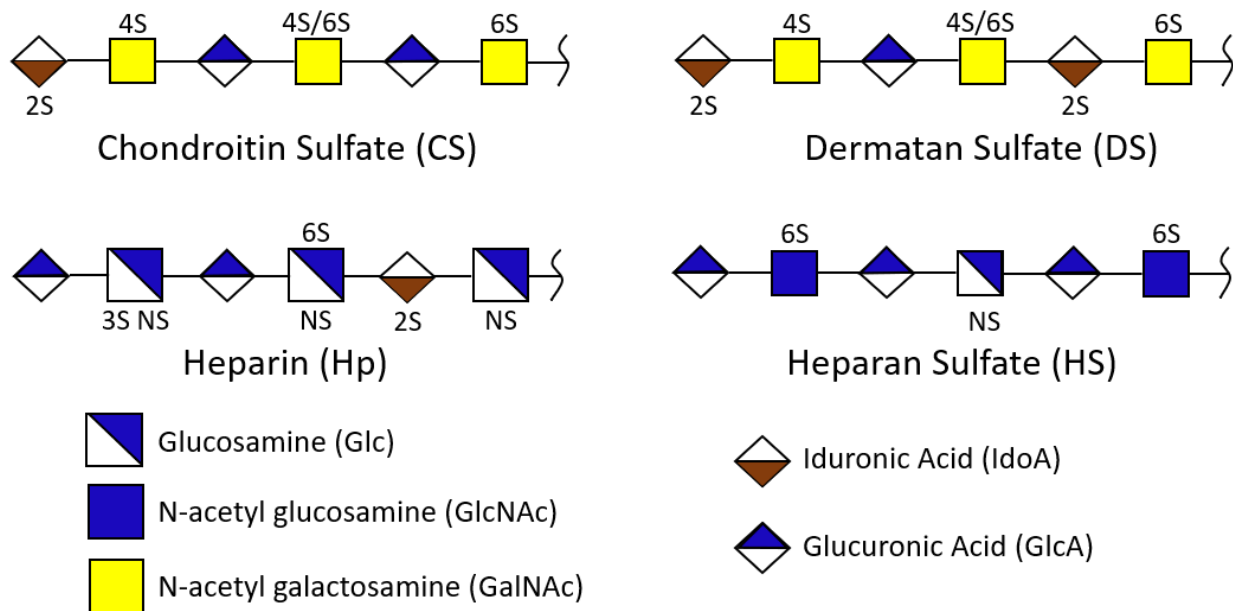


**Figure 1.1** Structures of chondroitin and dermatan sulfate (CS/DS) and heparin/heparan sulfate (Hp/HS) glycosaminoglycan oligosaccharides with their hexosamine and acidic building blocks.

The structural characterization of GAG chains is a significant analytical challenge [5-12]. Typically, GAG oligosaccharides are produced in limited quantities and cannot be amplified or overexpressed like other biopolymers, such as nucleic acids and proteins [13]. Nuclear magnetic resonance (NMR) spectroscopy has been utilized to identify the location and type of modifications on GAGs, but it requires pure samples in relatively high milligram amounts [14-16]. Mass spectrometry (MS) has become one of the standard methods for analyzing glycosaminoglycans due to its low sample requirements, micrograms or less, and ability to acquire information on mixtures [17-19]. Electrospray ionization (ESI) is most commonly used to analyze sulfated GAGs although several groups have used MALDI [20-28]. MALDI typically produces singly charged precursors limiting the size and complexity of GAG chains that can be sufficiently sequenced. ESI produces multiply charged precursors, and it can be coupled to

separation techniques making it more versatile [29-31]. The acidic nature of sulfate and carboxylic groups on sulfated GAGs lends itself to negative ion mode MS. Generally, composition analysis is the initial step in GAG analysis. It has been paired with disaccharide analysis to look into the motifs or building blocks of the sugar backbone [32, 33]. Using accurate mass measurement, composition information of multiple species, such as degree of polymerization (dp) and number of *O*- and *N*-sulfation and acetylation, can readily be determined.

### **Sequencing GAGs**

The structural characterization of GAGs requires tandem mass analysis to determine the location of modifications within individual residues. Glycosidic cleavages identify which residues are modified, and cross ring cleavages specify the position within a specific residue. A combination of glycosidic and cross ring cleavages are necessary to fully characterize a GAG chain. The main categories of ion activation that provide useful fragmentation are collisional activation, electron-based activation, ion-ion reactions, and photodissociation [19, 31, 34-45]. Since the work presented in this dissertation was completed using a Thermo Scientific Velos Pro Orbitrap Elite instrument, collisional activation and ion-ion reactions will be highlighted.

Collision induced dissociation (CID) was the first ion activation method that was combined with ESI-MS for GAG analysis [34-36]. Precursor ions interact and collide with neutral gas atoms during activation causing an increase in their internal kinetic energy. This cleaves the most labile bonds, specifically the important sulfate half-ester modification followed by the glycosidic backbone. As a result, CID produces an abundant amount of uninformative sulfate loss compared to other activation techniques. To improve the quality of fragmentation, the sulfate modification

can be stabilized through deprotonation or metal cation-hydrogen exchange resulting in more informative cleavages [30, 46-48]. By deprotonating or pairing the sulfate with a metal cation, the lability of the sulfate bond is drastically decreased. However, adding a metal cation into the sample can increase the complexity of the mass spectrum and decrease sensitivity. Although cross ring cleavages are not prevalent in CID spectra, highly ionized precursors can generate them as evidenced by Kailemia *et al.* [46]. In this work, sodium-hydrogen (Na-H) exchange was utilized to fully ionize the pentasaccharide Arixtra for sequencing studies.

CID is accessible on a wide variety of commercially available mass spectrometers. Reinhold *et al.* used CID on an ion trap instrument in a multistep MS<sub>n</sub> experiment to determine sequence information of highly sulfated GAGs [49]. Chemical derivatization, specifically permethylation with stable isotope analogs, allowed the authors to determine site specific sulfate location upon sequential MS/MS experiments performed in positive ion mode. Higher energy collision induced dissociation (HCD) is a similar type of collision fragmentation found specifically on Thermo Scientific Orbitrap instruments. HCD differs from CID in that it occurs in a collision cell located after the C-trap in a Thermo Orbitrap instrument. Additionally, a higher RF voltage is used to retain fragment ions in the C-trap before sending them into the Orbitrap. CID and HCD fragmentation occur on the order of milliseconds making it suitable to combine with different separation techniques. Recently, Sharp *et al.* sequenced mixtures of chemically derivatized heparan sulfate oligosaccharides using CID with an LC-MS separation [50, 51]. Derivatization prevented loss of sulfate modifications and resulted in informative fragmentation upon collisional dissociation. Although CID does not produce a significant amount of cross ring cleavages without additional modification in the form of metal cation-hydrogen exchange or derivatization, it can be

a vital tool for analyzing sparsely sulfated GAGs and combined with high throughput separation experiments.

Electron-based methods have been utilized and optimized by several laboratories to provide reliable and informative fragmentation for glycosaminoglycans. Electron detachment dissociation (EDD) and negative electron transfer dissociation (NETD) have been shown to readily provide both glycosidic and cross ring cleavages. In an EDD experiment, a multiply charged deprotonated ion is irradiated by a moderate energy electron ( $\sim 20\text{eV}$ ). After activation, an electron is detached producing odd and even electron fragment ions [6]. This leads to a higher abundance of cross ring cleavages compared to collisional activation. Previous studies completed using EDD on sulfated GAGs showed ample sequence coverage due to the high propensity of cross ring cleavages to locate specific sites of sulfation [19, 37, 38, 43-45]. In these studies, it was found that fully ionized precursors are not necessary for sequence coverage. As long as the ionization state equals the number of sulfate modifications, sulfate loss is minimized, and informative fragment ions are produced. Recently, Agyekum *et al.* published work that highlighted the ability to distinguish tetrasaccharide epimers as a result of preferential fragment ions based on the presence of glucuronic versus iduronic acid [44].

NETD is another type of electron activation, but it does not directly irradiate deprotonated precursor ions. It is the negative ion counterpart to electron transfer dissociation (ETD) [52, 53]. During the first step of this ion-ion reaction, electrons interact with a reagent, such as fluoranthene or xenon, to form a radical cation. The multiply charged deprotonated precursor ion transfers an electron to the radical cation which then produces a radical site in the anionic precursor. The resulting radical ion is much the same as the charge-reduced intermediate in an EDD experiment, and the product ions are similar by these two methods of ion activation. This radical derived

fragmentation predominately results in a higher abundance of cross ring cleavages analogous to EDD. Initial work using NETD to analyze GAGs was completed using an ion trap mass spectrometer by Wolff *et al.* [53]. Xenon and fluoranthene reagent ions were both studied, and sulfate loss was more pronounced with xenon, as expected due to its larger recombination energy. Additionally, NETD was able to distinguish epimers of GlcA and IdoA of purified samples. Recent experiments have focused on increasingly sulfated oligosaccharides using high resolution mass spectrometers [52, 54]. The mass accuracy associated with high resolution mass spectrometers allows the vast number of product ions of longer sugars to be assigned confidently confirming that NETD results are comparable with EDD performed on an FTICR-MS. The difference in 3-*O* and 6-*O* sulfation can be distinguished with cross ring cleavages using NETD activation as shown by Wu *et al.* [55]. NETD has the advantage of being performed on any MS instrument capable of ion-ion reactions. Furthermore, the NETD duty cycle is significantly shorter, enhancing its applicability to online separations. EDD experiments are typically 0.5-1.0 seconds per scan, and NETD occurs on the millisecond time scale. Consequently, NETD is ideal to pair with online separations for sulfated GAG oligosaccharide mixture characterization.

Tandem MS experiments work well to determine type and location of modifications. Nevertheless, purified samples are essential to accurately identify structures using this method. If more than one species is present during isolation, contradicting product ions could indicate more than one structure. Therefore, prior separation is useful to simplify mixtures for tandem MS experiments.

## Separations of Complex Mixtures

Biological extractions of GAGs are inherently complex and heterogeneous due to their non-template biosynthetic pathway [56]. Since GAGs have similar structures with modifications located in various positions, mixtures are hard to analyze using direct injection. Many of the species will present the same molecular ions in a mass spectrometer as isomeric compositions overlap. Powerful online separation methods are essential for reducing complex mixtures into simpler, easy to analyze components and differentiation of individual isomeric structures. Although full-length sulfated GAGs have been analyzed in top-down fashion by mass spectrometry, the general approach is to partially digest polysaccharides to mixtures containing oligosaccharides of moderate length to enable characterization [57, 58]. The complexity of these digest mixtures makes prior separation (online or off-line) desirable to facilitate analysis. Some approaches for separating GAGs coupled to MS include high performance liquid chromatography (HPLC), hydrophilic interaction liquid chromatography (HILIC), ion mobility spectrometry (IMS), and capillary zone electrophoresis (CZE) [59-63].

HPLC covers a broad range of separation techniques including size exclusion chromatography (SEC), strong anion exchange (SAX), reverse phase ion pairing (RPIP), and HILIC. These techniques are ideal for separating oligosaccharides with different degrees of polymerization (dp). However, in most cases they fall short for separation of GAG isomers without additional sample preparation. SEC is commonly used as the first purification step to separate oligosaccharides into various chain lengths by increments of dp 2. It is a simple and robust separation technique that provides profile information about compositions within the mixture, but it often presents multiple species with different sulfation patterns eluting at the same time. Zaia *et al.* and Zhang *et al.* performed experiments to separate complex mixtures of low

molecular weight heparins (LMWH) into chain lengths ranging from dp 2-30 [64, 65]. Figure 1.2a depicts the separation of Dalteparin using SEC combined with ion suppression to elute GAG chains of different sizes for MS analysis [64]. SEC has also been paired with other methods as a preliminary method to separate GAGs into different degrees of polymerization before further purification.

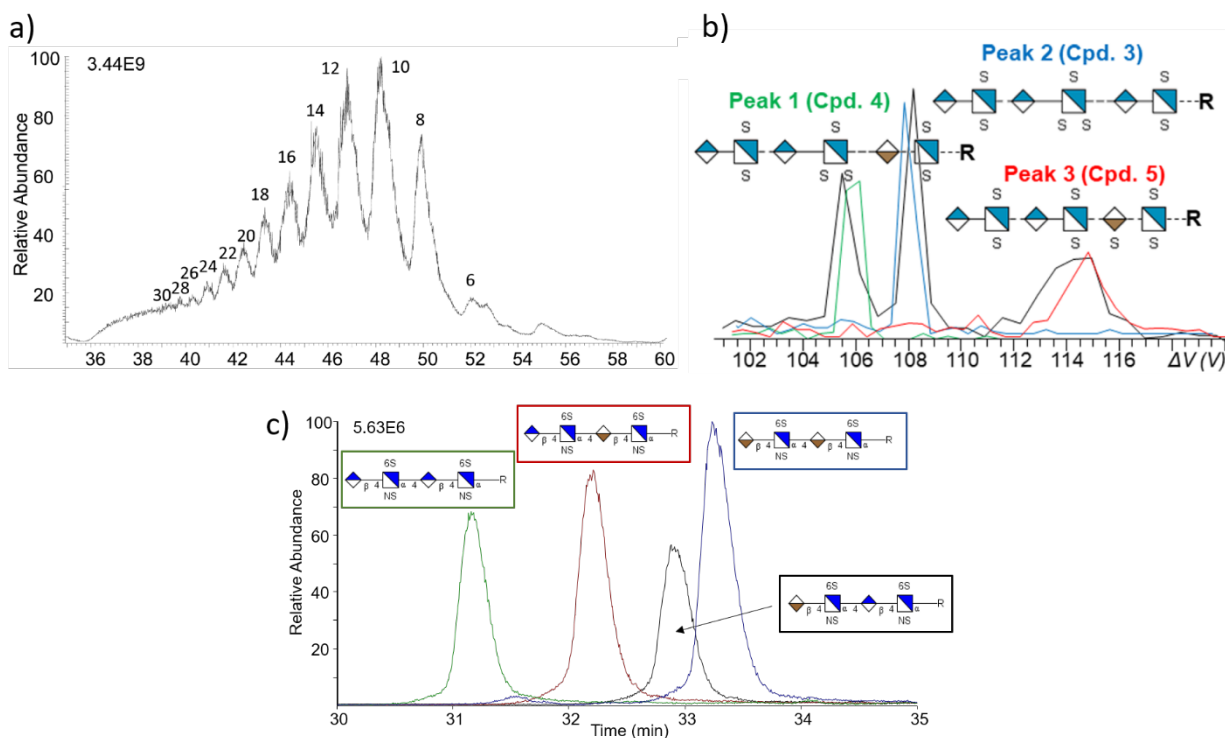


**Figure 1.2** Separation techniques for glycosaminoglycans. a) SEC-MS total ion chromatogram of enoxaparin. b) Gated-TIMS separation of dp6 isomers. Extracted ion mobility spectra ( $[M - 3H]^3-$ ) of Compound 3 (blue trace), Compound 4 (green), Compound 5 (red), and their mixture (black). c) Capillary zone electrophoresis (CZE) separation of dp4 epimers. Adapted with permission from a) *Anal. Chem.* **2016**, 88, 10654–10660 and b) *Anal. Chem.* **2019**, 91, 2994–3001.

Strong anion exchange (SAX) provides another step of purification for GAGs. This technique separates molecules based on their charge. Thus, GAGs with different numbers of sulfate modifications can be separated. However, SAX can be challenging to perform with online mass spectrometry due to the high amount of inorganic salts used for separation. MS contamination is common with this technique, but several groups have worked to reduce the type and abundance of salt present after separation [55, 64, 66]. Miller *et al.* published a combination of SEC and SAX to separate GAG oligosaccharides into fractions using volatile ammonium bicarbonate to reduce contamination [67]. Reverse phase ion pairing (RPIP) is another form of LC used to separate mixtures of GAGs prior to MS analysis. An ion pairing reagent is added to the mobile phase that interacts with the ionic sites on the GAG to retain them on the separation column for longer time periods to improve separation and resolution. Typically, ion pairing reagents are organic compounds, such as di- and tributyl amines [68]. Although this separates similar GAG species, it can complicate the MS and tandem MS analysis [49, 68-70]. Combined procedures that utilize techniques to suppress contamination are necessary to continue using online HPLC coupled with MS in a high throughput fashion.

HILIC is different from the other HPLC techniques described in this review as the separation is performed on a polar stationary phase. It separates molecules based on their polarity which is beneficial when working with highly anionic GAGs. The mobile phase typically used is acetonitrile and water which is advantageous for mass spectrometry. Furthermore, HILIC does not require pairing reagents, simplifying sample preparation and increasing MS sensitivity. Several groups have analyzed GAGs up to dp30 using HILIC-LC-MS [32, 71, 72]. Using a maltose modified HILIC column and high resolution MS, Sun *et al.* separated and identified 36 building blocks that comprise the nitrous acid depolymerized LMWH mixtures, dalteparin and



nadroparin [73]. Over 30 building blocks were separated within one hour without derivatization of the oligosaccharides. A combined method of HILIC LC-NETD-MS/MS was recently reported in which chemically synthesized tetra- and hexasaccharide isomers were separated and sequenced without permethylation [66]. To improve precursor sensitivity, an ion suppressor was implemented prior to MS analysis to reduce the abundance of salt present after separation. The GAG species were then fragmented with NETD and produced glycosidic and cross ring cleavages to determine the structures.

With heterogeneous GAG mixtures, it is important to determine all types of compositions whether they have different numbers of sulfo-modifications or the same, including positional isomers and epimers. In most cases, it is challenging to separate isomers and epimers using HPLC techniques. However, a few methods have been developed to address this issue as mentioned previously. Both ion mobility spectrometry and capillary zone electrophoresis have demonstrated multiple instances of separating GAG isomers and epimers with fast separations.

Gas phase separation, such as IMS, is one of the faster methods for separation and occurs post ionization. IMS separations are on the order of milliseconds up to seconds; whereas LC and CZE separations can take minutes or hours. Furthermore, post ionization separation can be used in tandem with direct injection and reduces adduct formation which simplifies the complexity of analysis. Wei *et al.* recently separated isomers using gated-trapped IMS (gated TIMS) combined with NETD to analyze highly sulfated GAGs [74]. Using gated-TIMS, stereoisomers were separated as shown in Figure 1.2b, and diagnostic ions produced from NETD confirmed their structure. Before that, Amster and coworkers used high field asymmetric waveform IMS, or FAIMS, to separate isobaric mixtures of oligosaccharides followed by structural characterization using EDD [75]. Another interesting area of development is a combination of IMS-MS with

cryogenic IR spectroscopy. The Rizzo group has demonstrated separation of isomeric CS and HS GAG disaccharides using this technique [76]. Some of the isomers have similar drift times, but with unique fingerprint IR spectra it is possible to distinguish the different types of disaccharides. Overall, there are multiple types of IMS which can be utilized to distinguish isomeric oligosaccharides on the millisecond timescale for high throughput applications.

Due to the ionic nature of sulfated GAGs, CZE is well-suited to separate these compounds as it operates based on charge, size, and shape. The majority of work completed on GAGs initially was performed in normal polarity mode which resulted in longer migration times [77-80]. Recent studies were performed using reverse polarity, in which a negative potential is applied to the separation capillary, to facilitate faster separation and improve the resolution of CZE for the separation of GAGs. This work began with disaccharides and has progressed to analyzing oligosaccharides. Specifically, CZE-MS analysis has been used to assign the degree of polymerization, sulfo-modification, and to show the presence of isomers [81, 82]. An example of this is shown in Figure 1.2c; four tetrasaccharide epimers were separated based on the difference of the C-5 stereochemistry on the uronic acid residues. Recently, NETD was used to characterize CZE separated HS tetrasaccharide standards and the low molecular weight heparin pharmaceutical enoxaparin [83]. Ion activation methods compatible with the CZE timescale, such as CID/HCD and NETD, will continue to be incorporated into CZE separation experiments.

Each of these separation techniques were developed to simplify the analysis of GAG mixtures. With these techniques combined with MS and MS/MS, researchers can investigate and solve specific biological and pharmaceutical problems. Nevertheless, continued development is necessary to improve the speed, sensitivity, and capability of distinguishing the components within a heterogeneous GAG sample.

## Applications

Mass spectrometry has been utilized for decades to tackle a variety of biological targets, including GAGs. Initially, most of the work focused on using a bottom-up approach in which enzymatic digestion of the GAG is performed prior to MS analysis to reduce the complexity of the sugars [12, 36, 84]. Disaccharide analysis is still performed routinely to statistically determine the components and disaccharide backbone motifs of longer chains, but it results in a loss of structural information such as linkage, order, and sulfation patterns [84, 85]. However, the location and organization of modification patterns on GAGs dictate their biological activity. Thus, the most recent endeavors have focused on partially digested sugars that retain biological function and full-length chains.

Low molecular weight heparins (LMWHs) are partially digested GAGs used in the pharmaceutical industry for medicinal purposes. In 2008, there were a number of complications associated with contaminated heparin [86]. Since then, there have been a multitude of experiments focused on analyzing the composition of pharmaceutical heparins [87]. Enoxaparin, dalteparin, and other versions of the LWMH drugs are produced through different enzymatic procedures; these heterogeneous mixtures range from dp2-30 with large variation in sulfation and sequence composition [73, 88, 89]. As one of the most sensitive analytical techniques, MS is well suited to tackle this issue when HPLC or CZE is used to separate the mixtures [12, 80].

For top down analysis, the longer chains in LMWH pharmaceuticals were analyzed using LC-MS by Linhardt and coworkers to determine the major structures present [71, 90, 91]. Over 80 compositions have been detected with these methods. Studies using CZE-MS have also found similar results [81]. The next step involves investigating longer sugars, such as the intact chains found on proteoglycans. The simplest proteoglycans, bikunin and decorin, were chosen first and

the GAG chains were analyzed using high resolution mass spectrometry. Bikunin and decorin have a single CS/DS GAG chain attached to the core protein; bikunin has a CS chain whereas decorin has a longer DS chain. Linhardt and Amster groups combined biological and analytical techniques to separate the GAGs from the protein into fractions of different chain lengths. The fractions were then analyzed with high resolution MS on both Orbitrap MS and FT-ICR MS instruments using MS for composition and CID/HCD MS/MS for sequencing. These analyses resulted in a common sulfation pattern for each GAG oligomer [92-94]. This work on decorin is represented in Figure 1.3 which shows the GAG chain connected to the protein core, a representative CID MS spectrum of a dp20 GAG, and the overall sequence motif for the GAG chain. Although top-down analysis of two proteoglycans have been studied, there is a driving need to continue analyzing different GAGs from biological species. Structure determination of GAGs can provide valuable insight into the impact of modification patterns for GAG-protein binding to answer a variety of biological issues.

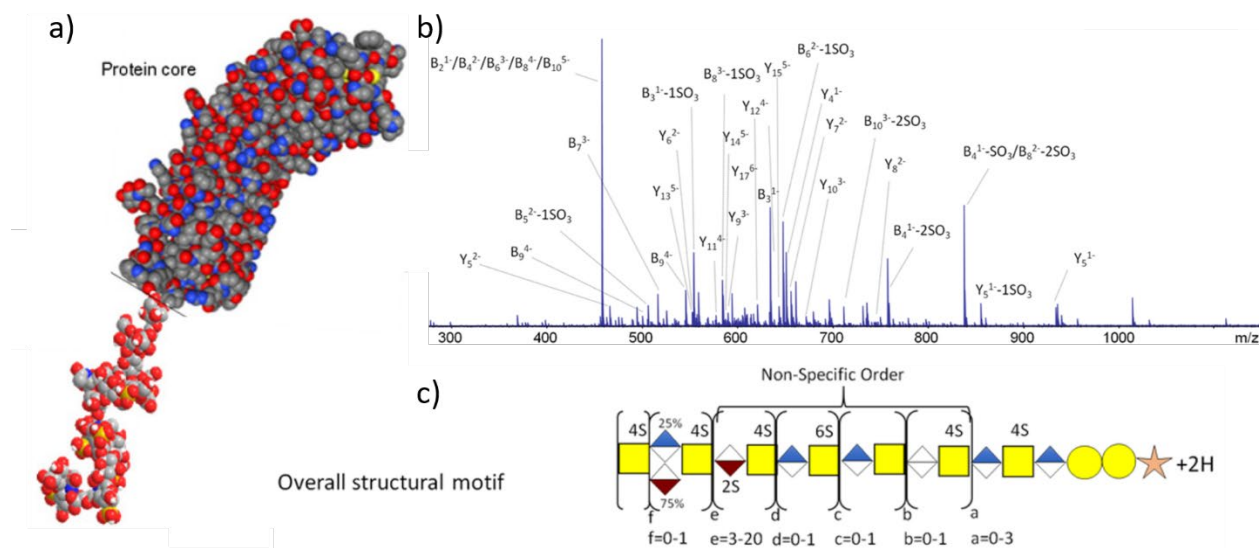


**Figure 1.3** Modeled structure and motif of decorin glycosaminoglycan. a) Space-filled structure of decorin PG, with the core protein from PDB (1XCD). Carbons (gray), hydrogens (white), oxygens (red), nitrogens (blue), and sulfurs (yellow) are shown. The O-linked GAG chain (dp20–8S) is shown with the reducing end (RE) and nonreducing end (NRE). b) CID tandem mass spectrum of decorin GAG chain dp 20 with 7 sulfo-modifications. c) Structural motif for decorin GAG chains determined by MS. Reprinted with permission. *J. Am. Chem. Soc.* **2017**, *139*, 16986-16995.

In **Chapter 2**, the experimental procedures to prepare and analyze the glycosaminoglycans samples are described in detail. GAG mixtures are prepared by enzymatic digestion of naturally occurring polysaccharides as well as chemical synthesis using a modular approach. Capillary zone electrophoresis separation and mass spectrometry techniques for characterization of mixtures are presented using collision induced dissociation and negative electron transfer dissociation.

The initial work to provide reliable and fast separations of sulfated GAGs is discussed in **Chapter 3**. Separations were completed using reverse polarity capillary electrophoresis on

purified standards before analyzing a complex pharmaceutical low molecular weight heparin mixture [81]. Capillaries were coated with neutral and cationic surfaces to decrease the separation time required for GAG analysis. In this work, more than 60 oligosaccharides ranging from dp3 to dp12 were separated and compositionally identified.

Urine from healthy human subjects were analyzed using the CZE-MS platform as demonstrated in **Chapter 4**. In this study, glycosaminoglycans found in male and female urine from young adults were compared using CZE-MS/MS [95]. CS/DS and HS were detected, but HA and KS were not. Molecular weight analysis suggests the presence of oligosaccharides from dp2-20 with a variety of sulfation patterns. Healthy young adult male and females gave similar profiles with the same ten most abundant species. These ten most abundant species were structurally characterized using NETD MS/MS with online CZE separation.

In **Chapter 5**, the previous work completed on bikunin using high resolution mass spectrometry was extended to incorporate separation prior to MS/MS analysis [92, 93]. Chondroitin/dermatan sulfate sugars were separated with the most highly sulfated sugars migrating through the capillary first. The most intense species were selected as precursors for fragmentation and characterized using CID/HCD activation. The smaller fractions contain shorter carbohydrates and chain length increases with increasing fraction size like the results shown previously [93]. From the separation information, there appeared to be minimal amount of epimers present in the samples. This is the first instance of separating sulfated GAGs ranging from dp20-dp57 using reverse polarity capillary zone electrophoresis and tandem mass spectrometry.

## REFERENCES

1. Varki, A., Biological roles of glycans. *Glycobiology* **2017**, 27 (1), 3-49.
2. Afratis, N.; Gialeli, C.; Nikitovic, D.; Tsegenidis, T.; Karousou, E.; Theocharis, A. D.; Pavão, M. S.; Tzanakakis, G. N.; Karamanos, N. K., Glycosaminoglycans: key players in cancer cell biology and treatment. *FEBS Journal* **2012**, 279 (7), 1177-1197.
3. Barbucci, R.; Magnani, A.; Lamponi, S.; Albanese, A., Chemistry and biology of glycosaminoglycans in blood coagulation. *Polym. Adv. Technol.* **1996**, 7 (8), 675-685.
4. Sasisekharan, R.; Shriver, Z.; Venkataraman, G.; Narayanasami, U., Roles of heparan-sulphate glycosaminoglycans in cancer. *Nat. Rev. Cancer* **2002**, 2 (7), 521.
5. Wolff, J. J.; Laremore, T. N.; Busch, A. M.; Linhardt, R. J.; Amster, I. J., Electron detachment dissociation of dermatan sulfate oligosaccharides. *J Am Soc Mass Spectrom* **2008**, 19 (2), 294-304.
6. Wolff, J. J.; Amster, I. J.; Chi, L.; Linhardt, R. J., Electron detachment dissociation of glycosaminoglycan tetrasaccharides. *J Am Soc Mass Spectrom* **2007**, 18 (2), 234-44.
7. Leach, F. E., 3rd; Wolff, J. J.; Xiao, Z.; Ly, M.; Laremore, T. N.; Arungundram, S.; Al-Mafraji, K.; Venot, A.; Boons, G. J.; Linhardt, R. J.; Amster, I. J., Negative electron transfer dissociation Fourier transform mass spectrometry of glycosaminoglycan carbohydrates. *Eur. J. Mass Spectrom.* **2011**, 17 (2), 167-76.
8. Laremore, T. N.; Leach, F. E.; Solakyildirim, K.; Amster, I. J.; Linhardt, R. J., Glycosaminoglycan characterization by electrospray ionization mass spectrometry including Fourier transform mass spectrometry. *Methods Enzymol.* **2010**, 478, 79-108.
9. Bielik, A. M.; Zaia, J., Multistage tandem mass spectrometry of chondroitin sulfate and dermatan sulfate. *Int J Mass Spectrom* **2011**, 305 (2-3), 131-137.

10. Zaia, J., Compositional analysis of glycosaminoglycans by electrospray mass spectrometry. *Anal. Chem.* **2001**, 73 (2), 233-239.
11. Zaia, J., Tandem mass spectrometry of sulfated heparin-like glycosaminoglycan oligosaccharides. *Analytical chemistry* **2003**, 75 (10), 2445.
12. Li, G.; Steppich, J.; Wang, Z.; Sun, Y.; Xue, C.; Linhardt, R. J.; Li, L., Bottom-Up Low Molecular Weight Heparin Analysis Using Liquid Chromatography-Fourier Transform Mass Spectrometry for Extensive Characterization. *Analytical Chemistry* **2014**, 86 (13), 6626-6632.
13. Kailemia, M. J.; Ruhaak, L. R.; Lebrilla, C. B.; Amster, I. J., Oligosaccharide Analysis by Mass Spectrometry: A Review of Recent Developments. *Analytical Chemistry* **2014**, 86 (1), 196-212.
14. Pomin, V. H.; Sharp, J. S.; Li, X.; Wang, L.; Prestegard, J. H., Characterization of Glycosaminoglycans by <sup>15</sup>N NMR Spectroscopy and in Vivo Isotopic Labeling. *Analytical Chemistry* **2010**, 82 (10), 4078-4088.
15. Langeslay, D. J.; Beecher, C. N.; Naggi, A.; Guerrini, M.; Torri, G.; Larive, C. K., Characterizing the Microstructure of Heparin and Heparan Sulfate Using N-Sulfoglucosamine <sup>1</sup>H and <sup>15</sup>N NMR Chemical Shift Analysis. *Analytical Chemistry* **2013**, 85 (2), 1247-1255.
16. Pomin, V. H., NMR chemical shifts in structural biology of glycosaminoglycans. *Analytical chemistry* **2013**, 86 (1), 65-94.
17. Staples, G. O.; Zaia, J., Analysis of Glycosaminoglycans Using Mass Spectrometry. *Curr Proteomics* **2011**, 8 (4), 325-336.
18. Zaia, J., Glycosaminoglycan glycomics using mass spectrometry. *Mol Cell Proteomics* **2013**, 12 (4), 885-92.



19. Zhou, W.; Håkansson, K., Structural Characterization of Carbohydrates by Fourier Transform Tandem Mass Spectrometry. *Current proteomics* **2011**, 8 (4), 297-308.
20. Pitt, J. J.; Gorman, J. J., Oligosaccharide Characterization and Quantitation Using 1-Phenyl-3-methyl-5-pyrazolone Derivatization and Matrix-Assisted Laser Desorption/Ionization Time-of-Flight Mass Spectrometry. *Analytical Biochemistry* **1997**, 248 (1), 63-75.
21. Kett, W. C.; Coombe, D. R., A structural analysis of heparin-like glycosaminoglycans using MALDI-TOF mass spectrometry. *Spectroscopy* **2004**, 18 (2).
22. Laremore, T. N.; Zhang, F.; Linhardt, R. J., Ionic Liquid Matrix for Direct UV-MALDI-TOF-MS Analysis of Dermatan Sulfate and Chondroitin Sulfate Oligosaccharides. *Analytical Chemistry* **2007**, 79 (4), 1604-1610.
23. Laremore, T. N.; Linhardt, R. J., Improved matrix-assisted laser desorption/ionization mass spectrometric detection of glycosaminoglycan disaccharides as cesium salts. *Rapid Communications in Mass Spectrometry* **2007**, 21 (7), 1315-1320.
24. Tissot, B.; Gasiunas, N.; Powell, A. K.; Ahmed, Y.; Zhi, Z.-l.; Haslam, S. M.; Morris, H. R.; Turnbull, J. E.; Gallagher, J. T.; Dell, A., Towards GAG glycomics: Analysis of highly sulfated heparins by MALDI-TOF mass spectrometry. *Glycobiology* **2007**, 17 (9), 972-982.
25. Przybylski, C.; Gonnet, F.; Bonnaffé, D.; Hersant, Y.; Lortat-Jacob, H.; Daniel, R., HABA-based ionic liquid matrices for UV-MALDI-MS analysis of heparin and heparan sulfate oligosaccharides. *Glycobiology* **2009**, 20 (2), 224-234.
26. Lesur, D.; Duhirwe, G.; Kovensky, J., High resolution MALDI-TOF-MS and MS/MS: Application for the structural characterization of sulfated oligosaccharides. *European Journal of Mass Spectrometry* **2019**, 0 (0), 1469066719851438.

27. Aichler, M.; Kunzke, T.; Buck, A.; Sun, N.; Ackermann, M.; Jonigk, D.; Gaumann, A.; Walch, A., Molecular similarities and differences from human pulmonary fibrosis and corresponding mouse model: MALDI imaging mass spectrometry in comparative medicine. *Laboratory Investigation* **2017**, *98*, 141.
28. Nimptsch, K.; Süß, R.; Schnabelrauch, M.; Nimptsch, A.; Schiller, J., Positive ion MALDI-TOF mass spectra are more suitable than negative ion spectra to characterize sulphated glycosaminoglycan oligosaccharides. *International Journal of Mass Spectrometry* **2012**, *310*, 72-76.
29. Zaia, J., Mass spectrometry and the emerging field of glycomics. *Chem Biol* **2008**, *15* (9), 881-92.
30. Zaia, J., Principles of mass spectrometry of glycosaminoglycans. *J Biomacromol Mass Spectrom* **2005**, *1* (1), 3-36.
31. Wolff, J. J.; Laremore, T. N.; Busch, A. M.; Linhardt, R. J.; Amster, I. J., Influence of charge state and sodium cationization on the electron detachment dissociation and infrared multiphoton dissociation of glycosaminoglycan oligosaccharides. *Journal of the American Society for Mass Spectrometry* **2008**, *19* (6), 790-798.
32. Gill, V. L.; Aich, U.; Rao, S.; Pohl, C.; Zaia, J., Disaccharide Analysis of Glycosaminoglycans Using Hydrophilic Interaction Chromatography and Mass Spectrometry. *Analytical Chemistry* **2013**, *85* (2), 1138-1145.
33. Hitchcock, A. M.; Bowman, M. J.; Staples, G. O.; Zaia, J., Improved Workup for Glycosaminoglycan Disaccharide Analysis using Capillary Electrophoresis with Laser-Induced Fluorescence Detection. *Electrophoresis* **2008**, *29* (22), 4538-4548.

34. Zaia, J.; McClellan, J. E.; Costello, C. E., Tandem Mass Spectrometric Determination of the 4S/6S Sulfation Sequence in Chondroitin Sulfate Oligosaccharides. *Analytical Chemistry* **2001**, *73* (24), 6030-6039.
35. Zamfir, A.; Seidler, D. G.; Kresse, H.; Peter-Katalinić, J., Structural characterization of chondroitin/dermatan sulfate oligosaccharides from bovine aorta by capillary electrophoresis and electrospray ionization quadrupole time-of-flight tandem mass spectrometry. *Rapid Communications in Mass Spectrometry* **2002**, *16* (21), 2015-2024.
36. Desaire, H.; Sirich, T. L.; Leary, J. A., Evidence of Block and Randomly Sequenced Chondroitin Polysaccharides: Sequential Enzymatic Digestion and Quantification Using Ion Trap Tandem Mass Spectrometry. *Analytical Chemistry* **2001**, *73* (15), 3513-3520.
37. Leach, F. E.; Xiao, Z.; Laremore, T. N.; Linhardt, R. J.; Amster, I. J., Electron detachment dissociation and infrared multiphoton dissociation of heparin tetrasaccharides. *International Journal of Mass Spectrometry* **2011**, *308* (2), 253-259.
38. Oh, H. B.; Leach, F. E.; Arungundram, S.; Al-Mafraji, K.; Venot, A.; Boons, G.-J.; Amster, I. J., Multivariate Analysis of Electron Detachment Dissociation and Infrared Multiphoton Dissociation Mass Spectra of Heparan Sulfate Tetrasaccharides Differing Only in Hexuronic acid Stereochemistry. *Journal of The American Society for Mass Spectrometry* **2011**, *22* (3), 582-590.
39. Wolff, J. J.; Laremore, T. N.; Leach, F. E.; Linhardt, R. J.; Amster, I. J., Electron Capture Dissociation, Electron Detachment Dissociation and Infrared Multiphoton Dissociation of Sucrose Octasulfate. *European Journal of Mass Spectrometry* **2009**, *15* (2), 275-281.
40. Klein, D.; Leach, F. I.; Amster, I.; Brodbelt, J., Structural Characterization of Glycosaminoglycan Carbohydrates using Ultraviolet Photodissociation. *Anal. Chem.* **2019**.

41. Ly, T.; Julian, R. R., Ultraviolet photodissociation: developments towards applications for mass-spectrometry-based proteomics. *Angewandte Chemie International Edition* **2009**, *48* (39), 7130-7137.
42. Racaud, A.; Antoine, R.; Dugourd, P.; Lemoine, J., Photoinduced dissociation of heparin-derived oligosaccharides controlled by charge location. *Journal of the American Society for Mass Spectrometry* **2010**, *21* (12), 2077-2084.
43. Leach, F. E.; Ly, M.; Laremore, T. N.; Wolff, J. J.; Perlow, J.; Linhardt, R. J.; Amster, I. J., Hexuronic Acid Stereochemistry Determination in Chondroitin Sulfate Glycosaminoglycan Oligosaccharides by Electron Detachment Dissociation. *Journal of The American Society for Mass Spectrometry* **2012**, *23* (9), 1488-1497.
44. Agyekum, I.; Zong, C.; Boons, G.-J.; Amster, I. J., Single Stage Tandem Mass Spectrometry Assignment of the C-5 Uronic Acid Stereochemistry in Heparan Sulfate Tetrasaccharides using Electron Detachment Dissociation. *Journal of The American Society for Mass Spectrometry* **2017**, 1-10.
45. Agyekum, I.; Patel, A. B.; Zong, C.; Boons, G.-J.; Amster, I. J., Assignment of hexuronic acid stereochemistry in synthetic heparan sulfate tetrasaccharides with 2-O-sulfo uronic acids using electron detachment dissociation. *International Journal of Mass Spectrometry* **2015**, *390* (Supplement C), 163-169.
46. Kailemia, M. J.; Li, L.; Ly, M.; Linhardt, R. J.; Amster, I. J., Complete Mass Spectral Characterization of a Synthetic Ultralow-Molecular-Weight Heparin Using Collision-Induced Dissociation. *Analytical Chemistry* **2012**, *84* (13), 5475-5478.
47. Kailemia, M. J.; Li, L.; Xu, Y.; Liu, J.; Linhardt, R. J.; Amster, I. J., Structurally Informative Tandem Mass Spectrometry of Highly Sulfated Natural and Chemoenzymatically

- Synthesized Heparin and Heparan Sulfate Glycosaminoglycans. *Molecular & Cellular Proteomics* **2013**, 12 (4), 979-990.
48. Zaia, J.; Costello, C. E., Tandem Mass Spectrometry of Sulfated Heparin-Like Glycosaminoglycan Oligosaccharides. *Analytical Chemistry* **2003**, 75 (10), 2445-2455.
49. Guo, Q.; Reinhold, V. N., Advancing MSn spatial resolution and documentation for glycosaminoglycans by sulfate-isotope exchange. *Analytical and Bioanalytical Chemistry* **2019**, 411 (20), 5033-5045.
50. Liang, Q.; Chopra, P.; Boons, G.-J.; Sharp, J. S., Improved de novo sequencing of heparin/heparan sulfate oligosaccharides by propionylation of sites of sulfation. *Carbohydrate Research* **2018**, 465, 16-21.
51. Huang, R.; Zong, C.; Venot, A.; Chiu, Y.; Zhou, D.; Boons, G.-J.; Sharp, J. S., De Novo Sequencing of Complex Mixtures of Heparan Sulfate Oligosaccharides. *Analytical Chemistry* **2016**, 88 (10), 5299-5307.
52. Leach, F. E.; Wolff, J. J.; Xiao, Z.; Ly, M.; Laremore, T. N.; Arungundram, S.; Al-Mafraji, K.; Venot, A.; Boons, G.-J.; Linhardt, R. J.; Amster, I. J., Negative electron transfer dissociation Fourier transform mass spectrometry of glycosaminoglycan carbohydrates. *European Journal of Mass Spectrometry (Chichester, England)* **2011**, 17 (2), 167-176.
53. Wolff, J. J.; Leach, F. E.; Laremore, T. N.; Kaplan, D. A.; Easterling, M. L.; Linhardt, R. J.; Amster, I. J., Negative electron transfer dissociation of glycosaminoglycans. *Analytical chemistry* **2010**, 82 (9), 3460-3466.
54. Leach, F. E.; Riley, N. M.; Westphall, M. S.; Coon, J. J.; Amster, I. J., Negative Electron Transfer Dissociation Sequencing of Increasingly Sulfated Glycosaminoglycan

Oligosaccharides on an Orbitrap Mass Spectrometer. *Journal of The American Society for Mass Spectrometry* **2017**, 28 (9), 1844-1854.

55. Wu, J.; Wei, J.; Hogan, J. D.; Chopra, P.; Joshi, A.; Lu, W.; Klein, J.; Boons, G.-J.; Lin, C.; Zaia, J., Negative Electron Transfer Dissociation Sequencing of 3-O-Sulfation-Containing Heparan Sulfate Oligosaccharides. *Journal of The American Society for Mass Spectrometry* **2018**, 29 (6), 1262-1272.

56. Varki, A.; Cummings, R. D.; Esko, J. D.; Freeze, H. H.; Stanley, P.; Bertozzi, C. R.; Hart, G. W.; Etzler, M. E., *Essentials of Glycobiology*. NY, 2009; Vol. 2.

57. Ly, M.; Laremore, T. N.; Linhardt, R. J., Proteoglycomics: Recent Progress and Future Challenges. *Omics: A journal of integrative biology* **2010**, 14 (4), 389-399.

58. Li, L.; Zhang, F.; Zaia, J.; Linhardt, R. J., Top-down approach for the direct characterization of low molecular weight heparins using LC-FT-MS. *Anal Chem* **2012**, 84 (20), 8822-9.

59. Zaia, J., On-line separations combined with MS for analysis of glycosaminoglycans. *Mass Spectrometry Reviews* **2009**, 28 (2), 254-272.

60. Volpi, N.; Galeotti, F.; Yang, B.; Linhardt, R. J., Analysis of glycosaminoglycan-derived, precolumn, 2-aminoacridone-labeled disaccharides with LC-fluorescence and LC-MS detection. *Nat. Protoc.* **2014**, 9 (3), 541-558.

61. Huang, Y.; Shi, X.; Yu, X.; Leymarie, N.; Staples, G. O.; Yin, H.; Killeen, K.; Zaia, J., Improved liquid chromatography-MS/MS of heparan sulfate oligosaccharides via chip-based pulsed makeup flow. *Anal Chem* **2011**, 83 (21), 8222-9.

62. Huang, R.; Liu, J.; Sharp, J. S., An approach for separation and complete structural sequencing of heparin/heparan sulfate-like oligosaccharides. *Anal Chem* **2013**, 85 (12), 5787-95.

63. Lemmnitzer, K.; Riemer, T.; Groessl, M.; Süß, R.; Knochenmuss, R.; Schiller, J., Comparison of ion mobility-mass spectrometry and pulsed-field gradient nuclear magnetic resonance spectroscopy for the differentiation of chondroitin sulfate isomers. *Analytical Methods* **2016**, 8 (48), 8483-8491.
64. Zaia, J.; Khatri, K.; Klein, J.; Shao, C.; Sheng, Y.; Viner, R., Complete Molecular Weight Profiling of Low-Molecular Weight Heparins Using Size Exclusion Chromatography-Ion Suppressor-High-Resolution Mass Spectrometry. *Analytical Chemistry* **2016**, 88 (21), 10654-10660.
65. Zhang, Q.; Chen, X.; Zhu, Z.; Zhan, X.; Wu, Y.; Song, L.; Kang, J., Structural Analysis of Low Molecular Weight Heparin by Ultraperformance Size Exclusion Chromatography/Time of Flight Mass Spectrometry and Capillary Zone Electrophoresis. *Analytical Chemistry* **2013**, 85 (3), 1819-1827.
66. Wu, J.; Wei, J.; Chopra, P.; Boons, G.-J.; Lin, C.; Zaia, J., Sequencing Heparan Sulfate Using HILIC LC-NETD-MS/MS. *Analytical Chemistry* **2019**.
67. Miller, R. L.; Guimond, S. E.; Shivkumar, M.; Blocksidge, J.; Austin, J. A.; Leary, J. A.; Turnbull, J. E., Heparin Isomeric Oligosaccharide Separation Using Volatile Salt Strong Anion Exchange Chromatography. *Analytical Chemistry* **2016**, 88 (23), 11542-11550.
68. Volpi, N.; Linhardt, R. J., High-performance liquid chromatography-mass spectrometry for mapping and sequencing glycosaminoglycan-derived oligosaccharides. *Nature protocols* **2010**, 5 (6), 993.
69. Du, J. Y.; Chen, L. R.; Liu, S.; Lin, J. H.; Liang, Q. T.; Lyon, M.; Wei, Z., Ion-pairing liquid chromatography with on-line electrospray ion trap mass spectrometry for the structural analysis of N-unsubstituted heparin/heparan sulfate. **2016**, 1028, 71-76.

70. Doneanu, C. E.; Chen, W.; Gebler, J. C., Analysis of Oligosaccharides Derived from Heparin by Ion-Pair Reversed-Phase Chromatography/Mass Spectrometry. **2009**, *81* (9), 3485-3499.
71. Li, L.; Zhang, F.; Zaia, J.; Linhardt, R. J., Top-Down Approach for the Direct Characterization of Low Molecular Weight Heparins Using LC-FT-MS. *Analytical Chemistry* **2012**, *84* (20), 8822-8829.
72. Antia, I. U.; Mathew, K.; Yagnik, D. R.; Hills, F. A.; Shah, A. J., Analysis of procainamide-derivatised heparan sulphate disaccharides in biological samples using hydrophilic interaction liquid chromatography mass spectrometry. *Analytical and Bioanalytical Chemistry* **2018**, *410* (1), 131-143.
73. Sun, X.; Guo, Z.; Yu, M.; Lin, C.; Sheng, A.; Wang, Z.; Linhardt, R. J.; Chi, L., Hydrophilic interaction chromatography-multiple reaction monitoring mass spectrometry method for basic building block analysis of low molecular weight heparins prepared through nitrous acid depolymerization. **2017**, *1479*, 121-128.
74. Wei, J.; Wu, J.; Tang, Y.; Ridgeway, M. E.; Park, M. A.; Costello, C. E.; Zaia, J.; Lin, C., Characterization and Quantification of Highly Sulfated Glycosaminoglycan Isomers by Gated-Trapped Ion Mobility Spectrometry Negative Electron Transfer Dissociation MS/MS. *Analytical Chemistry* **2019**, *91* (4), 2994-3001.
75. Muchena J. Kailemia, M. P., Desmond A. Kaplan, Andre Venot,; Geert-Jan Boons, L. L., Robert J. Linhardt, I. Jonathan Amster, High-field asymmetric-waveform ion mobility spectrometry and electron detachment dissociation of isobaric mixtures of glycosaminoglycans. *J. Am. Soc. Mass Spectrom.* **2013**.



76. Khanal, N.; Masellis, C.; Kamrath, M. Z.; Clemmer, D. E.; Rizzo, T. R., Glycosaminoglycan Analysis by Cryogenic Messenger-Tagging IR Spectroscopy Combined with IMS-MS. *Analytical Chemistry* **2017**, 89 (14), 7601-7606.
77. Prabhakar, V.; Capila, I.; Sasisekharan, R., The Structural Elucidation of Glycosaminoglycans. In *Glycomics: Methods and Protocols*, Packer, N. H.; Karlsson, N. G., Eds. Humana Press: Totowa, NJ, 2009; pp 147-156.
78. Volpi, N.; Maccari, F.; Linhardt, R. J., Capillary electrophoresis of complex natural polysaccharides. *Electrophoresis* **2008**, 29 (15), 3095-3106.
79. Zamfir, A. D., Applications of capillary electrophoresis electrospray ionization mass spectrometry in glycosaminoglycan analysis. *Electrophoresis* **2016**, 37 (7-8), 973-986.
80. Sun, X.; Lin, L.; Liu, X.; Zhang, F.; Chi, L.; Xia, Q.; Linhardt, R. J., Capillary Electrophoresis–Mass Spectrometry for the Analysis of Heparin Oligosaccharides and Low Molecular Weight Heparin. *Analytical Chemistry* **2016**, 88 (3), 1937-1943.
81. Sanderson, P.; Stickney, M.; Leach, F. E.; Xia, Q.; Yu, Y.; Zhang, F.; Linhardt, R. J.; Amster, I. J., Heparin/heparan sulfate analysis by covalently modified reverse polarity capillary zone electrophoresis-mass spectrometry. *Journal of Chromatography A* **2018**, 1545, 75-83.
82. Lin, L.; Liu, X.; Zhang, F.; Chi, L.; Amster, I. J.; Leach, F. E.; Xia, Q.; Linhardt, R. J., Analysis of heparin oligosaccharides by capillary electrophoresis–negative-ion electrospray ionization mass spectrometry. *Analytical and Bioanalytical Chemistry* **2017**, 409 (2), 411-420.
83. Stickney, M.; Sanderson, P.; Leach, F. E.; Zhang, F.; Linhardt, R. J.; Amster, I. J., Online capillary zone electrophoresis negative electron transfer dissociation tandem mass spectrometry of glycosaminoglycan mixtures. *International Journal of Mass Spectrometry* **2019**, 445, 116209.

84. Sun, X.; Li, L.; Overdier, K. H.; Ammons, L. A.; Douglas, I. S.; Burlew, C. C.; Zhang, F.; Schmidt, E. P.; Chi, L.; Linhardt, R. J., Analysis of Total Human Urinary Glycosaminoglycan Disaccharides by Liquid Chromatography–Tandem Mass Spectrometry. *Analytical Chemistry* **2015**, *87* (12), 6220-6227.
85. Turiák, L.; Tóth, G.; Ozohanics, O.; Révész, Á.; Ács, A.; Vékey, K.; Zaia, J.; Drahos, L., Sensitive method for glycosaminoglycan analysis of tissue sections. *Journal of Chromatography A* **2018**, *1544*, 41-48.
86. Liu, H.; Zhang, Z.; Linhardt, R. J., Lessons learned from the contamination of heparin. *Natural Product Reports* **2009**, *26* (3), 313-321.
87. Szajek, A. Y.; Chess, E.; Johansen, K.; Gratzl, G.; Gray, E.; Keire, D.; Linhardt, R. J.; Liu, J.; Morris, T.; Mulloy, B., The US regulatory and pharmacopeia response to the global heparin contamination crisis. *Nature biotechnology* **2016**, *34* (6), 625.
88. Mourier, P. A. J.; Agut, C.; Souaifi-Amara, H.; Herman, F.; Viskov, C., Analytical and statistical comparability of generic enoxaparins from the US market with the originator product. *Journal of Pharmaceutical and Biomedical Analysis* **2015**, *115*, 431-442.
89. Guerrini, M.; Rudd, T. R.; Mauri, L.; Macchi, E.; Fareed, J.; Yates, E. A.; Naggi, A.; Torri, G., Differentiation of Generic Enoxaparins Marketed in the United States by Employing NMR and Multivariate Analysis. *Analytical Chemistry* **2015**, *87* (16), 8275-8283.
90. Sun, X.; Sheng, A.; Liu, X.; Shi, F.; Jin, L.; Xie, S.; Zhang, F.; Linhardt, R. J.; Chi, L., Comprehensive Identification and Quantitation of Basic Building Blocks for Low-Molecular Weight Heparin. *Analytical Chemistry* **2016**, *88* (15), 7738-7744.
91. Ouyang, Y.; Zeng, Y.; Rong, Y.; Song, Y.; Shi, L.; Chen, B.; Yang, X.; Xu, N.; Linhardt, R. J.; Zhang, Z., Profiling Analysis of Low Molecular Weight Heparins by Multiple

Heart-Cutting Two Dimensional Chromatography with Quadruple Time-of-Flight Mass Spectrometry. **2015**, 87 (17), 8957-8963.

92. Chi, L.; Wolff, J. J.; Laremore, T. N.; Restaino, O. F.; Xie, J.; Schiraldi, C.; Toida, T.; Amster, I. J.; Linhardt, R. J., Structural Analysis of Bikunin Glycosaminoglycan. *Journal of the American Chemical Society* **2008**, 130 (8), 2617-2625.

93. Ly, M.; Leach, F. E., 3rd; Laremore, T. N.; Toida, T.; Amster, I. J.; Linhardt, R. J., The proteoglycan bikunin has a defined sequence. *Nat. Chem. Biol.* **2011**, 7 (11), 827-33.

94. Yu, Y.; Duan, J.; Leach, F. E.; Toida, T.; Higashi, K.; Zhang, H.; Zhang, F.; Amster, I. J.; Linhardt, R. J., Sequencing the Dermatan Sulfate Chain of Decorin. *Journal of the American Chemical Society* **2017**, 139 (46), 16986-16995.

95. Ha, X.; Sanderson, P.; Nesheiwat, S.; Lin, L.; Yu, Y.; Zhang, F.; Amster, I. J.; Linhardt, R. J., Structural Analysis of Urinary Glycosaminoglycans from Healthy Human Subjects. *Glycobiology* **2019**.

## CHAPTER 2

### EXPERIMENTAL METHODS

#### Preparation of Glycosaminoglycans

##### *GAG Standards*

GAG oligosaccharides were prepared by enzymatic depolymerization and purified using strong anion exchange high-pressure liquid chromatography (SAX-HPLC) for samples 1-6 from **Chapter 3** as shown in Table 3.1 [1]. Epimer pair heparan sulfate tetrasaccharides (Table 3.1, samples 7 GlcA-GlcNAc6S-IdoA-GlcNAc6S (GI) and 8 GlcA-GlcNAc6S-GlcA-GlcNAc6S (GG)) were chemically synthesized and purified as described in the literature [2]. Low molecular weight heparin, Enoxaparin, was from the USP (Rockville, MD). All samples were desalted with a 3 kDa Amicon Ultra centrifugal filter (Millipore, Temecula, CA) prior to separation and mass spectrometry analysis. Although the GAGs are below 3kDa, heparan sulfate tetrasaccharides and larger chains do not pass through the 3kDa membrane. The membrane permeability is based on size and shape. GAGs have a linear structure compared to proteins that often have a globular structure, and the linear structure makes it behave as a higher molecular weight to the centrifugal filter membrane. Filters were conditioned with water, and the sample was then washed with two filter volumes of water ( $14,000 \times g$  for 25 min each). Before analysis, GAG samples were diluted to 5  $\mu\text{g/mL}$  in water.

### *Urinary GAG Sample Preparation*

Urine samples were defrosted at 4°C and mixed well using a vortex mixer. 80 mL of each sample was used for GAG preparation. Small molecules and salts were removed by dialysis (molecular weight cut-off (MWCO) 150–500 Da) against distilled water and then freeze-dried to recover the crude GAGs. All lyophilized crude urinary GAGs were suspended in 10 mL of water, proteolyzed at 55 °C with 10 mg/mL actinase E for 24 h, and the mixture was then lyophilized. The lyophilized samples were dissolved in 5 mL of a solution of denaturing buffer (8 M urea containing 2 wt. % CHAPS), bound to a Vivapure Q Maxi H spin column, washed twice with 10 mL of denaturing buffer, and washed three-times with 10 mL of 0.2 M NaCl. The GAG components were then eluted from the spin column with three 10 mL volumes of 16% NaCl, and the salt in these fractions was removed by exhaustive dialysis (MWCO 500–1000 Da) against distilled water and freeze-dried to recover the purified GAGs.

### *Disaccharides Analysis of Urinary GAGs*

Purified urinary GAGs (approximately 5 µg) were dissolved in 300 µL of digestion buffer (50 mM ammonium acetate, 2 mM calcium chloride). Recombinant heparin lyase I, II, and III; chondroitin lyase ABC; and keratanase I and II (10 mU of each enzyme) were then added to the reaction buffer and placed in a 37 °C incubator overnight. The disaccharides were recovered by passing through a 3000 Da MWCO spin column. The filter unit was washed twice with 200 µL of distilled water, and the combined fractions were finally lyophilized. The dried samples were labeled with 2-aminoacridone (AMAC) by adding 10 µL of 0.1 M 2-aminoacridone in dimethyl sulfoxide/acetic acid (17/3, v/v) incubating at RT for 10 min, followed by adding 10 µL of 1 M aqueous sodium cyanoborohydride and incubating for 1 h at 45 °C. The resulting samples were

centrifuged at 13,200 rpm for 20 min. Supernatant was collected and analyzed by HPLC-MS on an Agilent 1200 LC/MSD instrument (Agilent Technologies, Inc. Wilmington, DE) equipped with a 6300 ion-trap and a binary pump. The column used was a Poroshell 120 C18 column (3.0 × 50 mm, 2.7 μm, Agilent, USA) at 45 °C. Eluent A was 50 mM ammonium acetate solution, and eluent B was methanol. The mobile phase passed through the column at a flow rate of 250 μL/min with 10 min linear gradients of 10–35% solution B. The electrospray interface was set in negative ionization mode with a skimmer potential of –40.0 V, a capillary exit of –40.0 V, and a source temperature of 350 °C, to obtain the maximum abundance of the ions in a full-scan spectrum (300–850 Da). Nitrogen (8 L/min, 40 psi) was used as a drying and nebulizing gas.

*Molecular Weight Distribution of Urinary GAGs using Polyacrylamide Gel Electrophoresis (PAGE)*

PAGE was used to determine the molecular weight distribution of GAGs. The purified urinary GAGs were separated by a 15% total acrylamide, which containing 14.08% (w/v) acrylamide, 0.92% (w/v) *N,N*-methylene-bis-acrylamide, and 5% (w/v) sucrose. The acrylamide monomer solutions were prepared in resolving buffer (0.1 M boric acid, 0.1 M Tris, 0.01 M disodium EDTA, pH 8.3). Stacking gel monomer solution was prepared in resolving buffer, containing 4.75% (w/v) acrylamide and 0.25% (w/v) *N,N*-methylene- bis-acrylamide and the pH adjusted to 6.3 using HCl. A 10 cm × 7 mm diameter resolving gel column was cast from 4 mL of 15% resolving gel solution containing 4 μL of tetramethylethylenediamine and 12 μL of 10% ammonium persulfate. A stacking gel was cast from 1 mL of stacking gel monomer solution containing 1 μL of tetramethylethylenediamine and 30 μL of 10% ammonium persulfate. Phenol red dye was added to the sample for visualization of the ion front during electrophoresis. In each

lane, ~5 µg of sample was subjected to electrophoresis. A standard composed mixture of heparin oligosaccharides with known molecular weights was prepared enzymatically from bovine lung heparin [3]. The gel was visualized with alcian blue staining and then digitized with UN-Scan-it to estimate molecular weight.

#### *Molecular Weight Distribution of Urinary GAGs using GPC*

Oligosaccharides separated by size exclusion column (Tosoh Bioscience TSKgel G3000SWxl and TSKgel G4000SWxl columns) with online differential refraction detector. Mobile phase was 50 mM ammonium acetate at 0.5 mL/min. GAGs were extracted by performing dialysis and treatment with actinase E to remove proteins on a mini Q cation column. Recovered GAGs were subjected to gel permeation chromatography (GPC) to obtain low molecular weight oligosaccharides before reconstituting in water for CZE-MS analysis.

#### *Glycosaminoglycan Samples Released from Bikunin*

The proteoglycan bikunin was purchased and purified using 30-kDa molecular weight centrifugal device as described in previous literature [4]. Actinase E was utilized for proteolysis of bikunin at pH 7.5 in 50 mM Tris-HCl in sodium acetate at 45°C for 18 hours before isolation of the digestion using strong anion exchange spin column chromatography. The glycosaminoglycan mixture was desalted using a 10-kDa molecular weight centrifugal filter with multiple deionized water washes.

Bikunin glycosaminoglycans were fractionated using continuous elution polyacrylamide gel electrophoresis (PAGE) [4]. Briefly, a 2 mg aliquot of purified bikunin glycosaminoglycan was loaded in a solution of phenol red and sucrose. Electrophoresis was performed for 8 hours at

constant power (12 W) with fraction collection set to 2 minutes. Strong anion exchange and desalting removed remaining salts and impurities. Separation was visualized using Alcian blue stain on a 15% total acrylamide monomer solution using native mini-slab PAGE gel. Molecular weight distribution of the glycosaminoglycans were estimated using PAGE densitometry and bikunin standards using UN-SCANIT (Silk Scientific) [5]. The resulting fractions were reconstituted in water for CZE-MS/MS analysis.

### **Capillary Coatings**

Bare fused silica capillaries were etched with concentrated hydrofluoric acid (HF) at one end to reduce the outer diameter of the capillary for use in the sheath flow CE interface described below. For the etching process, the outlet of the capillary was placed in concentrated HF for 45-60 min. The capillary tip was then washed profusely with water. The etched capillaries were coated with AHS to render a cation coated capillary and DMS to generate a neutral coated capillary. Coating solutions were prepared in toluene with 1% concentration of either AHS or DMS. To clean and prepare for coating, the capillary was rinsed with 0.1 M NaOH, water, methanol, dry acetone, and dry toluene, respectively, for 30 min each. The capillary was then coated by flowing 1% AHS or DMS for 1 h. The capillary was consecutively flushed with dry toluene, dry acetone, and methanol for 30 min to remove excess coating solution. Finally, the capillary was equilibrated with background electrolyte buffer (BGE, 25 mM ammonium acetate 70% MeOH) for 1 h. Once degradation becomes apparent, BFS capillaries can be easily cleaned by flushing sodium hydroxide for a short time; however, the coatings are stripped in basic conditions and must be reapplied by repeating the coating procedure. In some experiments, 0.1-1% formic acid (FA) or 0.02-0.1% diethylamine (DEA) was added to the BGE.



## **CZE-MS/MS of Oligosaccharides**

Experiments were conducted on an Agilent HP 3D capillary electrophoresis instrument (Wilmington, DE). The total length of the capillaries ranged from 50-80 cm, and the inner diameter was 50  $\mu\text{m}$ . The aqueous GAG samples were injected for 3-12 s at 950 mbar followed by a BGE injection for 10 s at 10 mbar. The ionic strength of the injected sample plug is 2-3 orders of magnitude less than that of the background electrolyte, so sample stacking is expected under these conditions and provides a sharp sample front. The capillary was then placed into a BGE vial for separation. A separation voltage of -30 kV was applied to the capillary for most experiments. A separation voltage of -15 kV was used for selected experiments as identified in following chapters.

An EMASS-II (CMP Scientific, Brooklyn, NY) CE-MS interface was employed to couple the CE with a Thermo Scientific Velos Orbitrap Elite mass spectrometer (Bremen, Germany) [6-8]. The etched capillary outlet was nested inside of a cation coated glass emitter tip with a 30  $\mu\text{m}$  tip orifice (CMP Scientific, Brooklyn, NY). The etched capillary was positioned 0.3-0.7 mm from the tip of the emitter orifice to create a mixing volume of ca. 15-18 nL, and the emitter tip was filled with sheath liquid (SL, 25 mM ammonium acetate 70% MeOH). Ammonium acetate (25 mM in 70% methanol) was used as the background electrolyte and sheath liquid to provide reproducible separations and optimal spray stability. An external power supply provided a nano-electrospray (nESI) voltage ranging from -1.7 to -1.9 kV to the emitter.

MS detection was performed in negative ion mode, and multiply deprotonated anions were observed for the GAG species. Prior to CZE-MS experiments, a semi-automatic optimization of source parameters was performed using sucrose octasulfate to improve sensitivity of sulfated GAGs and reduce sulfate loss during MS analysis. The Orbitrap was

scanned from  $m/z$  150-2000 for GAG oligosaccharides with a specified resolution of 120,000 for MS experiments.

For tandem mass spectrometry experiments, precursor ions were mass selected in the dual linear ion trap. Ions were activated using low energy collision (20-55 eV) or negative electron transfer dissociation (NETD) MS/MS. Both collision induced dissociation (CID) and higher energy collision induced dissociation (HCD) were used to analyze the oligosaccharides. Fluoranthene was used as the reagent cation for NETD activation. Multiply charged precursors were necessary for NETD activation. Doubly charged precursors were allowed to react for ~125 ms; whereas, only ~50 ms were required for triply charged precursors. Each peak from the electropherogram was averaged to obtain a tandem mass spectrum with mass accuracy of 10 ppm or better. Data analysis was performed using Glycoworkbench and in-lab developed software [9, 10]. Fragments were assigned and annotated using the Domon-Costello nomenclature [11].

## REFERENCES

1. Singh, A.; Kett, W. C.; Severin, I. C.; Agyekum, I.; Duan, J.; Amster, I. J.; Proudfoot, A. E. I.; Coombe, D. R.; Woods, R. J., The interaction of heparin tetrasaccharides with chemokine CCL5 is modulated by sulfation pattern and pH. *J. Biol. Chem.* **2015**.
2. Arungundram, S.; Al-Mafraji, K.; Asong, J.; Leach, F. E.; Amster, I. J.; Venot, A.; Turnbull, J. E.; Boons, G.-J., Modular Synthesis of Heparan Sulfate Oligosaccharides for Structure-Activity Relationship Studies. *Journal of the American Chemical Society* **2009**, *131* (47), 17394-17405.
3. Edens, R.; Al-Hakim, A.; Weiler, J.; Rethwisch, D.; Fareed, J.; Linhardt, R., Gradient polyacrylamide gel electrophoresis for determination of molecular weights of heparin preparations and low-molecular-weight heparin derivatives. *Journal of pharmaceutical sciences* **1992**, *81* (8), 823-827.
4. Ly, M.; Leach, F. E., 3rd; Laremore, T. N.; Toida, T.; Amster, I. J.; Linhardt, R. J., The proteoglycan bikunin has a defined sequence. *Nat. Chem. Biol.* **2011**, *7* (11), 827-33.
5. Ly, M.; Wang, Z.; Laremore, T. N.; Zhang, F.; Zhong, W.; Pu, D.; Zagorevski, D. V.; Dordick, J. S.; Linhardt, R. J., Analysis of E. coli K5 capsular polysaccharide heparosan. *Analytical and bioanalytical chemistry* **2011**, *399* (2), 737-745.
6. Lin, L.; Liu, X.; Zhang, F.; Chi, L.; Amster, I. J.; Leach, F. E.; Xia, Q.; Linhardt, R. J., Analysis of heparin oligosaccharides by capillary electrophoresis–negative-ion electrospray ionization mass spectrometry. *Analytical and Bioanalytical Chemistry* **2017**, *409* (2), 411-420.
7. Sun, L.; Zhu, G.; Zhao, Y.; Yan, X.; Mou, S.; Dovichi, N. J., Ultrasensitive and Fast Bottom-up Analysis of Femtogram Amounts of Complex Proteome Digests. *Angew. Chem., Int. Ed.* **2013**, *52* (51), 13661-13664.

8. Sun, L.; Zhu, G.; Zhang, Z.; Mou, S.; Dovichi, N. J., Third-generation electrokinetically pumped sheath-flow nanospray interface with improved stability and sensitivity for automated capillary zone electrophoresis–mass spectrometry analysis of complex proteome digests. *J. Proteome Res.* **2015**, *14* (5), 2312-2321.
9. Ceroni, A.; Maass, K.; Geyer, H.; Geyer, R.; Dell, A.; Haslam, S. M., GlycoWorkbench: a tool for the computer-assisted annotation of mass spectra of glycans. *Journal of proteome research* **2008**, *7* (4), 1650-1659.
10. Duan, J.; Jonathan Amster, I., An Automated, High-Throughput Method for Interpreting the Tandem Mass Spectra of Glycosaminoglycans. *Journal of The American Society for Mass Spectrometry* **2018**, *29* (9), 1802-1811.
11. Domon, B.; Costello, C. E., A systematic nomenclature for carbohydrate fragmentations in FAB-MS/MS spectra of glycoconjugates. *Glycoconjugate Journal* **1988**, *5* (4), 397-409.

## CHAPTER 3

### Heparin/Heparan Sulfate Analysis by Covalently Modified Reverse Polarity Capillary Zone

### Electrophoresis-Mass Spectrometry

<sup>1</sup>Sanderson, P.; Stickney, M.; Leach, F. E.; Xia, Q.; Yu, Y.; Zhang, F.; Linhardt, R. J.; Amster, I. J., Heparin/heparan sulfate analysis by covalently modified reverse polarity capillary zone electrophoresis-mass spectrometry. *Journal of Chromatography A* 2018, 1545, 75-83.  
anderson, P., and I.J. Amster. Reprinted with permission of publisher.

## **ABSTRACT**

Reverse polarity capillary zone electrophoresis coupled to negative ion mode mass spectrometry (CZE-MS) is shown to be an effective and sensitive tool for the analysis of glycosaminoglycan mixtures. Covalent modification of the inner wall of the separation capillary with neutral or cationic reagents produces a stable and durable surface that provides reproducible separations. By combining CZE-MS with a cation-coated capillary and a sheath flow interface, a rapid and reliable method has been developed for the analysis of sulfated oligosaccharides from dp4 to dp12. Several different mixtures have been separated and detected by mass spectrometry. The mixtures were selected to test the capability of this approach to resolve subtle differences in structure, such as sulfation position and epimeric variation of the uronic acid. The system was applied to a complex mixture of heparin/heparan sulfate oligosaccharides varying in chain length from dp3 to dp12 and more than 80 molecular compositions were identified by accurate mass measurement.

## INTRODUCTION

Sulfated glycosaminoglycan (GAG) carbohydrates are linear, acidic polysaccharide chains that are abundant on the surface of mammalian cells [1]. Several biological processes, such as developmental and disease functions, are impacted by GAGs within the body through protein-binding interactions [2-4]. The biosynthesis of GAG chains is a non-template process, facilitated by a number of enzymatic steps (elongation, deacetylation, sulfation, epimerization) that do not go to completion, and results in highly heterogeneous and complex mixtures [5]. There are several classes of GAGs that are defined by their linkage pattern and amino sugar (*N*-acetyl glucosamine (GlcNAc) or *N*-acetyl galactosamine (GalNAc)), with heparin and heparan sulfate as the most structurally diverse. Heparin and heparan sulfate consist of a repeating disaccharide unit of an *N*-acetyl glucosamine linked (1→4) to a hexuronic acid sugar. The GlcNAc can be modified by deacetylation and *N*-sulfo modification, and it can also have sulfation at the 6-*O*- or 3-*O*-position. The hexuronic acid sugar can also exist as one of two epimers: glucuronic acid (GlcA) or iduronic acid (IdoA) with sulfation most likely at the 2-*O*-position of IdoA but infrequently at the 2-*O*-position of GlcA [6].

The structural assignment of GAG chains is a significant analytical challenge and has been the target of several researchers [7-14]. Although full-length sulfated GAGs have been analyzed in top-down fashion by mass spectrometry [15, 16], the typical approach is to partially digest polysaccharides to oligosaccharide mixtures of moderate length (typically disaccharides to decasaccharide) to enable characterization. The structural analysis of sulfated GAGs can be accomplished using mass spectrometry, which has the advantages of high sensitivity and selectivity for structural characterization [10, 12, 13, 17, 18].

The complexity of these digest mixtures makes prior separation (on-line or off-line) desirable to facilitate analysis. Some approaches for separating GAGs include high performance liquid chromatography (HPLC), hydrophilic interaction liquid chromatography (HILIC), and capillary zone electrophoresis (CZE). HPLC is a large umbrella term that contains several different techniques based on the chosen column. Size exclusion (SEC), strong anion exchange (SAX), reversed phase ion pairing (RPIP), and graphitized carbon chromatography (GCC) are techniques that have been coupled to mass spectrometry for GAG analysis [19-22]. However, these techniques have disadvantages in comparison to CZE-MS. SEC and SAX utilize reagent cations at elevated concentrations that lead to ion suppression if not removed before MS analysis [23]. RPIP-LC-MS can lead to mass spectrometer contamination and may undermine system performance. HILIC uses a polar stationary phase and mobile phases much like those used in reverse-phase separations, making it more compatible for GAG separations and MS analysis [24, 25]. Unfortunately, HILIC separations resolve components mostly by their degree of polymerization (dp), and do not provide much resolution for isomers [14, 16]. GCC offers adsorption based separation with very stable graphite columns allowing a multitude of conditions to be implemented, such as high temperatures, variable pH, and low salt content [19, 26, 27]. Previous work using HPLC and HILIC demonstrated the ability to separate GAGs up to dp14 [20, 28].

Because of the ionic nature of sulfated GAG chains, CZE is a well-suited separation technique for this biomolecule class. Anionic biomolecules, such as oligonucleotides and metabolites, have been analyzed using CZE for several years [29-33]. Despite this advantage, CZE-MS analysis of GAG oligosaccharides remains an under-developed approach. Much of the early GAG CZE literature focuses on normal mode polarity where a positive potential is applied



to the capillary [34-36]. Using normal polarity, CZE separation of chondroitin sulfate, hyaluronic acid, keratan sulfate, heparan sulfate, and heparin; ranging from disaccharide to oligosaccharide length (up to dp20) has been demonstrated [37]. However, normal polarity is not well suited to the acidic nature of highly sulfated GAGs and generally leads to longer migration times (except with specific electrolytes) and low resolution [35, 36, 38]. Most of this work has been performed with optical detection and structural features cannot be assigned without the use of standards. Replacement of UV-absorbance with MS detection is a logical progression; however, the electrolytes used during UV detection experiments are non-volatile and often incompatible with MS limiting the number of well understood electrolytes that can be employed [39-41].

The optimal CZE-MS configuration for GAG oligosaccharide analysis is reverse polarity with negative mode ionization. In reverse polarity CZE, a negative potential is applied to the capillary inlet, generating an electrophoretic force for negatively charged GAGs in the direction of the mass spectrometer. By using reverse polarity, the migration times of GAGs will decrease and the sample peaks become narrower, improving resolution. A recent application of CZE-MS to GAGs has used reverse polarity CZE and negative mode MS detection [42]. This work focused on disaccharides and demonstrated fast and complete separations. Researchers have started to tackle larger oligosaccharides, which retain structural information, in an attempt to solve specific biological problems [37] and investigate common pharmaceuticals [42].

In addition to the electrophoretic force (EF), ions are also subject to an electroosmotic force (EOF). The EOF is driven by the bulk movement of solvated counterions near the inner surface of the capillary. With a conventional bare fused silica (BFS) capillary, the inner surface of the capillary presents silanol groups to the solution within the capillary. At neutral pH, the silanol groups are ionized, resulting in a negatively charged static layer which attracts cations

from the background electrolyte (BGE) to create a positively charged mobile layer [43, 44]. With reverse polarity CZE in a BFS capillary, the EOF opposes the EF and results in longer migration times, or may cause some less ionized components to migrate away from the MS interface and not be detected. Modification of the surface of the fused silica capillary can alter its properties and either turn off EOF by creating a neutral surface or make a static positively-charged surface, which would produce an EOF that moves in the same direction as the EF, thus reduces the migration time of the analytes [45, 46]. Prior work used dynamic coatings to create a static positive charge at the inner surface [47, 48]. These are simple to implement, but the stability of such non-covalent coatings is an issue that can be improved upon.

The present work focuses on the separation and detection of GAG oligosaccharide mixtures using reverse polarity CZE-MS. We have examined neutral and cation coated separation capillaries, using covalent modifications that are durable and stable. These were tested and compared to BFS capillaries to optimize separation parameters for GAGs. Baseline characterization of each coating was performed with binary mixtures of typical modifications in GAGs. The optimized conditions were used to examine a complex mixture of GAG oligosaccharides with up to 12 saccharide subunits. Although demonstrated on a high resolution MS system, the described methodology is amenable to most MS instrumentation.

## **MATERIALS AND METHODS**

### *Materials*

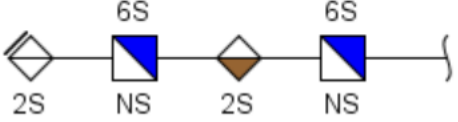
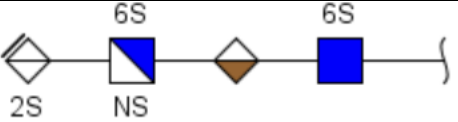
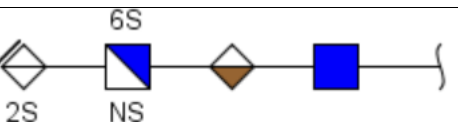
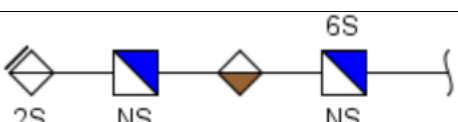
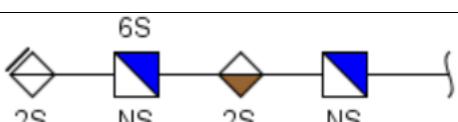
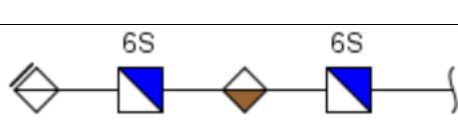
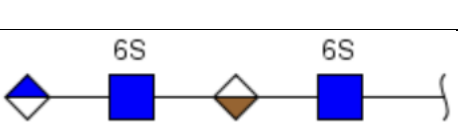
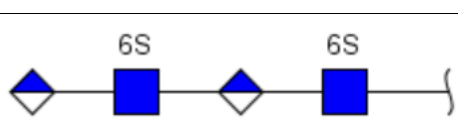
BFS capillaries (360  $\mu\text{m}$  o.d. x 50  $\mu\text{m}$  i.d.) were purchased from PolyMicro Technologies (Phoenix, AZ), and coated electrospray emitters (1.0 mm OD x 0.75 mm ID, E-BS-CC1-750-

1000-10 $\mu$ -B30) were obtained from CMP Scientific (Brooklyn, NY). Coating reagents, dichlorodimethylsilane (DMS, Sigma-Aldrich, St. Louis, MO) and N-(6-aminohexyl) aminomethyltriethoxysilane (AHS, Gelest, Morrisville, PA) were prepared in toluene. Ammonium acetate, formic acid, water, and methanol were of HPLC grade (Fisher Scientific, Hampton, NH). Diethylamine, sodium hydroxide, concentrated hydrofluoric acid (~48% wt), acetone, and toluene were purchased from Sigma-Aldrich (St. Louis, MO). All solutions were filtered with 0.45  $\mu$ m syringe filter (Millipore, Temecula, CA) before use.

### *GAG Standards*

GAG oligosaccharides were prepared by enzymatic depolymerization and purified using strong anion exchange high-pressure liquid chromatography (SAX-HPLC) for samples 1-6 as shown in Table 3.1 [49]. Epimer pair heparan sulfate tetrasaccharides (Table 3.1, samples 7 GlcA-GlcNAc6S-IdoA-GlcNAc6S (GI) and 8 GlcA-GlcNAc6S-GlcA-GlcNAc6S (GG)) were chemically synthesized and purified as described in the literature [50]. Low molecular weight heparin, Enoxaparin, was from the USP (Rockville, MD). All samples were desalted with a 3 kDa Amicon Ultra centrifugal filter (Millipore, Temecula, CA) prior to separation and mass spectrometry analysis. Although the GAGs are below 3kDa, heparan sulfate tetrasaccharides and larger chains do not pass through the 3kDa membrane. The membrane permeability is based on size and shape. GAGs have a linear structure compared to proteins that often have a globular structure, and the linear structure makes it behave as a higher molecular weight to the centrifugal filter membrane. Filters were conditioned with water, and the sample was then washed with two filter volumes of water ( $14,000 \times g$  for 25 min each). Before analysis, GAG samples were diluted to 5  $\mu$ g/mL in water.

**Table 3.1.** GAG tetrasaccharides used in this study

Tetrasaccharides	Structure Name	Molecular Weight (Da)	Structure
1	$\Delta$ UA2S-GlcNS6S- IdoA2S-GlcNS6S	1153.9427	
2	$\Delta$ UA2S-GlcNS6S- IdoA-GlcNAc6S	1036.0396	
3	$\Delta$ UA2S-GlcNS6S- IdoA-GlcNAc	914.0722	
4	$\Delta$ UA2S-GlcNS- IdoA-GlcNS6S	994.029	
5	$\Delta$ UA2S-GlcNS6S- IdoA2S-GlcNS	1073.9859	
6	$\Delta$ UA2S-GlcNS6S- IdoA-GlcNS6S	1073.9859	
7	GlcA-GlcNAc6S- IdoA-GlcNAc6S	936.1471	
8	GlcA-GlcNAc6S- GlcA-GlcNAc6S	936.1471	

## *Coatings*

Bare fused silica capillaries were etched with concentrated hydrofluoric acid (HF) at one end to reduce the outer diameter of the capillary for use in the sheath flow CE interface described below. For the etching process, the outlet of the capillary was placed in concentrated HF for 45-60 min. The capillary tip was then washed profusely with water. The etched capillaries were coated with AHS to render a cation coated capillary and DMS to generate a neutral coated capillary. Coating solutions were prepared in toluene with 1% concentration of either AHS or DMS. To clean and prepare for coating, the capillary was rinsed with 0.1 M NaOH, water, methanol, dry acetone, and dry toluene, respectively, for 30 min each. The capillary was then coated by flowing 1% AHS or DMS for 1 h. The capillary was consecutively flushed with dry toluene, dry acetone, and methanol for 30 min to remove excess coating solution. Finally, the capillary was equilibrated with background electrolyte buffer (BGE, 25 mM ammonium acetate 70% MeOH) for 1 h. Once degradation becomes apparent, BFS capillaries can be easily cleaned by flushing sodium hydroxide for a short time; however, the coatings are stripped in basic conditions and must be reapplied by repeating the coating procedure. In some experiments, 0.1-1% formic acid (FA) or 0.02-0.1% diethylamine (DEA) was added to the BGE.

## *Instrumentation*

Experiments were conducted on an Agilent HP 3D capillary electrophoresis instrument (Wilmington, DE). The total length of the capillary ranged from 52-54 cm, and its inner diameter was 50  $\mu\text{m}$  with a volume of approximately 1  $\mu\text{L}$ . The aqueous GAG sample was injected for 3 s at 950 mbar followed by a BGE injection for 10 s at 10 mbar. The injected volume was 0.1  $\mu\text{L}$ . The ionic strength of the injected sample plug is 2-3 orders of magnitude less than that of the

background electrolyte, so sample stacking is expected under these conditions and provides a sharp sample front. The capillary was then placed into a BGE vial for separation. A separation voltage of -30 kV was applied to the capillary for most experiments. A separation voltage of -15 kV was used for selected experiments as identified in the results below.

An EMASS-II (CMP Scientific, Brooklyn, NY) CE-MS interface was employed to couple the CE with a Thermo Scientific Velos Orbitrap Elite mass spectrometer (Bremen, Germany) [42, 51, 52]. The etched capillary outlet was nested inside of a cation coated glass emitter tip with a 30  $\mu\text{m}$  tip orifice (CMP Scientific, Brooklyn, NY). The etched capillary was positioned 0.3-0.5 mm from the tip of the emitter orifice to create a mixing volume of ca. 15 nL, and the emitter tip was filled with sheath liquid (SL, 25 mM ammonium acetate 70% MeOH). An external power supply provided a nano-electrospray (nESI) voltage ranging from -1.7 to -1.85 kV to the emitter. MS detection was performed in negative ion mode. Prior to CZE-MS experiments, a semi-automatic optimization of source parameters was performed using sucrose octasulfate to improve sensitivity of sulfated GAGs and reduce sulfate loss during MS analysis. The Orbitrap was scanned from  $m/z$  150-2000 for GAG oligosaccharides with a specified resolution of 120,000. Optimal conditions resulted when the S-lens RF level, multipole 00 offset, and lens 0 were set at 6 %, 7.20 V, and 8.50 V, respectively.

## RESULTS AND DISCUSSION

### *Coatings*

In capillary zone electrophoresis of mixtures, EF provides component separation due to differences in their mobilities. In contrast, EOF causes an analyte-independent migration of all

components. The magnitude and direction of the EOF with respect to the EF depends upon the chemical nature of the separation capillary's inner surface. In an uncoated BFS capillary, with a background electrolyte solution (BGE) of 25 mM ammonium acetate (pH=7.5) in 70% methanol, a static layer of negatively-charged silanol groups are presented at the inner wall of the capillary. These interact with the BGE to create a mobile layer of solvated positive ions. With reverse-polarity CZE, this mobile layer is attracted by the negative potential at the entrance of the separation capillary. This creates an EOF that opposes the EF for negatively charged analytes. In the case of highly-charged GAG oligosaccharide anions, the EF is greater than the EOF, so sample migrates toward the mass spectrometer interface. However, with EOF moving in the opposite direction, sample migration through the BFS capillary is slowed and results in increased migration times.

We have examined coated capillaries that eliminate the EOF, or reverse it so that it aligns with the EF to optimize the separation of GAG oligosaccharides. After optimization, migration time and peak widths are reduced while the peak capacity remains the same compared to prior work with BFS capillaries. Two different coatings, dichlorodimethylsilane (DMS) and N-(6-aminohexyl) aminomethyltriethoxysilane (AHS), were examined. Figure 3.1 compares the direction of EF and EOF for BFS, with that of capillaries with neutral (DMS) and cationic (AHS) coatings that were examined for this study.

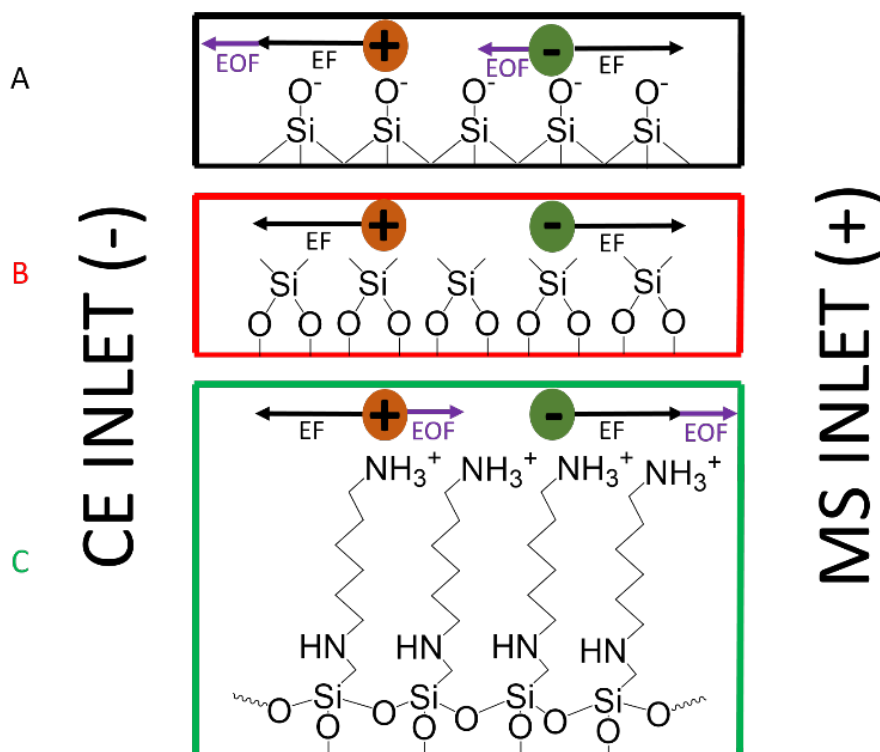


**Figure 3.1.** Diagram depicting the forces of electroosmotic flow (EOF) and electrophoretic forces (EF) that act on analytes during a CZE-MS experiment with three different inner capillary surfaces: (A) Bare fused silica (BFS), (B) DMS coated, and (C) AHS coated.

For DMS and AHS capillaries, the reagent forms a covalent ether linkage to silica at the surface of the inner wall of the capillary and produces a durable and stable layer. These fused silica surface modifications have been used by others for nanoparticle modification, protein immobilization supports, and other applications [53-55]. Non-covalent coating methods (also known as dynamic coating) are easier to implement than covalent coating, but the coating can dissociate from the inner surface over time. In our hands, when bovine serum albumin (BSA) is utilized as a non-covalent coating, a cation surface is produced on the inner surface of the capillary but is unstable over time and often leads to plug formation within the capillary as the



coating degrades. As shown in Figure 3.2, the covalently linked coatings are more durable than the BSA-coated capillaries. After 81 run iterations on a BSA capillary, degradation of the BSA coating caused plug formation and prevented further trials. The AHS and DMS coated capillaries are found to be quite stable, and the coating hydrolyzes slowly under the separation conditions with a very modest change in migration time from run to run. Furthermore, they do not lead to column plugging, and therefore can be refreshed by reapplication of the coating. In contrast, the BSA coated capillaries often become plugged by desorbed protein after several runs.

With a DMS-coated capillary, silanols are capped by neutral methyl groups. This eliminates the EOF in normal and reverse polarity and analytes migrate only under the influence of EF. For negatively-charged analytes under reverse-polarity conditions, the sample is expected to migrate through the capillary faster than in an uncoated BFS capillary. The AHS coated capillary will have an EOF that aligns with the EF for negatively-charged analytes in reverse-phase CZE and should exhibit even faster migration. Multiple amino silane reagents were considered, such as 3-aminopropyltriethoxysilane and N-(2-aminoethyl)-3-aminopropyltriethoxysilane. However, AHS was shown to be the most stable coating reagent because its chain length prevents hydrolysis by self-cyclization [53]. Short term durability tests demonstrated that covalent coatings are stable in optimized conditions (Figure 3.2), but long-term use showed signs of degradation in DMS coated capillaries. Both coatings degrade in high pH conditions ( $\text{pH} > 12$ ).

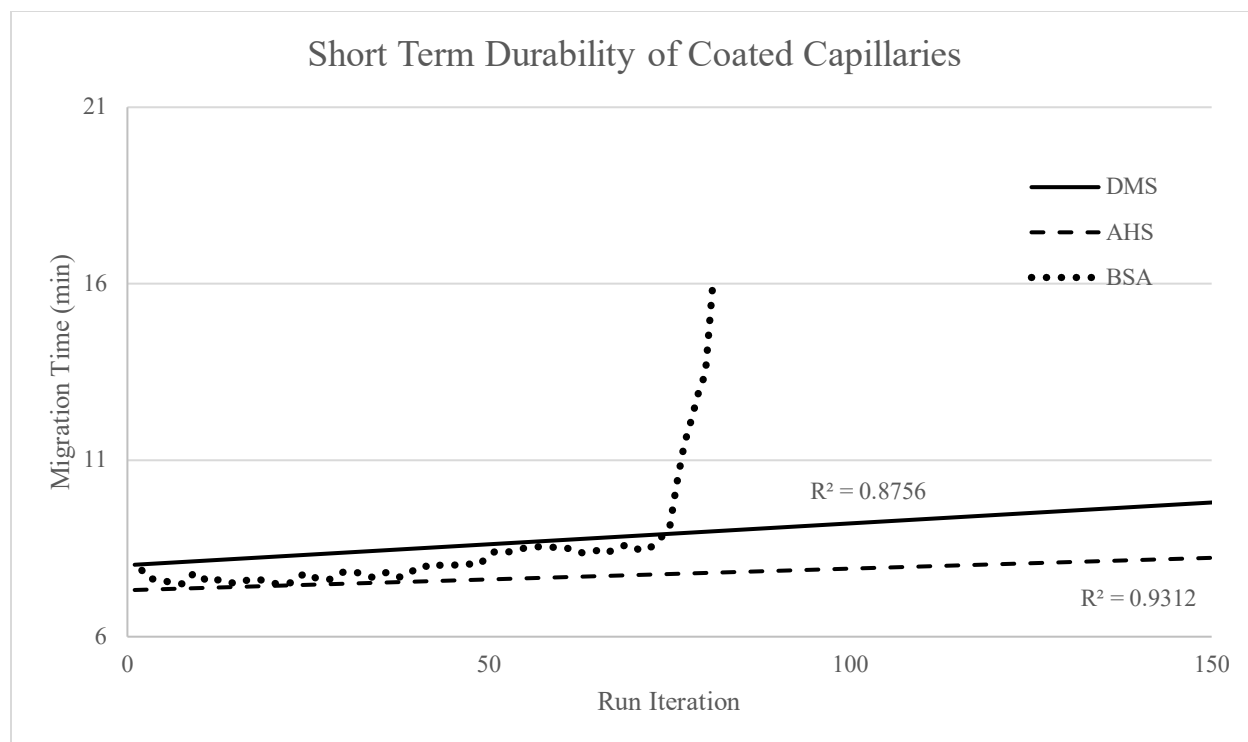


**Figure 3.2.** Short term durability of neutral (DMS, solid line) and cation (AHS, dashed line; BSA, circle dashed line) coated capillaries shown using sample 1 across 150 iterations. The BSA trial was terminated after 81 iterations due to coating failure.

### *CZE-MS of Tetrasaccharides*

Tetrasaccharide standards that contain common variations in GAG structure were used to test the efficacy of the coatings. A mixture of tetrasaccharides that differ in the number of sulfate modifications, ranging from 3 to 6 (samples 1-3), was analyzed first. Figure 3.3 compares the CZE migration profiles (base peak chromatogram) for this GAG tetrasaccharide mixture obtained with BFS, DMS, and AHS coatings on capillaries of similar length and identical experimental conditions. Sample 1 migrates through all of the capillaries first due to the higher number of sulfates present (six) compared to samples 2 and 3 with four and three sulfates, respectively. As expected from the EOF behavior described above, the compounds migrate most

rapidly with the AHS capillary and slowest with a BFS capillary. The peaks are narrowest with the AHS capillary, as longitudinal diffusion of a sample band increases linearly with its migration time. For sample 1, the peak widths at 50% peak height (FWHM) were 1.14, 0.49, and 0.2 min for BFS, DMS, and AHS capillaries, respectively. With a decrease in peak width, the sensitivity (limit of detection of 50 ng/mL) was improved using the AHS capillary and optimized experimental conditions. Shortened migration and reduced peak width were achieved with reverse polarity CZE on a cation coated capillary.

Next, compounds that contain single point variations in structure and produced mixtures of increasing separation difficulty were analyzed. Two GAG tetrasaccharides with different amino modifications, samples 4 and 2 (Table 3.1), were investigated. These tetrasaccharides have the same number of sulfate modifications, but one has an *N*-sulfo modification on the fourth residue; whereas, the other tetrasaccharide contains an *N*-acetyl group. Using reverse polarity CZE-MS on an AHS capillary, these tetrasaccharides are baseline separated in less than 20 min with approximately 2.5 min between the peaks. The FWHM for the peaks are 13.8 s (sample 4) and 15 s (sample 2). When compared with the DMS and BFS capillaries, the FWHM for the AHS capillary was reduced by a factor of two (DMS) or three (BFS). The two components of this mixture differ in composition by (*O*-sulfo + *N*-acetyl) versus (*OH* + *N*-sulfo), evidenced by the 42 Da difference in their mass spectra, shown in panels B and C of Figure 3.4.

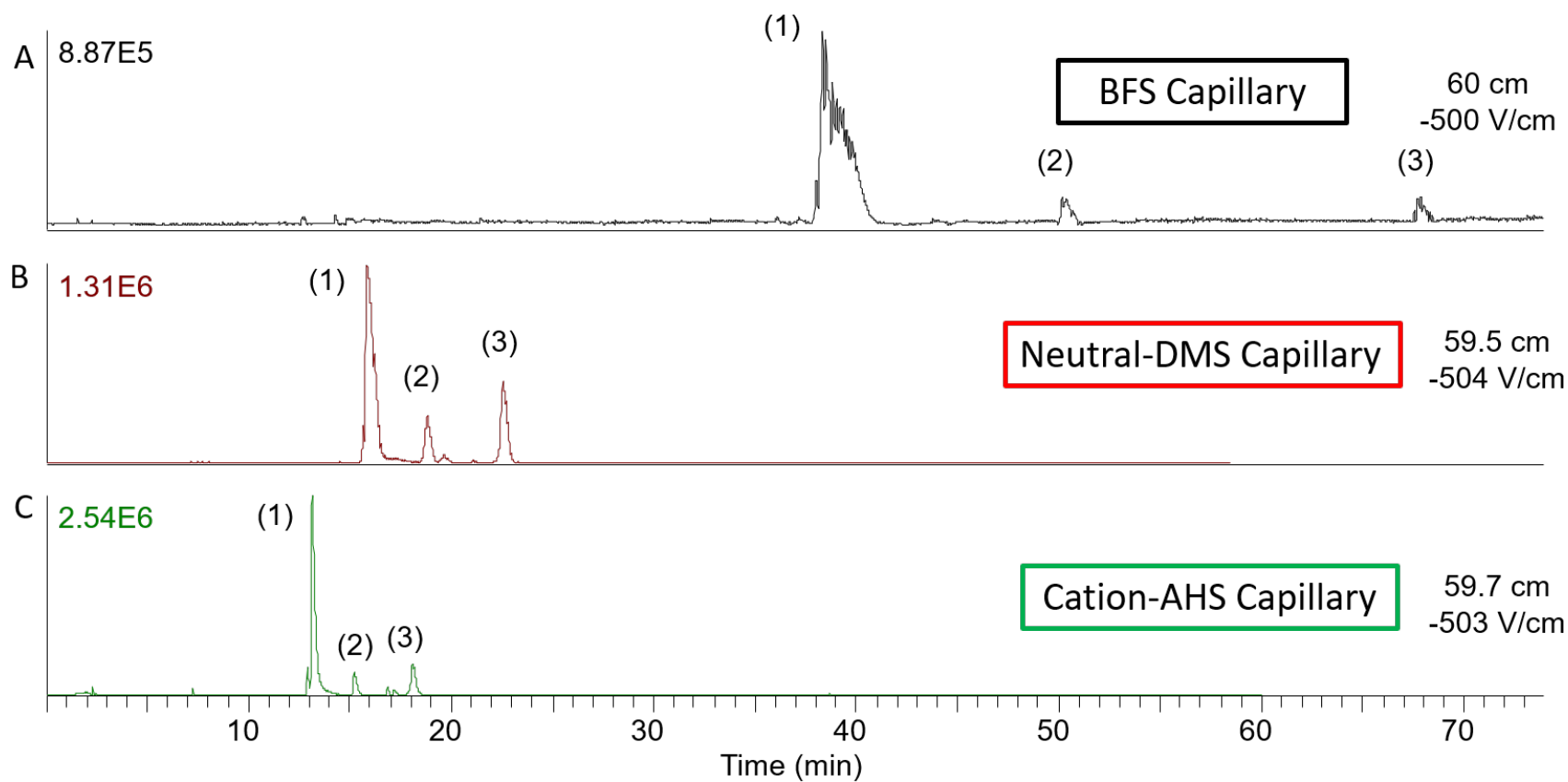


**Figure 3.3.** Electropherogram comparison of migration times based on different capillary coatings. Samples (1), (2), and (3) are tetrasaccharides with different numbers of sulfates. Sample (1) contains six sulfates, (2) has four sulfates, and (3) has three sulfates. Significant improvement in migration time and peak width is observed with neutral (DMS) and cation coated (AHS) capillaries.

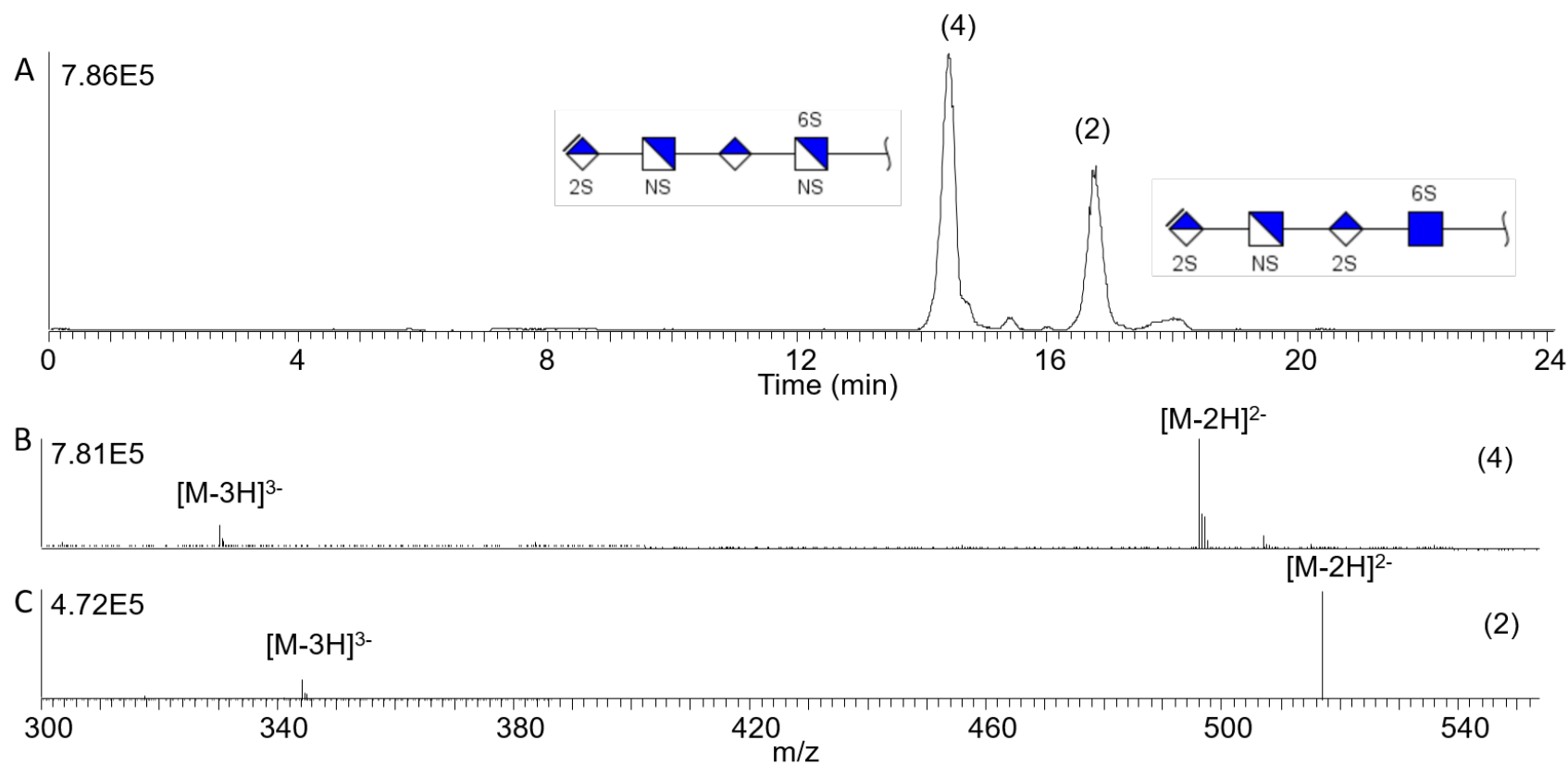


**Figure 3.4.** A) Baseline separation of tetrasaccharide mixture containing samples 4 and 2 with different amino modifications. Mass spectrum of sample 4 (B) and 2 (C) showing the mass difference due to amino modification.

A more challenging test are the isomeric tetrasaccharides, samples 5 and 6. The analyte structures are closely related and vary only in the position of one of the five sulfate modifications. Figure 3.5 shows the separation of this isomer pair (samples 5 and 6) using an AHS coated capillary, with baseline separation of the peaks. As these are positional isomers, their mass spectra are identical, and exhibit double, triply, and quadruply-charged molecular ions, as shown in the lower panel of Figure 3.5, for sample 5.

The most challenging analysis that often arises in GAG characterization using MS is the differentiation of stereoisomeric compounds arising from epimerization of uronic acids (GlcA vs. IdoA). We examined such a mixture of epimers, and the results are shown in Figure 3.6, for samples 7 (GI) and 8 (GG). These GAG tetrasaccharides vary only by the C-5 stereochemistry of the uronic acid near the reducing end. With reverse polarity CZE-MS on an AHS capillary, the two epimers are well separated. The early migrating peak, GI, exhibits a distinct shoulder. A similar result was found using differential ion mobility of these same compounds and was attributed to anomeric nature of the reducing end [56]. The rate of mutarotation of the anomeric carbon is slow compared to the migration time in CZE so this is a plausible cause of the extra peak in the sample. The lower panel in Figure 3.6 shows the mass spectrum of GI which is identical to that of GG (spectrum not shown). Since these are stereoisomers, all of the peaks in the electropherogram, including the shoulder, produce similar ESI mass spectra.

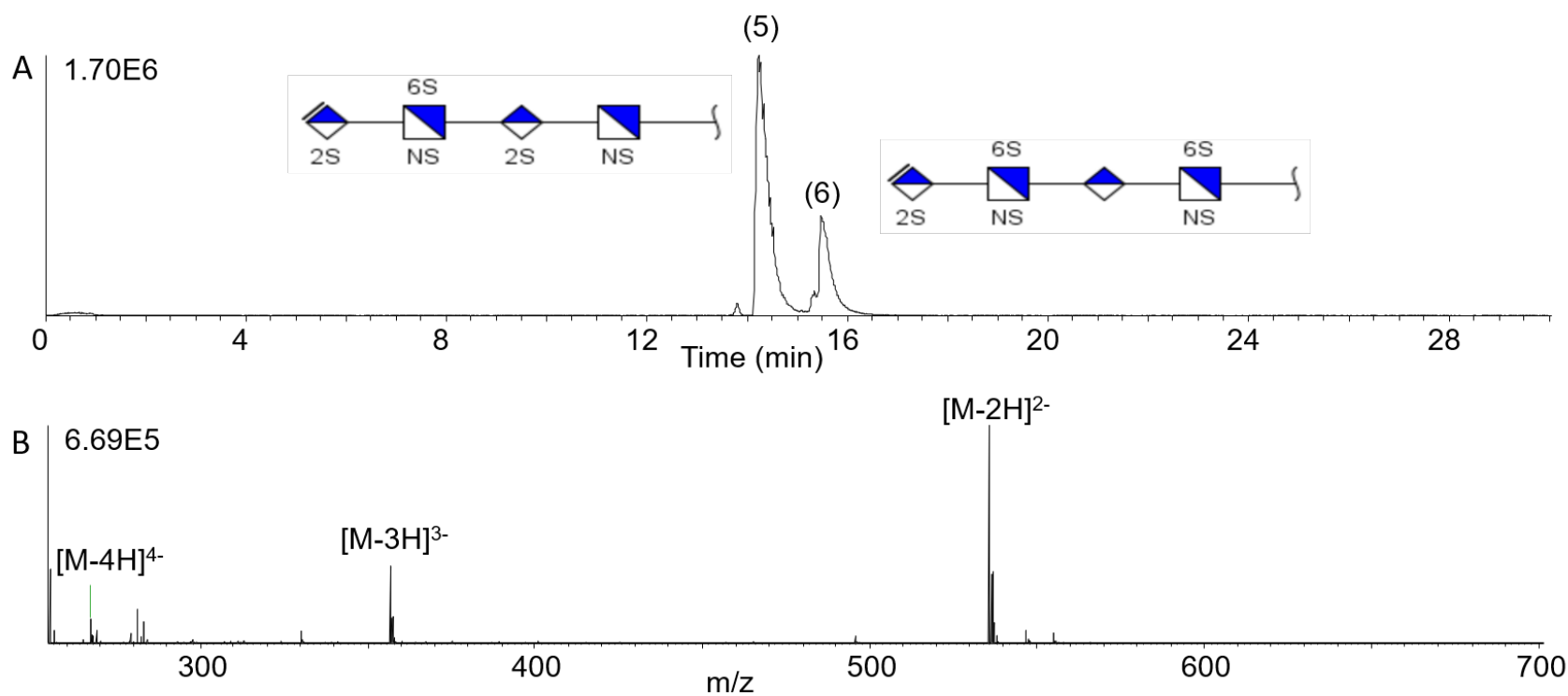


**Figure 3.5.** (A) Baseline CZE separation of a tetrasaccharide mixture on AHS capillary. Sample 5 and 6 are isomers with the same number of sulfate groups and exact mass, but differ in sulfate position on the last two sugar residues. (B) Mass spectrum of sample 5 demonstrating the observed charge state distribution.

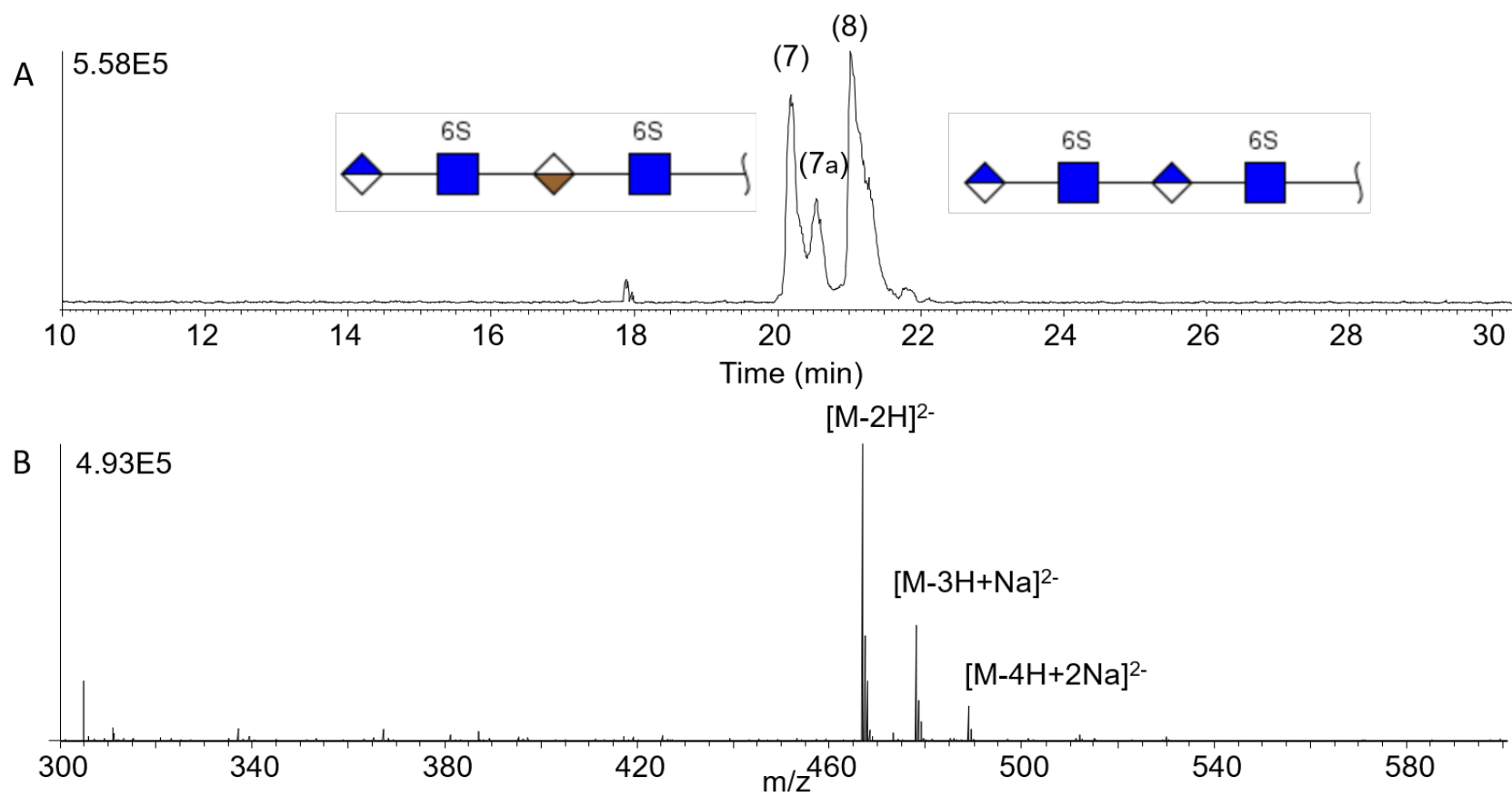


**Figure 3.6.** Baseline separation of a stereoisomer mixture (samples 7 and 8) on AHS capillary. Sample 7 migrates out first followed by sample 8. The shoulder peak labeled 7a is attributed to an anomeric form of sample 7.



### *CZE-MS of Enoxaparin (LMWH)*

Enoxaparin, a pharmaceutical product produced by alkaline depolymerization of heparin into low molecular weight components, was also analyzed using reverse polarity CZE and negative ion mode mass spectrometry. Others have analyzed Enoxaparin using on-line separations and mass spectrometry detection [14, 57-60]. This sample is known to be a complex mixture of oligosaccharides varying in degree of polymerization (dp) from dp 3 to dp 20. Figure 3.7A shows an ESI mass spectrum of the sample without any prior separation, demonstrating the innate complexity of this sample. Base peak electropherograms obtained using BFS, DMS, and AHS capillaries are shown Figure 3.7B. Enoxaparin migrates more quickly through the capillary on the cation coated capillary (AHS) compared to the neutral and uncoated capillaries.

Although the migration time decreases for the coated capillaries, peaks are not lost. The peaks become narrower when using coated capillaries, as shown previously with the tetrasaccharide mixtures, but they exhibit the same features as the BFS separation. This is a highly complex mixture, and we do not obtain baseline separation of all components. Nevertheless, the mass spectra obtained at any time point is highly simplified compared to the unseparated sample, and we can evaluate the components that are present. Oligosaccharides ranging from dp 3 to dp 12 were detected with a range of 4-17 sulfo groups present on the GAGs. The neutral masses extend from 753 to 3301 Da with less than 3.5 ppm error for the assigned compositions. Shorter oligosaccharides migrate through the capillary first and the GAG chain length increases over the migration period. The majority of the chains were dp 4 to dp 8 which is expected for the Enoxaparin mixture. Toward the end of the separation, dp 10 to dp 12 are observed in low intensity.

Sodium and ammonia adducts were also assigned for approximately half of the compositions. Sodium adducts are expected because Enoxaparin is manufactured as a sodium salt. The appearance of ammonia adducts can be explained by the choice of an ammonium acetate BGE. A supplemental list of all 83 unique compositions that were identified using the AHS capillary is included (Appendix A Supp. Table 1).

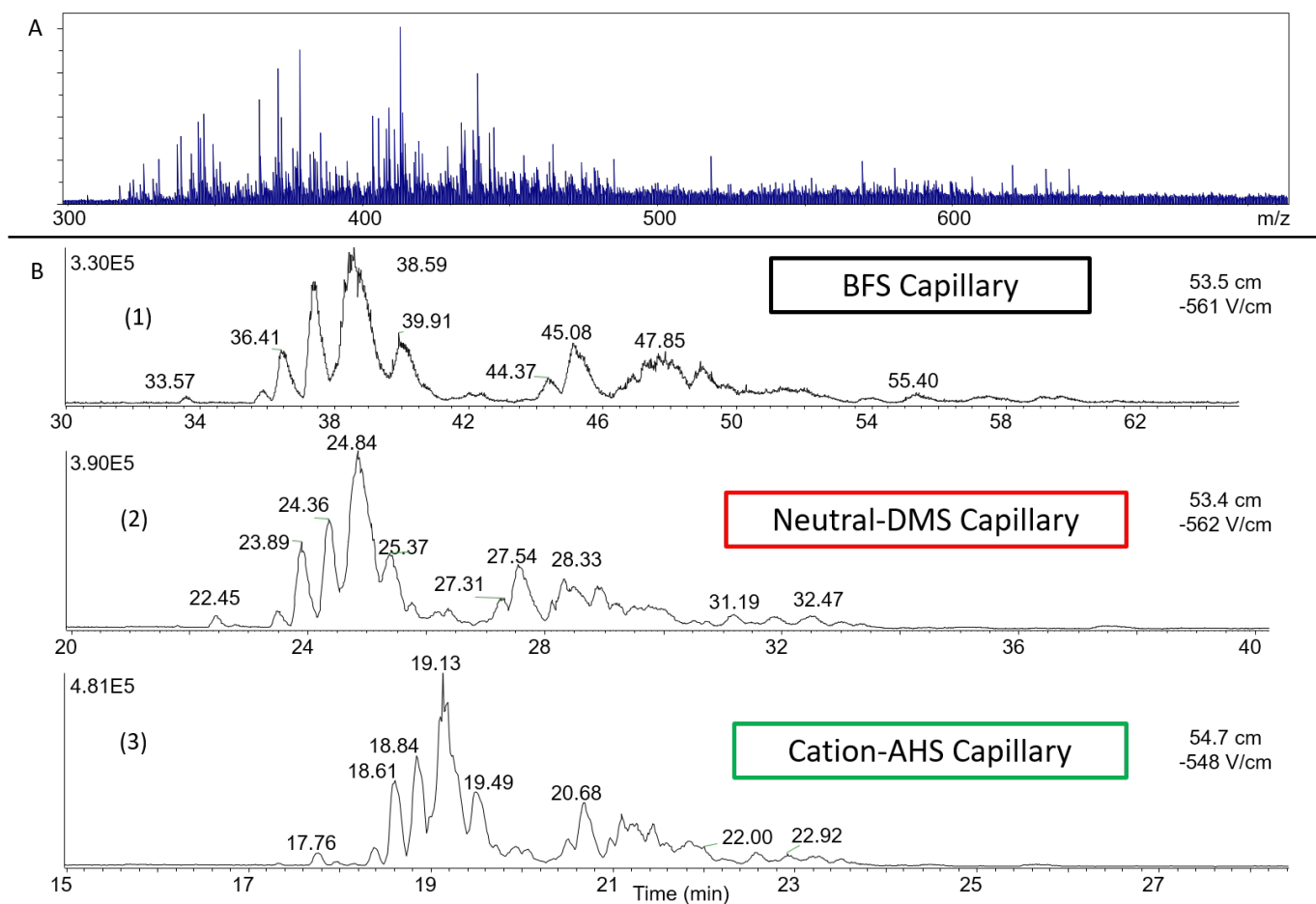


**Figure 3.7.** A) Mass spectrum of Enoxaparin (LMWH) without separation. B) Separation windows of Enoxaparin on uncoated and coated capillaries: (1) BFS (2) DMS, and (3) AHS with migration times decreasing from 1 to 3. The presented migration time window varies between panels 1-3 to enable comparison.

### *Additives for Separation*

While optimizing conditions for reverse polarity CZE with negative ionization mode MS, the use of background electrolyte solution (BGE) additives was explored. The role of pH can play a vital part in the extent of separation achieved based on the applied coating. EOF is directly influenced by the pH range of the BGE on capillaries that have a charge on the inner surface of the capillary. The neutral DMS capillary will not be affected by the pH of the BGE because the EOF is eliminated.

Formic acid (FA) and diethylamine (DEA) were used to adjust the pH to lower and higher values during separation, respectively. These reagents were selected for their volatility, which makes them compatible with on-line CZE-MS analysis. Acetic acid and formic acid were both tested as an additive to the BGE and sheath liquid. Using formic acid reduced the amount of background noise in the MS which improved the signal to noise ratio compared to acetic acid. Table 3.2 shows the effect of different BGE additives on the pH of the BGE. Without any additive, a BGE consisting of 25 mM ammonium acetate in 70% MeOH has a pH of 7.5. By adding FA to a concentration of 0.5%, the pH is reduced to 4.2. Conversely, with addition of 0.4 % DEA into the BGE, the pH increases to 10.1.

**Table 3.2.** Effect of BGE Additive on pH

BGE Additive	pH
0.5% FA	4.2
0.4% FA	4.3
0.3% FA	4.6
0.2% FA	4.8
0.1% FA	5.3
None	7.5
0.05% DEA	8.3
0.1% DEA	8.8
0.2% DEA	9.3
0.3% DEA	9.9
0.4% DEA	10.1
BGE: 25 mM ammonium acetate 70% MeOH	

For the AHS cation coated capillary, increasing the pH of the BGE reduces ionization of the modified surface of the capillary, reduces EOF, and results in longer migration times. In Figure 3.8, a mixture of tetrasaccharides containing an increasing number of sulfate groups, ranging from 3 to 6 sulfate groups (samples 1-3, and 6), is separated using 25 mM ammonium acetate in 70% MeOH with the addition of FA in the top electropherogram and DEA in the bottom electropherogram. The middle electropherogram is the separation in normal BGE without any pH adjustment. FA reduces the migration time and suppresses sodium adducts in the mass spectrum but does not affect the observed charge state. It also decreases the peak width in the electropherogram. The FWHM for sample 1 is reduced to 16 s using 0.1% FA compared to a FWHM of 22 s without any additive. In contrast, DEA increases migration times and the charge states of the ions of interest in the mass spectrum. As one would expect, DEA increases the peak width. For samples that migrate slower through the capillary, the peak widths increase. Peak broadening is diminished for samples that migrate faster through the capillary. Comparison of

sample 1 with or without DEA, the FWHM slightly increases from 21 to 22 s. However, for sample 2 and 3, the FWHM changed from 30 to 85.2 s and 22 to 28 s with the addition of 0.05% DEA, respectively. Overall, lower pH decreases migration time; while, higher pH increases migration time on an AHS cation coated capillary.

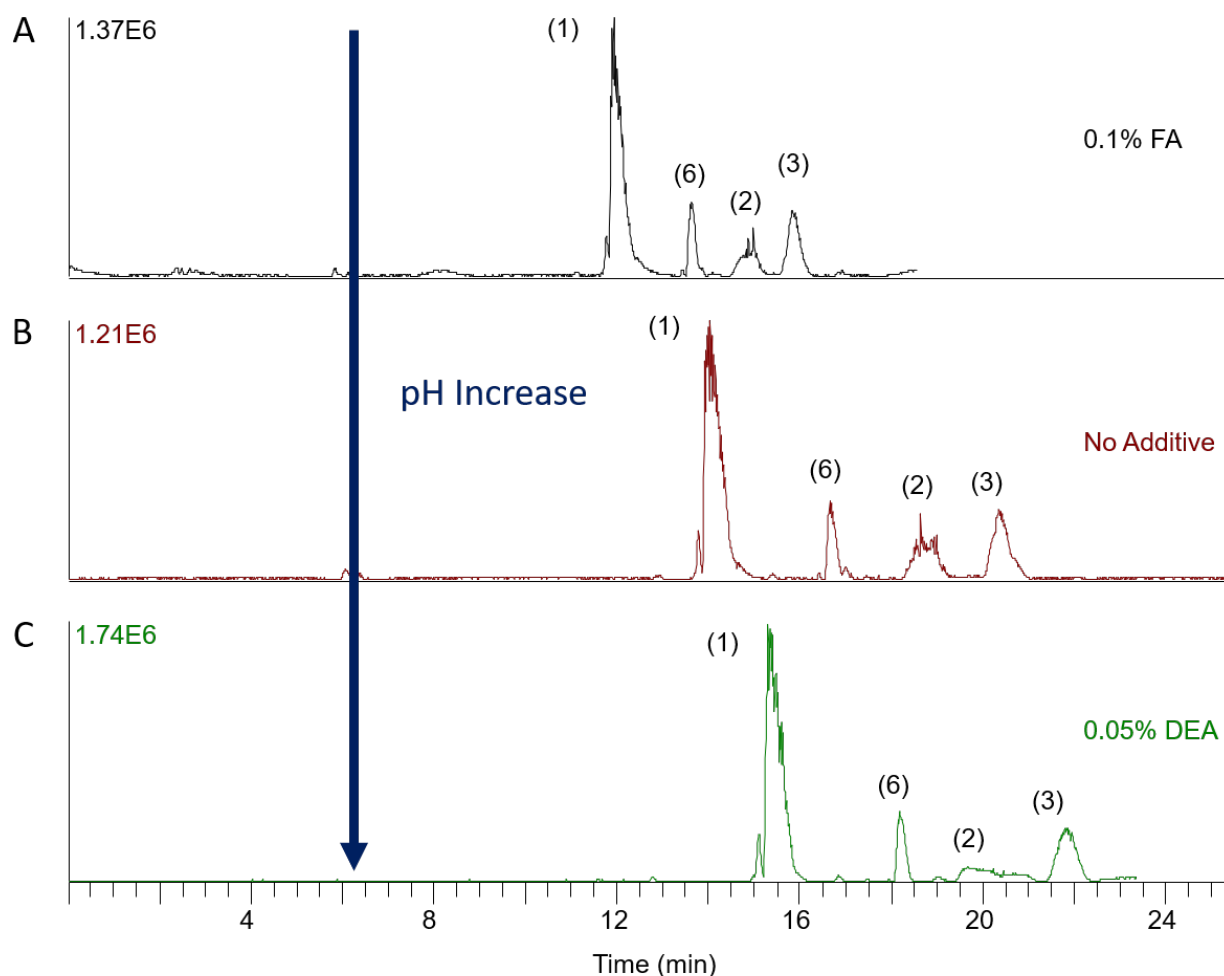


**Figure 3.8.** Effect of additives on four tetrasaccharide standards with an increasing number of sulfates (samples 1-3 and 6) through an AHS coated capillary. The pH of BGE in AHS coated capillaries modulates migration time. Lower pH, from addition of formic acid, leads to faster migration, and higher pH, from diethylamine, leads to slower migration.

## CONCLUSIONS

In this work, the advantages of using different coated capillaries with reverse polarity CZE-MS separations were demonstrated on oligosaccharide mixtures larger than disaccharides. Standard uncoated, neutral coated, and cation coated capillaries were investigated to determine

suitable CZE-MS conditions for sulfated glycosaminoglycans. Covalently coated capillaries were implemented through simple chemical reactions with silane reagents.

Using a cation coated capillary, structurally similar sulfated GAG oligosaccharides and complex mixtures were separated and analyzed with CZE-MS in a fast and reproducible manner. Positional isomers and stereoisomer tetrasaccharides were baseline separated. Although Enoxaparin was not baseline separated, the mass spectra were significantly simplified and would facilitate tandem mass spectrometry of the various components in this mixture. By incorporating a covalent cation coating, the migration time and peak widths were reduced while increasing the analytically useful lifetime of the separation capillary. Through the use of additives, the charge state distribution and migration time can be altered based on pH of the BGE. Future work will extend this method to incorporate tandem mass spectrometry for online sequence analysis of sulfated GAGs.

## **ACKNOWLEDGEMENTS**

The authors are grateful for generous financial support from the National Institutes of Health (R21HL136271 and P41GM103390). PS would like to acknowledge Jared Lamp (University of Notre Dame) for helpful discussions during manuscript preparation. The authors would like to acknowledge Geert Jan Boons (University of Georgia) and Deirdre Coombe (Curtin University) for previously provided samples utilized in this current study.



## REFERENCES

1. Varki, A., Biological roles of glycans. *Glycobiology* 2017, 27 (1), 3-49.
2. Afratis, N.; Gialeli, C.; Nikitovic, D.; Tsegenidis, T.; Karousou, E.; Theocharis, A. D.; Pavão, M. S.; Tzanakakis, G. N.; Karamanos, N. K., Glycosaminoglycans: key players in cancer cell biology and treatment. *FEBS Journal* 2012, 279 (7), 1177-1197.
3. Barbucci, R.; Magnani, A.; Lamponi, S.; Albanese, A., Chemistry and biology of glycosaminoglycans in blood coagulation. *Polym. Adv. Technol.* 1996, 7 (8), 675-685.
4. Sasisekharan, R.; Shriver, Z.; Venkataraman, G.; Narayanasami, U., Roles of heparan-sulphate glycosaminoglycans in cancer. *Nat. Rev. Cancer* 2002, 2 (7), 521.
5. Varki, A.; Cummings, R.; Esko, J.; Freeze, H.; Hart, G.; Marth, J., *Essentials of glycobiology*. Cold Spring Harbor Laboratory Press, New York 1998, (3rd edition).
6. Xiao, Z.; Zhao, W.; Yang, B.; Zhang, Z.; Guan, H.; Linhardt, R. J., Heparinase 1 selectivity for the 3,6-di-O-sulfo-2-deoxy-2-sulfamido- $\alpha$ -D-glucopyranose (1,4) 2-O-sulfo- $\alpha$ -L-idopyranosyluronic acid (GlcNS3S6S-IdoA2S) linkages. *Glycobiology* 2011, 21 (1), 13-22.
7. Wolff, J. J.; Laremore, T. N.; Busch, A. M.; Linhardt, R. J.; Amster, I. J., Electron detachment dissociation of dermatan sulfate oligosaccharides. *J Am Soc Mass Spectrom* 2008, 19 (2), 294-304.
8. Wolff, J. J.; Amster, I. J.; Chi, L.; Linhardt, R. J., Electron detachment dissociation of glycosaminoglycan tetrasaccharides. *J Am Soc Mass Spectrom* 2007, 18 (2), 234-44.
9. Leach, F. E., 3rd; Wolff, J. J.; Xiao, Z.; Ly, M.; Laremore, T. N.; Arungundram, S.; Al-Mafraji, K.; Venot, A.; Boons, G. J.; Linhardt, R. J.; Amster, I. J., Negative electron transfer dissociation Fourier transform mass spectrometry of glycosaminoglycan carbohydrates. *Eur. J. Mass Spectrom.* 2011, 17 (2), 167-76.

10. Laremore, T. N.; Leach, F. E.; Solakyildirim, K.; Amster, I. J.; Linhardt, R. J., Glycosaminoglycan characterization by electrospray ionization mass spectrometry including Fourier transform mass spectrometry. *Methods Enzymol.* 2010, 478, 79-108.
11. Bielik, A. M.; Zaia, J., Multistage tandem mass spectrometry of chondroitin sulfate and dermatan sulfate. *Int J Mass Spectrom* 2011, 305 (2-3), 131-137.
12. Zaia, J., Compositional analysis of glycosaminoglycans by electrospray mass spectrometry. *Anal. Chem.* 2001, 73 (2), 233-239.
13. Zaia, J., Tandem mass spectrometry of sulfated heparin-like glycosaminoglycan oligosaccharides. *Analytical chemistry* 2003, 75 (10), 2445.
14. Li, G.; Steppich, J.; Wang, Z.; Sun, Y.; Xue, C.; Linhardt, R. J.; Li, L., Bottom-Up Low Molecular Weight Heparin Analysis Using Liquid Chromatography-Fourier Transform Mass Spectrometry for Extensive Characterization. *Analytical Chemistry* 2014, 86 (13), 6626-6632.
15. Ly, M.; Leach, F. E.; Laremore, T. N.; Toida, T.; Amster, I. J.; Linhardt, R. J., The proteoglycan bikunin has a defined sequence. *Nat. Chem. Biol.* 2011, 7 (11), 827-833.
16. Li, L.; Zhang, F.; Zaia, J.; Linhardt, R. J., Top-down approach for the direct characterization of low molecular weight heparins using LC-FT-MS. *Anal Chem* 2012, 84 (20), 8822-9.
17. Chi, L.; Amster, J.; Linhardt, R. J., Mass Spectrometry for the Analysis of Highly Charged Sulfated Carbohydrates. *Current Analytical Chemistry* 2005, 1 (3), 223-240.
18. Laremore, T. N.; Zhang, F.; Dordick, J. S.; Liu, J.; Linhardt, R. J., Recent progress and applications in glycosaminoglycan and heparin research. *Curr. Opin. Chem. Biol.* 2009, 13 (5-6), 633-40.

19. Zaia, J., On-line separations combined with MS for analysis of glycosaminoglycans. *Mass Spectrom. Rev.* 2009, 28 (2), 254-72.
20. Volpi, N.; Galeotti, F.; Yang, B.; Linhardt, R. J., Analysis of glycosaminoglycan-derived, precolumn, 2-aminoacridone-labeled disaccharides with LC-fluorescence and LC-MS detection. *Nat. Protoc.* 2014, 9 (3), 541-558.
21. Huang, Y.; Shi, X.; Yu, X.; Leymarie, N.; Staples, G. O.; Yin, H.; Killeen, K.; Zaia, J., Improved liquid chromatography-MS/MS of heparan sulfate oligosaccharides via chip-based pulsed makeup flow. *Anal Chem* 2011, 83 (21), 8222-9.
22. Huang, R.; Liu, J.; Sharp, J. S., An approach for separation and complete structural sequencing of heparin/heparan sulfate-like oligosaccharides. *Anal Chem* 2013, 85 (12), 5787-95.
23. Zaia, J.; Khatri, K.; Klein, J.; Shao, C.; Sheng, Y.; Viner, R., Complete molecular weight profiling of low-molecular weight heparins using size exclusion chromatography-ion suppressor-high-resolution mass spectrometry. *Anal Chem* 2016, 88 (21), 10654-10660.
24. Gill, V. L.; Aich, U.; Rao, S.; Pohl, C.; Zaia, J., Disaccharide analysis of glycosaminoglycans using hydrophilic interaction chromatography and mass spectrometry. *Anal Chem* 2013, 85 (2), 1138-45.
25. Buszewski, B.; Noga, S., Hydrophilic interaction liquid chromatography (HILIC)—a powerful separation technique. *Anal. Bioanal. Chem.* 2012, 402 (1), 231-247.
26. Pereira, L., Porous graphitic carbon as a stationary phase in HPLC: theory and applications. *J. Liq. Chromatogr. Relat. Technol.* 2008, 31 (11-12), 1687-1731.
27. Ruhaak, L. R.; Deelder, A. M.; Wührer, M., Oligosaccharide analysis by graphitized carbon liquid chromatography-mass spectrometry. *Anal. Bioanal. Chem.* 2009, 394 (1), 163-74.

28. Karlsson, N. G.; Schulz, B. L.; Packer, N. H.; Whitelock, J. M., Use of graphitised carbon negative ion LC–MS to analyse enzymatically digested glycosaminoglycans. *Journal of Chromatography B* 2005, 824 (1), 139-147.
29. Durney, B. C.; Criefield, C. L.; Holland, L. A., Capillary electrophoresis applied to DNA: determining and harnessing sequence and structure to advance bioanalyses (2009–2014). *Anal. Bioanal. Chem.* 2015, 407 (23), 6923-6938.
30. Soga, T.; Igarashi, K.; Ito, C.; Mizobuchi, K.; Zimmermann, H.-P.; Tomita, M., Metabolomic profiling of anionic metabolites by capillary electrophoresis mass spectrometry. *Anal. Chem.* 2009, 81 (15), 6165-6174.
31. Hirayama, A.; Wakayama, M.; Soga, T., Metabolome analysis based on capillary electrophoresis-mass spectrometry. *Trends Anal. Chem.* 2014, 61 (Supplement C), 215-222.
32. Karabiber, F.; McGinnis, J. L.; Favorov, O. V.; Weeks, K. M., QuShape: Rapid, accurate, and best-practices quantification of nucleic acid probing information, resolved by capillary electrophoresis. *RNA* 2013, 19 (1), 63-73.
33. Heller, C.; Slater, G. W.; Mayer, P.; Dovichi, N.; Pinto, D.; Viovy, J.-L.; Drouin, G., Free-solution electrophoresis of DNA. *J. Chromatogr. A* 1998, 806 (1), 113-121.
34. Prabhakar, V.; Capila, I.; Sasisekharan, R., The structural elucidation of glycosaminoglycans. *Methods. Mol. Biol.* 2009, 534, 147-56.
35. Volpi, N.; Maccari, F.; Linhardt, R. J., Capillary electrophoresis of complex natural polysaccharides. *Electrophoresis* 2008, 29 (15), 3095-106.
36. Campa, C.; Coslovi, A.; Flamigni, A.; Rossi, M., Overview on advances in capillary electrophoresis-mass spectrometry of carbohydrates: a tabulated review. *Electrophoresis* 2006, 27 (11), 2027-50.

37. Zamfir, A. D., Applications of capillary electrophoresis electrospray ionization mass spectrometry in glycosaminoglycan analysis. *Electrophoresis* 2016, 37 (7-8), 973-86.
38. Sun, X.; Lin, L.; Liu, X.; Zhang, F.; Chi, L.; Xia, Q.; Linhardt, R. J., Capillary Electrophoresis–Mass Spectrometry for the Analysis of Heparin Oligosaccharides and Low Molecular Weight Heparin. *Analytical Chemistry* 2016, 88 (3), 1937-1943.
39. Ampofo, S. A.; Wang, H. M.; Linhardt, R. J., Disaccharide compositional analysis of heparin and heparan sulfate using capillary zone electrophoresis. *Anal. Biochem.* 1991, 199 (2), 249-255.
40. Mitropoulou, T. N.; Lamari, F.; Syrokou, A.; Hjerpe, A.; Karamanos, N. K., Identification of oligomeric domains within dermatan sulfate chains using differential enzymic treatments, derivatization with 2-aminoacridone and capillary electrophoresis. *Electrophoresis* 2001, 22 (12), 2458-2463.
41. Toida, T.; Linhardt, R. J., Detection of glycosaminoglycans as a copper (II) complex in capillary electrophoresis. *Electrophoresis* 1996, 17 (2), 341-346.
42. Lin, L.; Liu, X.; Zhang, F.; Chi, L.; Amster, I. J.; Leach, F. E.; Xia, Q.; Linhardt, R. J., Analysis of heparin oligosaccharides by capillary electrophoresis–negative-ion electrospray ionization mass spectrometry. *Analytical and Bioanalytical Chemistry* 2017, 409 (2), 411-420.
43. Shintani, H., Handbook of capillary electrophoresis applications. Springer Science & Business Media: 2012.
44. Kuhn, R.; Hoffstetter-Kuhn, S., Capillary electrophoresis: principles and practice. Springer Science & Business Media: 2013.
45. Whatley, H., Basic Principles and Modes of Capillary Electrophoresis. Humana Press: Totowa, NJ, 2001; p 21-58.

46. Grossman, P. D.; Colburn, J. C., *Capillary electrophoresis: Theory and practice*. Academic Press: 2012.
47. Man, Y.; Lv, X.; Iqbal, J.; Jia, F.; Xiao, P.; Hasan, M.; Li, Q.; Dai, R.; Geng, L.; Qing, H.; Deng, Y., Adsorptive BSA Coating Method for CE to Separate Basic Proteins. *Chromatographia* 2013, 76 (1), 59-65.
48. Chang, W. W.; Hobson, C.; Bomberger, D. C.; Schneider, L. V., Rapid separation of protein isoforms by capillary zone electrophoresis with new dynamic coatings. *Electrophoresis* 2005, 26 (11), 2179-2186.
49. Singh, A.; Kett, W. C.; Severin, I. C.; Agyekum, I.; Duan, J.; Amster, I. J.; Proudfoot, A. E. I.; Coombe, D. R.; Woods, R. J., The interaction of heparin tetrasaccharides with chemokine CCL5 is modulated by sulfation pattern and pH. *J. Biol. Chem.* 2015.
50. Arungundram, S.; Al-Mafraji, K.; Asong, J.; Leach, F. E.; Amster, I. J.; Venot, A.; Turnbull, J. E.; Boons, G.-J., Modular Synthesis of Heparan Sulfate Oligosaccharides for Structure-Activity Relationship Studies. *Journal of the American Chemical Society* 2009, 131 (47), 17394-17405.
51. Sun, L.; Zhu, G.; Zhao, Y.; Yan, X.; Mou, S.; Dovichi, N. J., Ultrasensitive and Fast Bottom-up Analysis of Femtogram Amounts of Complex Proteome Digests. *Angew. Chem., Int. Ed.* 2013, 52 (51), 13661-13664.
52. Sun, L.; Zhu, G.; Zhang, Z.; Mou, S.; Dovichi, N. J., Third-generation electrokinetically pumped sheath-flow nanospray interface with improved stability and sensitivity for automated capillary zone electrophoresis–mass spectrometry analysis of complex proteome digests. *J. Proteome Res.* 2015, 14 (5), 2312-2321.

53. Zhu, M.; Lerum, M. Z.; Chen, W., How to prepare reproducible, homogeneous, and hydrolytically stable aminosilane-derived layers on silica. *Langmuir* 2012, 28 (1), 416-23.
54. Liu, X.; Xing, J.; Guan, Y.; Shan, G.; Liu, H., Synthesis of amino-silane modified superparamagnetic silica supports and their use for protein immobilization. *Colloids Surf., A* 2004, 238 (1), 127-131.
55. Kneuer, C.; Sameti, M.; Haltner, E. G.; Schiestel, T.; Schirra, H.; Schmidt, H.; Lehr, C.-M., Silica nanoparticles modified with aminosilanes as carriers for plasmid DNA. *Int. J. Pharm.* 2000, 196 (2), 257-261.
56. Kailemia, M. J.; Park, M.; Kaplan, D. A.; Venot, A.; Boons, G.-J.; Li, L.; Linhardt, R. J.; Amster, I. J., High-field asymmetric-waveform ion mobility spectrometry and electron detachment dissociation of isobaric mixtures of glycosaminoglycans. *J. Am. Soc. Mass Spectrom.* 2014, 25 (2), 258-268.
57. Galeotti, F.; Volpi, N., Online Reverse Phase-High-Performance Liquid Chromatography-Fluorescence Detection-Electrospray Ionization-Mass Spectrometry Separation and Characterization of Heparan Sulfate, Heparin, and Low-Molecular Weight-Heparin Disaccharides Derivatized with 2-Aminoacridone. *Analytical Chemistry* 2011, 83 (17), 6770-6777.
58. Li, D.; Chi, L.; Jin, L.; Xu, X.; Du, X.; Ji, S.; Chi, L., Mapping of low molecular weight heparins using reversed phase ion pair liquid chromatography–mass spectrometry. *Carbohydr. Polym.* 2014, 99, 339-344.
59. Zaia, J.; Khatri, K.; Klein, J.; Shao, C.; Sheng, Y.; Viner, R., Complete Molecular Weight Profiling of Low-Molecular Weight Heparins Using Size Exclusion Chromatography-Ion

Suppressor-High-Resolution Mass Spectrometry. *Analytical Chemistry* 2016, 88 (21), 10654-10660.

60. Sun, X.; Sheng, A.; Liu, X.; Shi, F.; Jin, L.; Xie, S.; Zhang, F.; Linhardt, R. J.; Chi, L., Comprehensive Identification and Quantitation of Basic Building Blocks for Low-Molecular Weight Heparin. *Analytical Chemistry* 2016, 88 (15), 7738-7744.



## CHAPTER 4

### Structural Analysis of Urinary Glycosaminoglycans from Healthy Human Subjects

<sup>2</sup> Sanderson, P.; Ha, X.; Nesheiwat, S.; Lin, L.; Yu, Y.; Zhang, F.; Amster, I. J.; Linhardt, R. J., Structural Analysis of Urinary Glycosaminoglycans from Healthy Human Subjects. *Glycobiology* **2019**. Reprinted with permission of publisher.

## **ABSTRACT**

Urinary glycosaminoglycans (GAGs) can reflect the health condition of a human being, and the GAGs composition can be directly related to various diseases. In order to effectively utilize such information, a detailed understanding of urinary GAGs in healthy individuals can provide insight into the levels and structures of human urinary GAGs. In this study, urinary GAGs were collected and purified from healthy males and females of adults and young adults. The total creatinine-normalized urinary GAG content, molecular weight distribution, and disaccharide compositions were determined. Using capillary zone electrophoresis (CZE)-mass spectrometry (MS) and CZE-MS/MS relying on negative electron transfer dissociation (NETD), the major components of healthy human urinary GAGs were determined. The structures of ten GAG oligosaccharides representing the majority of human urinary GAGs were determined.

## INTRODUCTION

Urine is a biofluid generated by the kidneys that collects in the bladder and is then excreted through the urethra. Kidneys function as a blood filtration system in the human body. They excrete excess water and soluble metabolism byproducts from the bloodstream, such as nitrogenous waste from amino acid and nucleic acid metabolism (urea and uric acid), and creatinine from muscle metabolism [1, 2]. Kidneys also help our body maintain a stable internal environment by extracting glucose to regulate blood sugar levels, and by removing excess ions to maintain electrolyte (sodium, calcium, phosphorus, potassium, magnesium, chloride, bicarbonate, and phosphates) balance, and also removing toxins, hormones and other waste products from blood [1].

Since urine contains the majority of water soluble waste products from the human metabolism system and blood regulatory system, the chemical composition of these byproducts can provide valuable information indicative of human health. Modern clinic urinalysis is one of the most common medical diagnostic methods. The major target parameters of urinalysis include the amounts of ions and trace metals, proteins and enzymes, blood cells, and glucose. Among these analytes, glucose is a particularly important indicator of diabetes mellitus [3]. Recent developments in medical science have shown other diseases that can be diagnosed or monitored through the types and amount of urinary glycans. Mucopolysaccharidoses (MPSs), a group of lysosomal storage disorders caused by lack of enzymes for glycosaminoglycan (GAG) metabolism, are one such disease family identified through the presence of urinary GAGs [4, 5]. MPS results in a large increase of GAG concentration in the urine, such as heparan sulfate (HS) and keratan sulfate (KS) [6]. GAGs in this easily accessed biofluid can be used to detect and monitor kidney pathogenesis [7], bladder disease [8], and metastatic prostatic cancer [9, 10]. Urinary GAG analysis has been helpful in understanding glomerular-related disease [11],

interstitial cystitis [12], sepsis severity [13], and urinary tract infection [14]. In most of these pathologies there is a large increase in the concentration of urinary GAGs simplifying their analysis. However, in the urine of healthy individuals GAG levels are generally quite low ( $\mu\text{g/mL}$  levels) making their analysis quite difficult.

The total healthy human urinary GAGs have been quantified by various methods, including dimethylmethylene blue colorimetric dye-binding analysis [15, 16], by gel electrophoresis with silver staining [17, 18], by cetylpyridinium chloride (CPC) precipitation methods [19], and using ELISA kits for certain human GAGs [20]. Disaccharide analysis of human urinary GAGs has been studied by 2-aminoacridine (AMAC)-derivatized capillary electrophoresis-laser induced fluorescence (CE-LIF) [21, 22], and LC-MS/MS by multiple reaction monitoring (MRM) [23]. The results of these different measurements resulted similar conclusions that the amount of GAG in healthy human urine was relatively low ( $\mu\text{g/mL}$  levels) and showed a high individual variability. The observed differences in total GAG amount were not gender specific but varied somewhat based on an individual's age. The majority of urinary GAG were chondroitin sulfate (CS) (on average over 70%), followed by heparan sulfate (HS) (from 10%-30% based on detection method). Trace amounts of dermatan sulfate (DS) and hyaluronic acid (HA) were also reported.

However, because technical limitations, in the analysis of the small quantities of GAGs in the urine of healthy individuals little, if any, detailed structural analysis has been performed on urinary GAGs. Molecular weight distribution of urinary GAGs has been previously studied by electrophoresis. However, in most of the studies, GAGs from healthy human urine only functioned as a control to MPS or other disease affected patients' urine samples [24, 25]. Specifically, there has been no study of their molecular weight distributions, GAG compositions, or sequence of the GAGs present in healthy human urine detailed. A high-sensitivity, information-rich analytical

technique is required for such detailed structural analysis. Separation is also paramount to adequately investigate complex biological samples, such as urinary GAGs. High resolution SEC method can also achieve a robust separation efficiency and resolution [26]. Due to the highly ionic nature of sulfated GAGs, capillary zone electrophoresis (CZE) is ideally suited for separation of these molecules as it separates based on size, charge, and molecular shape [27-30]. Coupling CZE to mass spectrometry (MS) provides high sensitivity and selectivity for structural characterization of sulfated GAGs [31-35]. Decades of research has been performed on sulfated GAGs using various mass spectrometry fragmentation techniques [36-41]. In particular, electron based activation, such as electron detachment dissociation (EDD) and negative electron transfer dissociation (NETD), has provided more informative fragment ions to determine sequence coverage [36-40, 42, 43]. Combining NETD with online CZE-MS simplifies complex GAG samples and should provide sequence information for the GAG species present.

MPS and other disease related urinary GAGs have been extensively studied by various methods in the past several years, including LC-MS, CE-LIF, and other advanced analytical instrumentation [21, 22, 44]. But none of these studies have reported a profile of the GAGs present in healthy human urine. Furthermore, there have been no detailed structural and compositional studies on either the GAGs present in human urine from healthy individuals or MPS patients. Herein we report the first molecular weight compositional analysis on the urinary GAGs of healthy males and females isolated using gel permeation chromatography (GPC). HS and CS/DS components ranging from disaccharides to nonasaccharides are found with a range of sulfation patterns. The ten most abundant GAGs observed by CE-MS were fragmented using NETD MS/MS to determine modification location and structural assignments.

## EXPERIMENTAL

**Materials.** All chemicals and reagents were obtained from commercial sources and used as received unless otherwise specified. Health human urine samples from healthy males and six healthy females were purchased from BioreclamationIVT (Westbury, NY) (see Appendix B Supporting Information Table SI). No information on protection of human subjects was required for this study based on NIH guidelines, as unidentified biospecimens from living individuals obtained from a commercial provider are not considered human subjects research. Seventeen unsaturated HA, HS and CS disaccharide standards purchased from Iduron, Cheshire, UK. Actinase E was from KaKen Biochemicals (Tokyo, Japan). Recombinant *Flavobacterium heparinum* heparin lyases I, II, and III, and *Proteus vulgaris* chondroitin lyase ABC and keratinase 2 were expressed in *Escherichia coli* and purified in our laboratory as previously described. Keratinase 1 from *Pseudomonas sp.* was obtained from Sigma (St. Louis, MO). TSK gel 3000 SWxl and 4000 SWxl were from Tosoh Bioscience (King of Prussia, PA). BFS capillaries (360  $\mu\text{m}$  o.d.  $\times$  50  $\mu\text{m}$  i.d.) were purchased from PolyMicro Technologies (Phoenix, AZ), and coated electrospray emitters (1.0 mm OD  $\times$  0.75 mm ID, E-BS-CC1-750-1000–10  $\mu$ -B30) were obtained from CMP Scientific (Brooklyn, NY). Coating reagent *N*-(6-aminohexyl) aminomethyltriethoxysilane (AHS, Gelest, Morrisville, PA) was prepared in toluene and applied to the capillary as previously described [21]. Dialysis membranes were from Spectrum Chemical (New Brunswick, NJ).

## **Sample Preparation**

Urine samples were defrosted at 4°C and mixed well using a vortex mixer. 80 mL of each sample was used for GAG preparation. Small molecules and salts were removed by dialysis (molecular weight cut-off (MWCO) 150–500 Da) against distilled water and then freeze-dried to recover the crude GAGs. All lyophilized crude urinary GAGs were suspended in 10 mL of water, proteolyzed at 55 °C with 10 mg/mL actinase E for 24 h, and the mixture was then lyophilized. The lyophilized samples were dissolved in 5 mL of a solution of denaturing buffer (8 M urea containing 2 wt. % CHAPS), bound to a Vivapure Q Maxi H spin column, washed twice with 10 mL of denaturing buffer, and washed three-times with 10 mL of 0.2 M NaCl. The GAG components were then eluted from the spin column with three 10 mL volumes of 16% NaCl, and the salt in these fractions was removed by exhaustive dialysis (MWCO 500–1000 Da) against distilled water and freeze-dried to recover the purified GAGs.

## **Disaccharides Analysis**

Purified urinary GAGs (approximately 5 µg) were dissolved in 300 µL of digestion buffer (50 mM ammonium acetate, 2 mM calcium chloride). Recombinant heparin lyase I, II, and III; chondroitin lyase ABC; and keratanase I and II (10 mU of each enzyme) were then added to the reaction buffer and placed in a 37 °C incubator overnight. The disaccharides were recovered by passing through a 3000 Da MWCO spin column. The filter unit was washed twice with 200 µL of distilled water, and the combined fractions were finally lyophilized. The dried samples were labeled with 2-aminoacridone (AMAC) by adding 10 µL of 0.1 M 2-aminoacridone in dimethyl sulfoxide/acetic acid (17/3, v/v) incubating at RT for 10 min, followed by adding 10 µL of 1 M aqueous sodium cyanoborohydride and incubating for 1 h at 45 °C. The resulting samples were

centrifuged at 13,200 rpm for 20 min. Supernatant was collected and analyzed by HPLC-MS on an Agilent 1200 LC/MSD instrument (Agilent Technologies, Inc. Wilmington, DE) equipped with a 6300 ion-trap and a binary pump. The column used was a Poroshell 120 C18 column (3.0 × 50 mm, 2.7 μm, Agilent, USA) at 45 °C. Eluent A was 50 mM ammonium acetate solution, and eluent B was methanol. The mobile phase passed through the column at a flow rate of 250 μL/min with 10 min linear gradients of 10–35% solution B. The electrospray interface was set in negative ionization mode with a skimmer potential of –40.0 V, a capillary exit of –40.0 V, and a source temperature of 350 °C, to obtain the maximum abundance of the ions in a full-scan spectrum (300–850 Da). Nitrogen (8 L/min, 40 psi) was used as a drying and nebulizing gas.

#### **Molecular Weight Distribution of Urinary GAGs using Polyacrylamide Gel Electrophoresis (PAGE).**

PAGE was used to determine the molecular weight distribution of GAGs. The purified urinary GAGs were separated by a 15% total acrylamide, which containing 14.08% (w/v) acrylamide, 0.92% (w/v) *N,N*-methylene-bis-acrylamide, and 5% (w/v) sucrose. The acrylamide monomer solutions were prepared in resolving buffer (0.1 M boric acid, 0.1 M Tris, 0.01 M disodium EDTA, pH 8.3). Stacking gel monomer solution was prepared in resolving buffer, containing 4.75% (w/v) acrylamide and 0.25% (w/v) *N,N*-methylene- bis-acrylamide and the pH adjusted to 6.3 using HCl. A 10 cm × 7 mm diameter resolving gel column was cast from 4 mL of 15% resolving gel solution containing 4 μL of tetramethylethylenediamine and 12 μL of 10% ammonium persulfate. A stacking gel was cast from 1 mL of stacking gel monomer solution containing 1 μL of tetramethylethylenediamine and 30 μL of 10% ammonium persulfate. Phenol red dye was added to the sample for visualization of the ion front during electrophoresis. In each



lane, ~5 µg of sample was subjected to electrophoresis. A standard composed mixture of heparin oligosaccharides with known molecular weights was prepared enzymatically from bovine lung heparin [45]. The gel was visualized with alcian blue staining and then digitized with UN-Scan-it to estimate molecular weight.

### **Molecular Weight Distribution of Urinary GAGs using GPC.**

Oligosaccharides separated by size exclusion column (Tosoh Bioscience TSKgel G3000SWxl and TSKgel G4000SWxl columns) with online differential refraction detector. Mobile phase was 50 mM ammonium acetate at 0.5 mL/min. GAGs were extracted by performing dialysis and treatment with actinase E to remove proteins on a mini Q cation column. Recovered GAGs were subjected to gel permeation chromatography (GPC) to obtain low molecular weight oligosaccharides before reconstituting in water for CZE-MS analysis.

### **CZE-MS/MS of Oligosaccharides.**

CZE separations were performed on an Agilent HP 3D CE instrument using a cation-coated capillary with a -30 kV potential applied. Ammonium acetate (25 mM in 70% methanol) was used as the background electrolyte and sheath liquid to provide reproducible separations and optimal spray stability. Conditions and parameters were consistent with previously reported literature used for purified GAG standards [21]. Samples were injected for 9 s at 950 mbar followed by a BGE injection for 10 s at 10 mbar.

An EMASS-II (CMP Scientific, Brooklyn, NY) CE-MS interface was employed to couple the CE with a Thermo Scientific Velos Orbitrap Elite mass spectrometer (Bremen, Germany) [46, 47]. The etched capillary outlet was nested inside of a cation coated glass emitter tip with a 30 µm

tip orifice. The etched capillary was positioned 0.3–0.5 mm from the tip of the emitter orifice to create a mixing volume of ~15 nL which was filled with sheath liquid. Nano-electrospray ionization (nESI) voltage was applied by an external power supply ranging from –1.85 to –1.9 kV to the emitter.

MS detection was performed in negative-ion mode, and multiply deprotonated anions were observed for each species. Sucrose octasulfate was utilized prior to CZE-MS experiments to perform a semi-automatic optimization of source parameters. This improved sensitivity of sulfated GAGs and decreased sulfate loss during MS analysis. The Orbitrap was scanned from  $m/z$  150–2000 for GAG oligosaccharides with a specified resolution of 120,000 for MS and MS/MS experiments. Tandem mass spectrometry experiments were performed using negative electron transfer dissociation (NETD) MS/MS with fluoranthene as the reagent cation for activation. Mass selection of the precursors occurred in the dual linear ion trap. Activation with fluoranthene for doubly and triply charged precursors was ~125 ms and ~50 ms, respectively. Each peak from the electropherogram was averaged to obtain a tandem mass spectrum with mass accuracy of 10 ppm or better. Data analysis was performed using Glycoworkbench [48] and in-lab developed software [49]. Fragments were assigned based on the Domon-Costello nomenclature [50].

## **RESULTS AND DISCUSSION**

### **Isolation and quantification of total GAGs in human urine**

Two sets of healthy male and female donors were selected, six young adults (23-25 years of age) and adults (35-45 years of age) (Appendix B Table SI). Samples were first dialyzed using controlled pore dialysis membranes (MWCO 150-500 Da and 500-1000 Da) to remove salt, urea, and other small molecules in the urine samples without loss of GAGs or GAG oligosaccharides.

After digestion with actinase E to degrade proteins/peptides, urinary GAGs were purified through strong anion exchange Vivapure Q Maxi H spin column.

Total GAG amounts for each urine sample were measured by disaccharide analysis based on carbazole assay and MS-MRM. The results were normalized based on creatinine concentration to normalize the hydration levels of the individual donors (Appendix B Table SII). The values determined by carbazole assay showed a higher level of variation (including negative concentrations) due to the interference of this colorimetric assay due to urine color. Thus, the total GAG present as determined by GAG disaccharide analysis based on MRM-MS was used to compound GAG content, which ranged from 7-70  $\mu\text{g/mL}$  (Figure 4.1A). MRM-MS analysis showed the total GAG was comprised solely of HS and CS/DS with no HA or KS observed. When samples from males and females were compared (Figure 4.1B), on average female urine showed higher levels of heparan sulfate than male urine at 75.7% as compared to 68.1%, respectively. In contrast male urine showed higher average composition of CS than female urine, 31% as compared to 24%, respectively. Both sexes, however, displayed a smaller percentage of urinary CS than HS. Despite the differences in average values, these differences were not significant. Since an individual's age can have an impact on excreted GAGs [51], we split the urine samples into two sets, M1-3\*/F1-3\* (young adults) and M1-3/F1-3 (adults) and compared the percentage of HS and CS in these two groups. Based on age, the urine from young adults showed a higher average percentage of HS and a lower average percentage of CS than their adult urine counterparts (Figure 4.1C). These differences, based on an individual's age, were just barely significant.

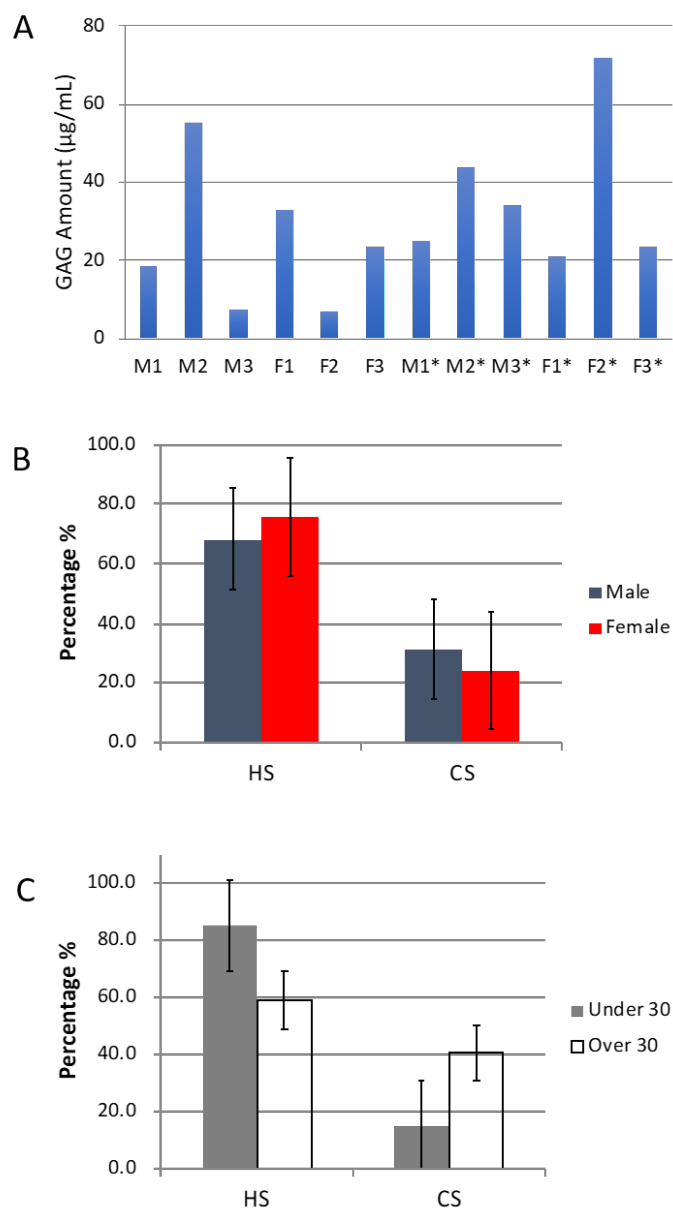


**Figure 4.1.** Analysis of total GAG content of human urine samples. A. Total GAG amount in urine sample determined through disaccharide analysis using MRM and normalized based on creatinine levels. B. Comparison of HS and CS composition differences by gender in urine samples obtained from healthy male and female volunteers. C. Comparison of HS and CS composition differences by age in urine samples obtained from young adults (23-25 y) and adults (35-45 y).

### **Disaccharide compositional analysis of GAGs in healthy human urine.**

The disaccharide composition of the HS and CS in each sample following enzymatic depolymerization was next determined (Table 4.1 and Table SIII, Appendix B). These data show that 0S was the most abundant disaccharide in the urinary HS of both males and females and in both age groups. After 0S, both male and female samples showed decreasing amounts of NS, NS2S, 6S and NS6S and TriS, respectively. Again it should be noted that the urine from females had higher average amounts of HS disaccharides than the urine from males. The HS disaccharide composition of the urine from young adults showed a higher percentage of 0S than that from the adult group. There was less uniformity between the sexes in the disaccharide composition of CS. Female urine showed higher percentages 4S and 6S of CS disaccharides. CS of urine from young adults showed higher levels of 4S than from the urine of adults, this trend was also reflected in 4S6S, 2S4S and TriS CS disaccharides. This observation is consistent with an understanding that cartilage (comprised primarily of chondroitin 6S) breakdown increases with an individual's age [52]. In both age groups, 4S showed the highest levels, followed by 6S. There is a general higher sulfation level in the CS from urine samples obtained from adults compared to young adults. This is also consistent with the increased sulfation of cartilage CS with age [53]. The high level of variability in the disaccharide composition in individuals makes it difficult to draw strong conclusions as to the overall significance of these observed differences.

**Table 4.1.** HS and CS compositional analysis.

HS disaccharide composition (mole %)								
Disaccharide	TriS	NS6S	NS2S	NS	2S6S	6S	2S	0S
Range (mg/mL)	0-0.35	0.11-2.66	0.14-3.06	0.37-6.47	0-0.02	0.16-2.64	0-0.21	2.94-30.57
Mean (mg/mL)	0.14	0.68	0.91	2.39	0	0.92	0.05	13.17
Std. dev.	0.11	0.83	0.80	1.90	0.01	0.71	0.06	9.58
CS disaccharide composition (mole %)								
Disaccharide	TriS	2S4S	2S6S	4S6S	4S	6S	2S	0S
Range (mg/mL)	0-2.28	0.13-2.14	0.08-0.85	0.12-4.01	3.37-27.36	0.54-13.96	0.01-1.52	0.22-2.86
Mean (mg/mL)	0.20	0.73	0.42	1.21	11.46	2.85	0.27	1.12
Std. dev.	0.66	0.59	0.27	1.10	8.51	3.75	0.42	0.93

### **Molecular weight determination of urinary GAGS.**

The molecular weight properties of the 12 urinary GAG samples were next examined by electrophoresis on 15% polyacrylamide gels (Figures 4.2A & B). These gels qualitatively show similar molecular distributions for all 12 samples that can be broken into three major components, high molecular weight (top third of each lane above the degree of polymerization (dp)~20 standard), intermediate molecular weight (middle third at the dp~20 standard) and low molecular weight (lower third at and below the dp~10 standard). Nearly all of the urine samples shows a band between the dp~20 and dp~10 bands. The sharpness and relative intensity of this band suggests that it may not be a GAG or GAG oligosaccharide but rather a highly charged metabolite (such as sulfated steroids) or xenobiotic generally present in urine. Two representative samples, M2\* and F2\*, containing sufficiently high levels of GAGs for analytical and preparative GPC, were used to more quantitatively examine molecular weight distributions by gel permeation chromatography (GPC) using refractive index detection and are shown in Figure 4.2C. The high molecular weight components are shown in the void volume by the small peak at 17-20 min. The intermediate molecular weight components at 25-32 min, corresponding to the size of heparin ( $MW_{avg}$  19 kDa), can be observed as a small broad peak. The low molecular weight components at 33-40 min, corresponding to (or smaller than) a low molecular weight heparin ( $MW_{avg}$  4-5 kDa) can be observed as a large broad peak. These major low molecular weight components were analyzed by CZE-MS/MS.

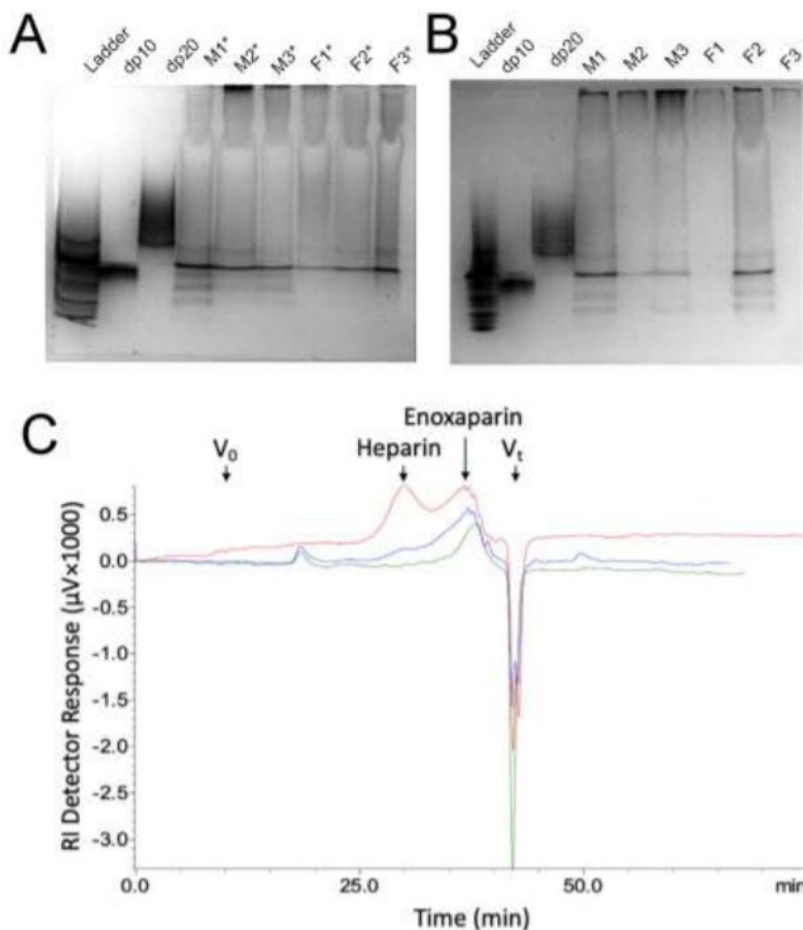


**Figure 4.2.** Molecular weight distribution of human urinary GAGs. A. & B. show PAGE results on 15% gel stained with alcian blue and imaged with Biorad gel imaging software. Samples were from young adults (M1\*, M2\*, M3\*, F1\*, F2\*, F3\*) in gel A and samples from young adults (M1, M2, M3, F1, F2, F3) in gel B. Standards run in each gel include a ladder of oligosaccharides prepared from the partial digestion of bovine lung heparin [45]. The dp~10 (MWavg 3,325) and dp~20 (MWavg 6,650) standards were prepared by fractionating bovine lung heparin oligosaccharides by low pressure GPC [45]. C. Shows the GPC analysis using refractive index detection of two urine samples M2\* (blue trace) and F2\* (black trace). A mixture of unfractionated heparin (MWavg 19,000) and enoxaparin (a low molecular weight heparin, MWavg 4,500) are shown as standards (red trace).



### **CZE-MS Analysis of low molecular weight human urinary GAGs.**

The high sensitivity of CZE-MS allows detection and separation of GAGs at low concentrations to determine various GAG compositions in urine. The low molecular weight components (MW < 5 kDa) recovered by GPC from two of the urine samples, M2\* and F2\*, were analyzed using CZE-MS/MS. After reconstituting these low molecular weight GAG components from the GPC fractions in 30  $\mu$ L of water they were separated by CZE-MS. A variety of compositions were determined by extracting the m/z and charge of the ions and using in-lab automated software developed for assignment [49].

The majority of the species identified in the M2\* and F2\* samples were similar, with GAG chains ranging in size from dp 2-9 containing both HS and CS/DS components (Figure 4.3). The M2\* sample was at a higher concentration and resulted in detection of 81 different compositions while the lower amount of the F2\* contained only 28 compositions. The variability between the compositions comprising the M2\* and F2\* samples is shown in Figure 4.3A. Pentasaccharides were the most abundant chain lengths with 17 different compositions for M2\* and 7 for F2\*. Urine is a complex biological sample with a multitude of GAGs present. Thus, after composition analysis, each GAG precursor was manually interrogated to determine the number of isomers present in the samples (Figure 4.3B). As expected based on the compositional information, the number of isomers was higher for M2\* (158) than for F2\* (60) sample with dp 4-6 representing the largest number of isomers present for both sexes. The composition and isomer components are provided in the supplemental material (Table SIV, Appendix B).

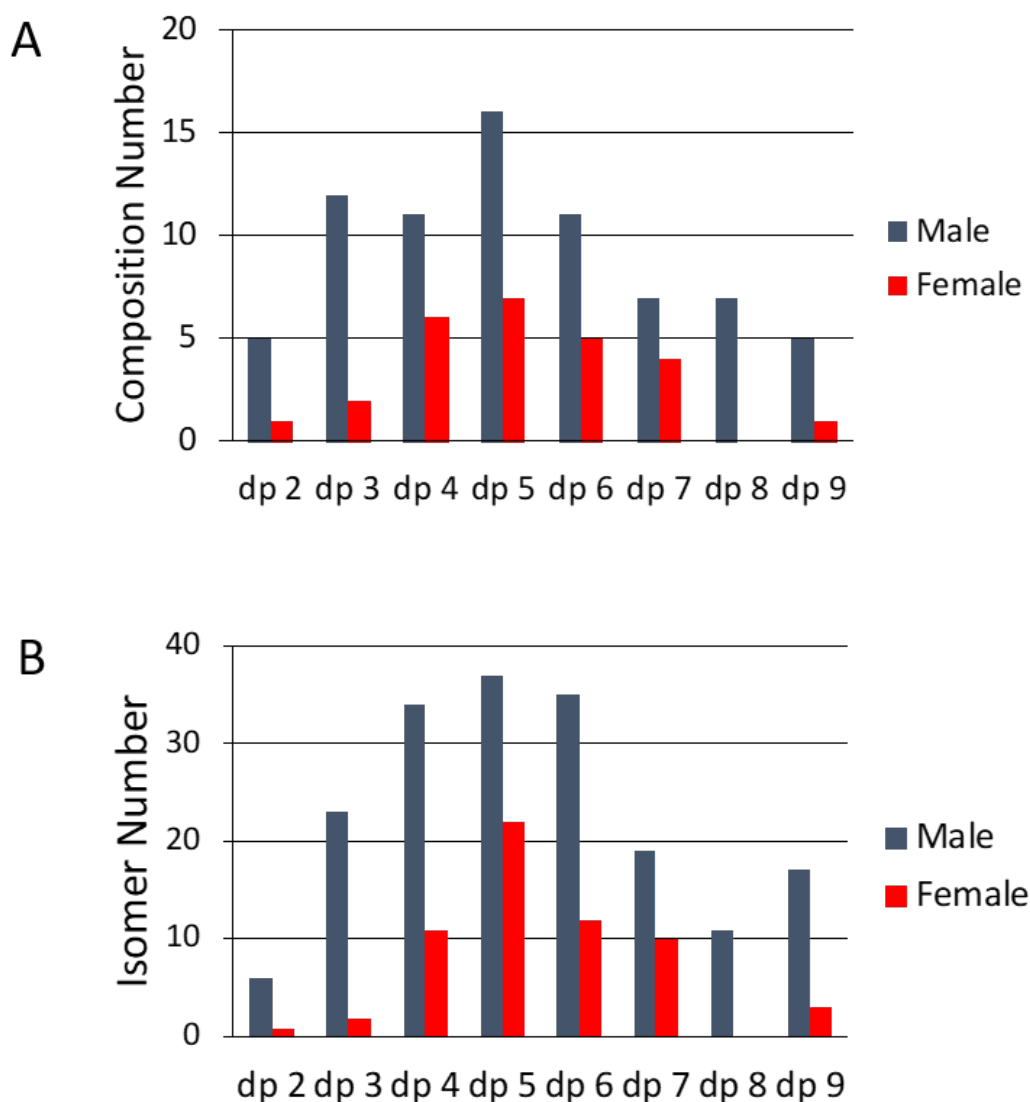


**Figure 4.3.** Comparison of the sulfated GAGs recovered from urine coming from a healthy, young adult male (M2\*) and female (F2\*) individual. A. Composition matches of varying chain lengths containing both HS and CS/DS. B. Amount of isomers detected for each degree of polymerization.

Of particular interest are the structures found in peaks 1, 3, 4 and 5 (Figure 4.4) as these suggest the presence of an unsaturated (-18 amu)  $\Delta$ UA residue at the non-reducing end of these four HS oligosaccharides. Such  $\Delta$ UA residues are commonly observed on the treatment of GAGs with a microbial polysaccharide lyase but such enzymes are not found in mammals [54]. A heparin lyase has been isolated from the human colonic bacterium, *Bacillus stercoris* [55], suggesting that these HS oligosaccharides might have a dietary source.

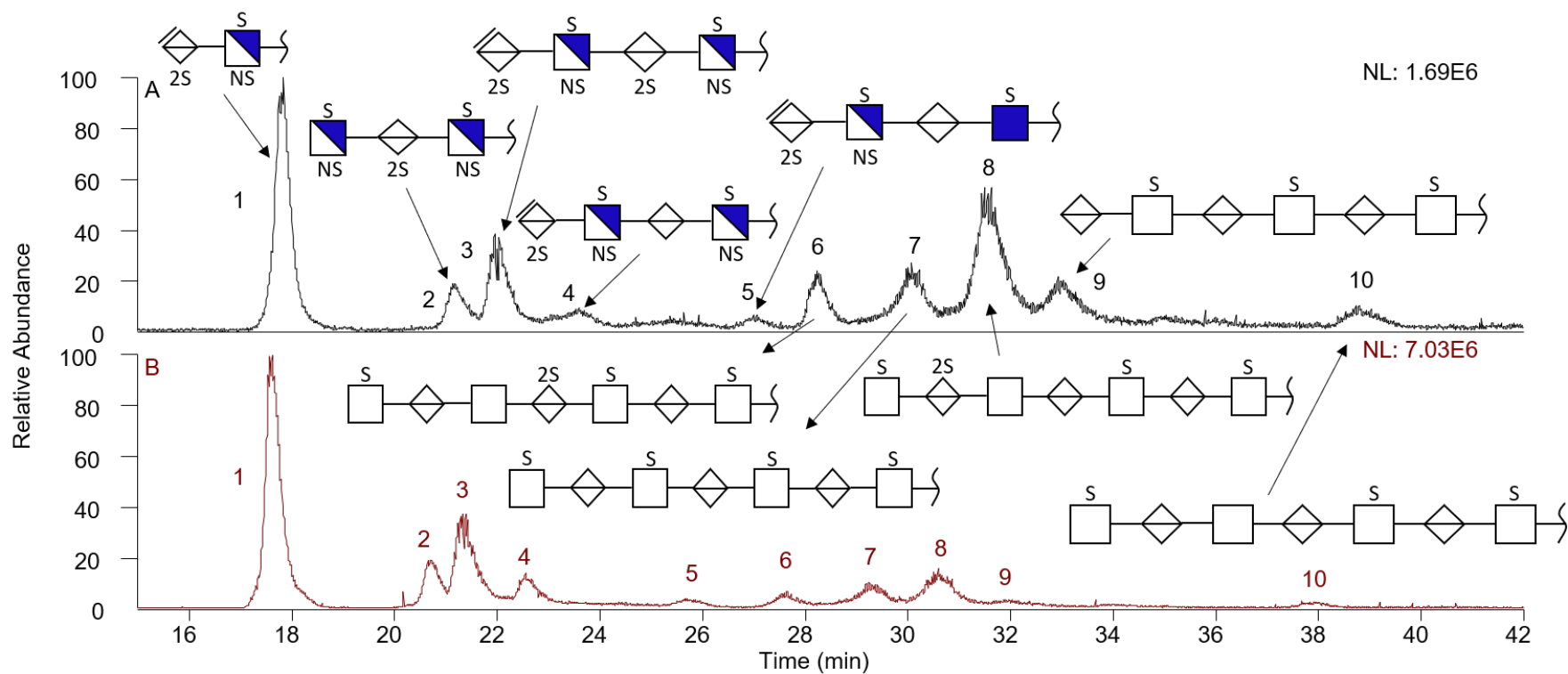


**Figure 4.4.** Extracted ion electropherograms (EIEs) from the CE-MS analysis of the ten most abundant GAG oligosaccharides recovered from the urine of healthy, young adult donors. A. EIE of the major low molecular weight GAGs recovered from the urine of a female donor, F2\*. B. EIE of the major low molecular weight GAGs recovered from the urine of a male donor, M2\*. Structures were determined using NETD MS/MS (as shown in Figure 4.5) are the same for both sexes designated by the peak number.

### CZE-MS/MS analysis of low molecular weight human urinary GAGs.

Further investigation into the sample relied on online tandem mass spectrometry experiments. By combining negative electron transfer dissociation (NETD) experiments with CZE-MS, the top ten most abundant species in both the M2\* and F2\* samples were structurally analyzed. The CZE separations are shown in their extracted ion electropherograms (EIEs) (Figure 4.4). The EIEs of both samples are strikingly similar showing the same set of peaks at similar relative intensities but the M2\* with a higher concentration showed higher abundance of GAGs when using the same conditions and injection volumes. The ten most abundant GAG precursor mass values extracted from the low molecular weight GAGs from F2\* (Figure 4.4A) and M2\* (Figure 4.4B) urine are identified. The structures provided were determined using NETD MS/MS, and they are the same for both sexes designated by the peak number.

The NETD mass spectrum of a trisaccharide containing five sulfo groups is displayed in Figure 4.5. This HS trisaccharide is the second GAG to migrate through the capillary (peak 2, Figure 4.5, A&B). The averaged NETD MS/MS spectrum is from M2\* at 20.89 minutes, but the corresponding F2\* peak 2 mass spectrum looks similar. Fragment ions are depicted using the Domon-Costello nomenclature. Glycosidic cleavages are the most abundant fragments aside from the neutral losses. The glycosidic cleavages in addition to the mass of the precursor enable assignment of the *N*-sulfo modification on the hexosamine residues. In addition, the glycosidic cleavages indicate the hexosamine residues have two sulfo groups with the uronic acid containing a single sulfo group. While it is not possible to determine the stereochemistry of *C*-5 on the acidic sugar, is represented by a white diamond with the sulfate located at the 2-*O* position. There are three cross ring assignments represented by red boxes ( $^{1,5}\text{X}_2$ ,  $^{2,5}\text{X}_2$ , and  $^{0,2}\text{A}_3$ ). The cross ring assignments occur on the hexosamines, but do not distinguish between 6-*O* and 3-*O* sulfation on

these residues. Thus, the sulfo groups might be in either the 3-*O* or 6-*O* position are represented as “S” on the structure in Figure 5. The structure based on human HS biosynthesis most likely corresponding to GlcNS6S (1→4) IdoA2S (1→4) GlcNS6S. The remaining GAG species from F2\* and M2\* and their associated MS/MS spectra fragment lists can be found in the supplemental section (Table SIV, Appendix B).



From the fragmentation patterns, it was possible to identify which residues contain sites of modification, such as sulfation or *N*-acetylation, for each polysaccharide. Additionally, separation and characterization of positional isomers was accomplished on dp7 carbohydrates with three different sulfation patterns (Figure 4A & 4B, peaks 6-8). The five peaks that migrate through the capillary first appear to potentially be HS species based on the number of sulfo modifications in addition to the presence of abundant of *N*-sulfation. The latter five species appear to be CS/DS based on the moderate sulfation patterns (one per disaccharide) and number of *N*-acetyl groups present. However, this is not confirmed at this time so the hexosamines are presented by white squares if they do not contain *N*-sulfation. Further analysis will required to more completely to delineate these structures.

Although it was not possible to distinguish between 6-*O* from 3-*O* sulfation for HS (and the 4-*O* from the 6-*O* sulfation for CS/DS), the number of sulfo modifications on sugar residues was determined for 10 sulfated GAGs. The most abundant GAG species found in both samples was a disaccharide with three sulfo modifications. Overall, the abundance was higher for M2\* compared to F2\*, but both samples had similar profiles and compositions for the 10 most abundant GAGs. The variation in the number of compositions and isomers could be a result of the concentration difference between the samples.

## CONCLUSIONS

A detailed structural and compositional GAGs profile of healthy urinary GAGs has been reported in this study. Urinary GAGs collected and purified from individuals of different age (young adults under 30 and adults over 30) and from males and females were analyzed in this work. The total creatinine-normalized GAG concentrations ranged from 7-70 µg/mL. HS was the



most prominent urinary GAG followed by CS and no HA and KS were detected. Disaccharide compositional analysis based on LC-MS MRM showed that OS is the predominant HS disaccharide and 4S was the predominant CS disaccharide. Molecular weight analysis suggested the presence of intact GAGs as well as GAG oligosaccharides with the majority of urinary GAGs being oligosaccharides of chain sizes from dp 2-20. Urine from males had slightly more CS and urine samples collected from people young adults have a higher percentage HS. The CZE-MS/MS analysis of urinary GAG oligosaccharides from two samples for urine collected from a healthy young adult male and female gave similar profiles having the same 10 most abundant GAG oligosaccharides. Interestingly, four of these oligosaccharides contain  $\Delta$ UA residues at their non-reducing end suggesting they might originate from dietary sources. Since this study examines only a relatively small number of non-diverse individuals who are not controlled for diet, hydration level, nor individually evaluated for health, the results presented do not define the ‘normal’ ranges of GAG concentration and structure but instead represent only typical values in healthy individuals. Additional well-controlled clinical studies will be required to set ‘normal’ ranges of GAG concentration and structure.

## **ACKNOWLEDGEMENTS**

The authors gratefully acknowledge generous financial support from the National Institutes of Health, grants CA231074, DK111958, HL136271, and GM103390.

## REFERENCES

1. Bouatra, S.; Aziat, F.; Mandal, R.; Guo, A. C.; Wilson, M. R.; Knox, C.; Bjorndahl, T. C.; Krishnamurthy, R.; Saleem, F.; Liu, P., The human urine metabolome. *PloS one* 2013, 8 (9), e73076.
2. Echeverry, G.; Hortin, G. L.; Rai, A. J., Introduction to urinalysis: historical perspectives and clinical application. In *the Urinary Proteome*, Springer: 2010; pp 1-12.
3. Armstrong, J., Urinalysis in Western culture: a brief history. *Kidney international* 2007, 71 (5), 384-387.
4. Coutinho, M. F.; Lacerda, L.; Alves, S., Glycosaminoglycan storage disorders: a review. *Biochemistry research international* 2012, 2012.
5. Lehman, T. J.; Miller, N.; Norquist, B.; Underhill, L.; Keutzer, J., Diagnosis of the mucopolysaccharidoses. *Rheumatology* 2011, 50 (suppl\_5), v41-v48.
6. Spranger, J. W.; Brill, P. W.; Hall, C.; Superti-Furga, A.; Unger, S., Bone dysplasias: an atlas of genetic disorders of skeletal development. Oxford University Press, USA: 2018.
7. Gatto, F.; Maruzzo, M.; Magro, C.; Basso, U.; Nielsen, J., Prognostic value of plasma and urine glycosaminoglycan scores in clear cell renal cell carcinoma. *Frontiers in oncology* 2016, 6, 253.
8. Atahan, Ö.; Kayigil, Ö.; Hizel, N.; Yavuz, Ö.; Metin, A., Urinary glycosaminoglycan excretion in bladder carcinoma. *Scandinavian journal of urology and nephrology* 1996, 30 (3), 173-177.

9. De Klerk, D.; Werely, C., Urinary glycosaminoglycan excretion in metastatic prostate cancer. *World Journal of Urology* 1986, 4 (4), 200-204.
10. Egidi, M.; Guelfi, G.; Cochetti, G.; Poli, G.; Barillaro, F.; Zampini, D., Characterization of kallireins and microRNAs in urine sediment for the discrimination of prostate cancer from benign prostatic hyperplasia. *J. Cancer Sci. Ther* 2015, 7 (4).
11. Wiggins, J. E.; Goyal, M.; Wharram, B. L.; Wiggins, R. C., Antioxidant ceruloplasmin is expressed by glomerular parietal epithelial cells and secreted into urine in association with glomerular aging and high-calorie diet. *Journal of the American Society of Nephrology* 2006, 17 (5), 1382-1387.
12. Lose, G.; Fransden, B., Subcutaneous heparin in the treatment of interstitial cystitis. In *Interstitial Cystitis*, Springer: 1990; pp 153-156.
13. Zhang, X.; Han, X.; Xia, K.; Xu, Y.; Yang, Y.; Oshima, K.; Haeger, S. M.; Perez, M. J.; McMurtry, S. A.; Hippensteel, J. A., Circulating heparin oligosaccharides rapidly target the hippocampus in sepsis, potentially impacting cognitive functions. *Proceedings of the National Academy of Sciences* 2019, 116 (19), 9208-9213.
14. Taganna, J.; de Boer, A. R.; Wuhrer, M.; Bouckaert, J., Glycosylation changes as important factors for the susceptibility to urinary tract infection. Portland Press Ltd.: 2011.
15. Alonso-Fernández, J.; Fidalgo, J.; Colon, C., Neonatal screening for mucopolysaccharidoses by determination of glycosaminoglycans in the eluate of urine-impregnated paper: preliminary results of an improved DMB-based procedure. *Journal of clinical laboratory analysis* 2010, 24 (3), 149-153.

16. Dave, M.; Chawla, P.; Dherai, A.; Ashavaid, T., Urinary Glycosaminoglycan Estimation as a Routine Clinical Service. *Indian Journal of Clinical Biochemistry* 2015, 30 (3), 293-297.
17. Mu, A. K.-W.; Lim, B.-K.; Hashim, O. H.; Shuib, A. S., Detection of differential levels of proteins in the urine of patients with endometrial cancer: Analysis using two-dimensional gel electrophoresis and O-glycan binding lectin. *International journal of molecular sciences* 2012, 13 (8), 9489-9501.
18. Al-Hakim, A.; Linhardt, R. J., Electrophoresis and detection of nanogram quantities of exogenous and endogenous glycosaminoglycans in biological fluids. *Applied and theoretical electrophoresis: the official journal of the International Electrophoresis Society* 1991, 1 (6), 305-312.
19. Gallegos-Arreola, M. P.; Machorro-Lazo, M. V.; Flores-Martínez, S. E.; Zúñiga-González, G. M.; Figuera, L. E.; González-Noriega, A.; Sánchez-Corona, J., Urinary glycosaminoglycan excretion in healthy subjects and in patients with mucopolysaccharidoses. *Archives of medical research* 2000, 31 (5), 505-510.
20. Mashima, R.; Sakai, E.; Tanaka, M.; Kosuga, M.; Okuyama, T., The levels of urinary glycosaminoglycans of patients with attenuated and severe type of mucopolysaccharidosis II determined by liquid chromatography-tandem mass spectrometry. *Molecular genetics and metabolism reports* 2016, 7, 87-91.
21. Sanderson, P.; Stickney, M.; Leach, F. E.; Xia, Q.; Yu, Y.; Zhang, F.; Linhardt, R. J.; Amster, I. J., Heparin/heparan sulfate analysis by covalently modified reverse polarity capillary zone electrophoresis-mass spectrometry. *Journal of Chromatography A* 2018, 1545, 75-83.

22. Chang, Y.; Yang, B.; Weyers, A.; Linhardt, R. J., Capillary electrophoresis for the analysis of glycosaminoglycan-derived disaccharides. In *Capillary Electrophoresis of Biomolecules*, Springer: 2013; pp 67-77.
23. Sun, X.; Li, L.; Overdier, K. H.; Ammons, L. A.; Douglas, I. S.; Burlew, C. C.; Zhang, F.; Schmidt, E. P.; Chi, L.; Linhardt, R. J., Analysis of total human urinary glycosaminoglycan disaccharides by liquid chromatography–tandem mass spectrometry. *Anal. Chem.* 2015, 87 (12), 6220-6227.
24. Tanyalcin, M. T., Urinary Glycosaminoglycan Electrophoresis With Optimized Keratan Sulfate Separation Using Peltier System for the Screening of Mucopolysaccharidoses. *Journal of Inborn Errors of Metabolism and Screening* 2015, 3, 2326409815613805.
25. Maccari, F.; Gheduzzi, D.; Volpi, N., Anomalous structure of urinary glycosaminoglycans in patients with pseudoxanthoma elasticum. *Clinical chemistry* 2003, 49 (3), 380-388.
26. Zhang, Q.; Chen, X.; Zhu, Z.; Zhan, X.; Wu, Y.; Song, L.; Kang, J., Structural Analysis of Low Molecular Weight Heparin by Ultraperformance Size Exclusion Chromatography/Time of Flight Mass Spectrometry and Capillary Zone Electrophoresis. *Analytical Chemistry* 2013, 85 (3), 1819-1827.
27. Prabhakar, V.; Capila, I.; Sasisekharan, R., The structural elucidation of glycosaminoglycans. *Methods. Mol. Biol.* 2009, 534, 147-56.
28. Volpi, N.; Maccari, F.; Linhardt, R. J., Capillary electrophoresis of complex natural polysaccharides. *Electrophoresis* 2008, 29 (15), 3095-106.

29. Campa, C.; Coslovi, A.; Flamigni, A.; Rossi, M., Overview on advances in capillary electrophoresis-mass spectrometry of carbohydrates: a tabulated review. *Electrophoresis* 2006, 27 (11), 2027-50.
30. Zamfir, A. D., Applications of capillary electrophoresis electrospray ionization mass spectrometry in glycosaminoglycan analysis. *Electrophoresis* 2016, 37 (7-8), 973-86.
31. Chi, L.; Amster, J.; Linhardt, R. J., Mass Spectrometry for the Analysis of Highly Charged Sulfated Carbohydrates. *Current Analytical Chemistry* 2005, 1 (3), 223-240.
32. Laremore, T. N.; Leach, F. E.; Solakyildirim, K.; Amster, I. J.; Linhardt, R. J., Glycosaminoglycan characterization by electrospray ionization mass spectrometry including Fourier transform mass spectrometry. *Methods Enzymol.* 2010, 478, 79-108.
33. Laremore, T. N.; Zhang, F.; Dordick, J. S.; Liu, J.; Linhardt, R. J., Recent progress and applications in glycosaminoglycan and heparin research. *Curr. Opin. Chem. Biol.* 2009, 13 (5-6), 633-40.
34. Zaia, J.; Costello, C. E., Compositional Analysis of Glycosaminoglycans by Electrospray Mass Spectrometry. *Analytical Chemistry* 2001, 73 (2), 233-239.
35. Zaia, J.; Costello, C. E., Tandem Mass Spectrometry of Sulfated Heparin-Like Glycosaminoglycan Oligosaccharides. *Analytical Chemistry* 2003, 75 (10), 2445-2455.
36. Bielik, A. M.; Zaia, J., Multistage tandem mass spectrometry of chondroitin sulfate and dermatan sulfate. *Int J Mass Spectrom* 2011, 305 (2-3), 131-137.
37. Leach, F. E.; Riley, N. M.; Westphall, M. S.; Coon, J. J.; Amster, I. J., Negative Electron Transfer Dissociation Sequencing of Increasingly Sulfated Glycosaminoglycan

Oligosaccharides on an Orbitrap Mass Spectrometer. *Journal of The American Society for Mass Spectrometry* 2017, 28 (9), 1844-1854.

38. Leach, F. E.; Wolff, J. J.; Xiao, Z.; Ly, M.; Laremore, T. N.; Arungundram, S.; Al-Mafraji, K.; Venot, A.; Boons, G.-J.; Linhardt, R. J.; Amster, I. J., Negative electron transfer dissociation Fourier transform mass spectrometry of glycosaminoglycan carbohydrates.

*European Journal of Mass Spectrometry* (Chichester, England) 2011, 17 (2), 167-176.

39. Wolff, J. J.; Amster, I. J.; Chi, L.; Linhardt, R. J., Electron detachment dissociation of glycosaminoglycan tetrasaccharides. *J Am Soc Mass Spectrom* 2007, 18 (2), 234-44.

40. Wolff, J. J.; Laremore, T. N.; Busch, A. M.; Linhardt, R. J.; Amster, I. J., Electron detachment dissociation of dermatan sulfate oligosaccharides. *J Am Soc Mass Spectrom* 2008, 19 (2), 294-304.

41. Klein, D. R.; Leach III, F. E.; Amster, I. J.; Brodbelt, J. S., Structural Characterization of Glycosaminoglycan Carbohydrates Using Ultraviolet Photodissociation. *Analytical chemistry* 2019.

42. Leach, F. E.; Xiao, Z.; Laremore, T. N.; Linhardt, R. J.; Amster, I. J., Electron detachment dissociation and infrared multiphoton dissociation of heparin tetrasaccharides. *International Journal of Mass Spectrometry* 2011, 308 (2), 253-259.

43. Wolff, J. J.; Leach, F. E.; Laremore, T. N.; Kaplan, D. A.; Easterling, M. L.; Linhardt, R. J.; Amster, I. J., Negative electron transfer dissociation of glycosaminoglycans. *Analytical chemistry* 2010, 82 (9), 3460-3466.

44. Auray-Blais, C.; Lavoie, P.; Zhang, H.; Gagnon, R.; Clarke, J. T.; Maranda, B.; Young, S. P.; An, Y.; Millington, D. S., An improved method for glycosaminoglycan analysis by LC–MS/MS of urine samples collected on filter paper. *Clinica Chimica Acta* 2012, 413 (7-8), 771-778.
45. Edens, R.; Al-Hakim, A.; Weiler, J.; Rethwisch, D.; Fareed, J.; Linhardt, R., Gradient polyacrylamide gel electrophoresis for determination of molecular weights of heparin preparations and low-molecular-weight heparin derivatives. *Journal of pharmaceutical sciences* 1992, 81 (8), 823-827.
46. Lin, L.; Liu, X.; Zhang, F.; Chi, L.; Amster, I. J.; Leach, F. E.; Xia, Q.; Linhardt, R. J., Analysis of heparin oligosaccharides by capillary electrophoresis–negative-ion electrospray ionization mass spectrometry. *Analytical and Bioanalytical Chemistry* 2017, 409 (2), 411-420.
47. Sun, L.; Zhu, G.; Zhang, Z.; Mou, S.; Dovichi, N. J., Third-generation electrokinetically pumped sheath-flow nanospray interface with improved stability and sensitivity for automated capillary zone electrophoresis–mass spectrometry analysis of complex proteome digests. *J. Proteome Res.* 2015, 14 (5), 2312-2321.
48. Ceroni, A.; Maass, K.; Geyer, H.; Geyer, R.; Dell, A.; Haslam, S. M., GlycoWorkbench: a tool for the computer-assisted annotation of mass spectra of glycans. *Journal of proteome research* 2008, 7 (4), 1650-1659.
49. Duan, J.; Jonathan Amster, I., An Automated, High-Throughput Method for Interpreting the Tandem Mass Spectra of Glycosaminoglycans. *Journal of The American Society for Mass Spectrometry* 2018, 29 (9), 1802-1811.



50. Domon, B.; Costello, C. E., A systematic nomenclature for carbohydrate fragmentations in FAB-MS/MS spectra of glycoconjugates. *Glycoconjugate Journal* 1988, 5 (4), 397-409.
51. Lee, E.-Y.; Kim, S.-H.; Whang, S.-K.; Hwang, K.-Y.; Yang, J.-O.; Hong, S.-Y., Isolation, identification, and quantitation of urinary glycosaminoglycans. *American journal of nephrology* 2003, 23 (3), 152-157.
52. Li, Y.; Wei, X.; Zhou, J.; Wei, L., The age-related changes in cartilage and osteoarthritis. *BioMed research international* 2013, 2013.
53. Lauder, R. M.; Huckerby, T. N.; BROWN, G. M.; Bayliss, M. T.; Nieduszynski, I. A., Age-related changes in the sulphation of the chondroitin sulphate linkage region from human articular cartilage aggrecan. *Biochemical Journal* 2001, 358 (2), 523-528.
54. Linhardt, R.; Galliher, P.; Cooney, C., Polysaccharide lyases. *Applied biochemistry and biotechnology* 1987, 12 (2), 135-176.
55. Ahn, M. Y.; Shin, K. H.; Kim, D.-H.; Jung, E.-A.; Toida, T.; Linhardt, R. J.; Kim, Y. S., Characterization of a *Bacteroides* species from human intestine that degrades glycosaminoglycans. *Canadian journal of microbiology* 1998, 44 (5), 423-429.

## CHAPTER 5

Capillary Zone Electrophoresis and Mass Spectrometry for the Analysis of Chondroitin Sulfate

Glycosaminoglycans Released from Bikunin

<sup>3</sup>Sanderson, P., R.J. Linhardt, and I.J. Amster, To be submitted to *Journal of Chromatography A*

## ABSTRACT

Glycosylation is one of the most complex post translational modifications that alters a protein's functionality due to the non-template driven synthesis of carbohydrates. Proteins modified with a sulfated glycosaminoglycan (GAG) chain are referred to as proteoglycans, and the simplest one is bikunin. Bikunin is a plasma proteinase inhibitor with a single covalently-attached chondroitin sulfate (CS) chain. In this study, fractions containing a collection of bikunin CS GAG chains of similar size with varying sulfation levels were separated using capillary zone electrophoresis coupled to mass spectrometry (CZE-MS/MS) for detection and structure analysis. The glycosaminoglycan chains ranged from dp20 up to dp57 with four to eleven sulfates. Based on accurate mass measurement from high resolution MS, 179 compositions were detected. Using low energy collisional activation (CID/HCD), the most abundant species were structurally characterized. Although these GAG chains have minimal amount of sulfation, this is the first instance of using reverse polarity CZE-MS/MS to characterize glycosaminoglycans of this size.

## INTRODUCTION

Post-translational modifications (PTMs) are chemical modifications to proteins that play a vital role in protein function. PTMs are some of most important and variable steps in the biosynthetic pathway of proteins which occur toward the end, and they have the potential to drastically alter the protein mechanism. Phosphorylation, glycosylation, methylation, and acetylation are a few examples of PTMs that influence aspects of cell biology [1]. In particular, glycosylation is one of the most heterogeneous and complex PTMs. Glycoconjugates are common in mammalian biospecimens and permit a variety of different biological functions to proceed accordingly [2].

Proteoglycans are a specific class of glycoconjugates in which one or more glycosaminoglycan (GAG) chains are covalently linked to a core protein [3]. Proteins are synthesized in a reproducible stepwise manner starting from DNA transcription to RNA then translation from RNA to amino acid polymerization into proteins. Carbohydrates are not biologically synthesized in the same manner. There is not a template guided process, but instead enzymes add sugar residues to elongate the carbohydrate chain. Once elongation is complete, a variety of enzymes will modify the residues within the carbohydrate chain. For GAGs, the most common modifications are deacetylation of hexosamine residues, epimerization of the uronic acid, and *N*- and *O*-sulfation. Since the enzymatic reactions do not go to completion, heterogeneous mixtures of GAG chains are produced. To understand the functional role of proteoglycans, it is important to determine the structure of the GAG component. Two proteoglycans, bikunin and decorin, have been the subject of “top-down” structure characterization, that is, analysis of their full-length GAG chains without any prior enzymatic processing of the carbohydrate portion [4-6]. Bikunin is by far the simplest proteoglycan with a

single chondroitin sulfate (CS) chain containing 25-60 sugar residues and fewer than 10 sulfo modifications. Chondroitin sulfate glycosaminoglycans are moderately sulfated with repeating units of N-acetylgalactosamine and glucuronic acid residues. In the case of bikunin, disaccharide analysis has established that the only modification to the basic structure is sulfation at the 4-*O* position of N-acetylgalactosamine. The full structural characterization of the bikunin GAGs requires only the identification of which residues contain a sulfo modification.

Characterization of sulfated GAGs is a significant analytical challenge due to limited quantities produced and the inability to amplify or overexpress GAGs [7-14]. Mass spectrometry (MS) and nuclear magnetic resonance spectroscopy (NMR) are the main techniques used to identify and location modifications on sulfated carbohydrates [15-20]. Mass spectrometry has the advantages of high sensitivity, selectivity, and compatibility with online separation methods to detect and characterize GAGs [19, 21]. With accurate mass measurement, GAG compositions can be determined, but additional structure information requires tandem MS. When carbohydrates are fragmented, glycosidic and cross ring cleavages specify the position and type of modifications. Glycosidic cleavages indicate which residues have modifications, but cross ring cleavages identify the specific location within a sugar residue. Various activation methods have been applied to sulfated GAGs [20, 22-34]. For sparsely sulfated GAGs, collisional activation can provide adequate sequence coverage, while electron-based or photodissociation techniques are better suited to more highly sulfated GAGs to minimize sulfate loss and promote cross ring fragmentation.

Methods used to analyze purified standards are not always adequate for biological samples. Such samples are often complex mixtures of positional isomers and diastereomers which are difficult to isolate for tandem MS experiments. For this reason, biological GAG

mixtures need alternative ways to separate the components prior to structure analysis. Liquid chromatography (LC), ion mobility spectrometry (IMS), and capillary zone electrophoresis (CZE) are a few of the common methods used to separate sulfated GAG chains coupled to mass spectrometry [35-39].

Liquid chromatography is widely used to separate oligosaccharides of different degrees of polymerization (dp). Reverse phase (RP) chromatography is frequently used for derivatized glycans, but it requires additional preparation steps or ion pairing reagents to separate sulfated GAG sugars [21]. For sulfated GAGs, hydrophilic interaction liquid chromatography (HILIC) is more commonly used as the column has a polar stationary phase which retains the highly anionic GAGs without ion pairing reagents. Multiple groups have analyzed disaccharides up to dp30 using HILIC-LC-MS [40-42]. IMS separations are gas phase separations that occur post ionization on the millisecond to second time scale. Consequently, sulfated GAGs do not require additional preparation or reagents which simplifies the complexity of analysis. Isomers have been separated using different types of IMS, but highly complex mixtures are difficult to separate using this method based on the speed of the separation.

Capillary zone electrophoresis (CZE) separates molecules based on charge, size, and shape. The anionic nature of sulfated GAGs lends itself well to separation by CZE. Previous literature has shown that reverse polarity CZE can separate a wide range of GAG chains [43-45]. GAGs containing different numbers of sulfates have been baseline resolved in addition to separating isomers and epimers. CZE separations are on the order of minutes which take longer than IMS separations, but this allows mixtures containing a large number of components to be separated.

In this study, fractions of glycosaminoglycans mixtures released from bikunin were separated and characterized using reverse polarity CZE-MS/MS. Previous studies of these bikunin glycosaminoglycans fractions used direct injection on both an ESI-LTQ-Orbitrap-FTMS and Nano-ESI-FTICR-MS for analysis [5]. From the published results, each fraction was a mixture of GAG chains of similar molecular size. The fractions covered a size range from 25-50 sugars in length. Surprisingly, the direct injection results showed a conserved pattern of sulfation on the CS chains. The present work is the first attempt to separate GAG chains released from a proteoglycan using online CZE-MS/MS. These GAGs are longer than previously analyzed chains using CZE-MS/MS, but the limited amount of sulfo-modifications make them ideal candidates for experiments using CID/HCD activation. In under an hour, chondroitin sulfate glycosaminoglycans ranging from dp20 to dp55 were separated. The major saccharides were selected for low energy collision activation to make structural assignments.

## **MATERIAL AND METHODS**

### *Materials*

All chemicals and reagents were purchased from commercial sources and used as received unless otherwise specified. Bare fused silica (BFS) capillaries (360  $\mu\text{m}$  o.d.  $\times$  50  $\mu\text{m}$  i.d.) and electrospray emitters (1.0 mm OD  $\times$  0.75 mm ID) were obtained from PolyMicro Technologies (Phoenix, AZ) and CMP Scientific (Brooklyn, NY), respectively. Reagents *N*-(6-aminohexyl) aminomethyltriethoxysilane (AHS, Gelest, Morrisville, PA) and dichlorodimethylsilane (DMS, Sigma-Aldrich, St. Louis, MO) was prepared in toluene to coat the capillaries as previously described [43]. All solutions were filtered with 0.45  $\mu\text{m}$  syringe filter (Millipore, Temecula, CA) before use.

### *Glycosaminoglycan Samples*

The proteoglycan bikunin was purchased and purified using 30-kDa molecular weight centrifugal device as described in previous literature [5]. Actinase E was utilized for proteolysis of bikunin at pH 7.5 in 50 mM Tris-HCl in sodium acetate at 45°C for 18 hours before isolation of the digestion using strong anion exchange spin column chromatography. This released the carbohydrate chain from the protein, with a serine residue present at the reducing end of the linker region. The glycosaminoglycan mixture was desalted using a 10-kDa molecular weight centrifugal filter with multiple deionized water washes.

Bikunin glycosaminoglycans were fractionated using continuous elution polyacrylamide gel electrophoresis (PAGE) [5]. Briefly, a 2 mg aliquot of purified bikunin glycosaminoglycan was loaded in a solution of phenol red and sucrose. Electrophoresis was performed for 8 hours at constant power (12 W) with fraction collection set to 2 minutes. Strong anion exchange and desalting removed remaining salts and impurities. Separation was visualized using Alcian blue stain on a 15% total acrylamide monomer solution using native mini-slab PAGE gel. Molecular weight distribution of the glycosaminoglycans were estimated using PAGE densitometry and bikunin standards using UN-SCANIT (Silk Scientific) [46]. The resulting fractions were reconstituted in water for CZE-MS/MS analysis.

### *Instrumentation*

Capillary zone electrophoresis (CZE) separations were performed on an Agilent HP 3D CE instrument using cation- and neutral-coated capillaries with a -30 kV potential applied. Ammonium acetate (25 mM in 70% methanol) was used as the background electrolyte and sheath liquid. Conditions and parameters were consistent with previously reported literature used for



purified GAG standards [43]. Samples were injected for 12 s at 950 mbar followed by a BGE injection for 10 s at 10 mbar.

An EMASS-II (CMP Scientific, Brooklyn, NY) CE-MS interface coupled the CE to a Thermo Scientific Velos Orbitrap Elite mass spectrometer (Bremen, Germany) [47, 48]. The capillary outlet was etched and nested inside of a glass emitter tip with a 30  $\mu\text{m}$  tip orifice. The etched capillary was positioned 0.4–0.7 mm from the tip of the emitter orifice to create a mixing volume of ~18 nL which was filled with sheath liquid. Nano-electrospray ionization (nESI) voltage was applied by an external power supply ranging from –1.70 to –1.85 kV to the emitter.

MS detection was performed in negative-ion mode, and multiply deprotonated anions were observed for each species. To improve sensitivity of glycosaminoglycans and reduce sulfate loss during MS analysis, sucrose octasulfate and arixtra were utilized prior to CZE-MS experiments to perform a semi-automatic optimization of source parameters. The Orbitrap was scanned from  $m/z$  250–2000 for glycosaminoglycans with a specified resolution of 120,000 for MS and MS/MS experiments. Composition assignments were determined using in-lab developed software. For tandem mass spectrometry experiments, precursor ions were mass selected in the dual linear ion trap and activated using low energy collision (20–55 eV) MS/MS. Each peak from the electropherogram was averaged to obtain a tandem mass spectrum with mass accuracy of 10 ppm or better. Data analysis was performed using Glycoworkbench and in-lab developed software [49, 50]. CID/HCD fragments were assigned and annotated using the Domon-Costello nomenclature [51].

## RESULTS AND DISCUSSION

### *CZE-MS & Compositional Analysis*

Seven fractions containing size similar CS glycosaminoglycan chains released from bikunin were analyzed using online reverse polarity CZE-MS. By applying a strong separation potential of -30 kV, sulfated GAG chains were separated based on the number of sulfate groups and molecular size of the chain. By extracting the  $m/z$  values and charge of the ions, accurate mass compositions were determined using in-lab automated software with a mass tolerance of 10 ppm [50]. As expected, the fraction containing the lowest average molecular weight (5.37 kDa, f50) had the shortest carbohydrate chains ranging from dp20 to dp37 with four to nine sulfo modifications. The fraction with the longest chains and highest average molecular weight (9.77 kDa, f117) contained dp43 to dp 57 with five to nine sulfo modifications. These results are similar to the direct injection FTMS published results [5]. The other five fractions contain chain lengths within these ranges with ten being the greatest number of sulfo modifications on a chain. Adjacent fractions have sulfated GAG compositions that overlap, but the major species in each fraction is different. As these fractions were separated using continuous PAGE, overlap between the fractions is expected.

Figure 5.1 shows the base peak electropherogram from  $m/z$  700-2000 (A) and extracted ion electropherograms (B-F) of the five most abundant GAG species found in the smallest fraction, f50. In this fraction, the most abundant species were dp27-7-Ser (B), dp27-6-Ser (C), dp26-5-Ser (D), and dp25-5-Ser (E). Separation is predominantly determined based on the number of sulfate modifications on the glycosaminoglycan chains. The highly sulfated glycosaminoglycan chains migrate through the capillary first with dp27-7-Ser followed by dp27-6-Ser. As the sulfate number decreases, the electrophoretic force on the GAG chains decreases

resulting in longer migration times. However, as mentioned previously, the separation is not only reliant on charge or number of sulfate modifications. GAG chains that have the same number of sulfate groups are also separated based on their size and shape as displayed in Figure 5.1 (D) and (E). Both odd and even chains are observed during the separations with a wide variety of chain lengths. Table 5.1 indicates the glycosaminoglycan chains that are detected for f50 of which there are 35 different compositions. The electropherograms and composition lists for the remaining fractions can be found in the supplemental material (Appendix C) and have similar properties but contain longer chains.

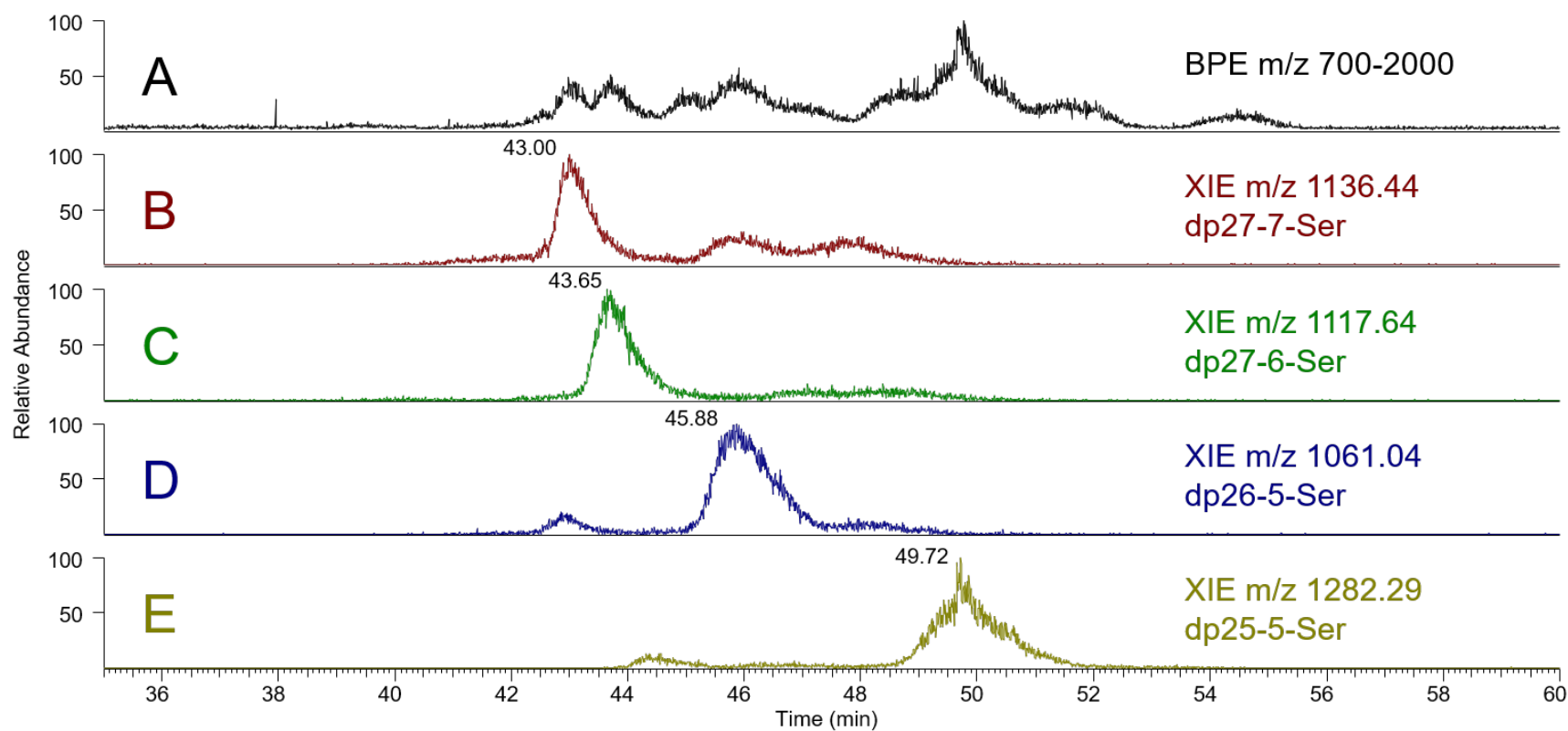


**Figure 5.1.** Base peak (A, BPE) and extraction ion electropherograms (B-E, XIE) of the four most abundant glycosaminoglycans in fraction 50: B) dp27-7-Ser, C) dp27-6-Ser, D) dp26-5-Ser, and E) dp25-5-Ser.

**Table 5.1.** Glycosaminoglycan chains detected in fraction 50 based on accurate mass measurement.

<b>dp</b>	<b>Number of Sulfate Modifications</b>			
20	4			
21	4	5		
22	4			
23	4	5	6	
24	3	4	5	6
25	4	5	6	7
26	4	5	6	7
27	5	6	7	8
28	6	7	8	
29	7	8	9	
30	5			
31	6	8		
33	6			
35	6			
37	5			

Although there is slight peak overlap within the electropherograms for chains that have similar size and sulfate modifications, there are only a few species present in each mass spectrum for the major glycosaminoglycan chains. As chain size increases, there is more overlap of the similar size and charge. The number of sulfate modifications is increasing by small amount even as chain length increases. Since these fractions contain a large number of components, general overlap between similar size and charge are expected.

A representative mass spectrum of dp27-7-Ser from fraction 50 was averaged from 42.9-43.1 min to demonstrate the charge state distribution and molecular species present. Generally, the most abundant ions have lower charge states ( $[M-5H]^{5-}$  and  $[M-4H]^{4-}$ ), but multiple charge states are detected ( $[M-4H]^{4-}$  to  $[M-13H]^{13-}$ , Figure 5.2). This lower charge state behavior is characteristic of CZE-MS separations using ammonium acetate as the background electrolyte

because ammonium acetate decreases the degree of ionization for sulfated GAGs [44].

Additionally, with lower charge states, ammonium-hydrogen exchange ( $\text{NH}_4^+$ -H ex) is observed for the highly sulfated chains. The most abundant molecular ion in Figure 5.2 is the dp27-7-Ser precursor with the addition of  $\text{NH}_4^+$ -H ex ( $m/z$  1137.0405). The molecular ion without  $\text{NH}_4^+$ -H ex is ~35% abundance ( $m/z$  1133.0347). The next most abundant peak is the four charge state ( $m/z$  1425.8091) of the same precursor with addition of  $\text{NH}_4^+$ -H ex. This phenomenon was consistent for all fractions and glycosaminoglycan chains for the four and five charge states depending on the level of sulfation. Ammonium-hydrogen exchange was not observed for the higher charge states (above  $[\text{M}-6\text{H}]^{6-}$ ).

The mass spectrum for each peak in the electropherogram is greatly simplified compared to a direct infusion experiment of the same fraction that contains all compositions in a single mass spectrum. In most cases, each peak in the electropherogram contains only a few species. Figure 5.2 illustrates three species found in the mass spectrum of the peak from 42.9-43.1 minutes. In addition to the main species, dp27-7-Ser,  $m/z$  1061.0187<sup>5-</sup> and 1331.0317<sup>4-</sup> represents dp25-7-Ser with a single  $\text{NH}_4^+$ -H exchange. Dp28-6-Ser was also observed by  $m/z$  1156.4365<sup>5-</sup> and dp30-6-Ser from  $m/z$  1232.0591<sup>5-</sup>. These species are similar in number of sulfates and chain lengths; therefore, it is not surprising that these species have similar migration times.

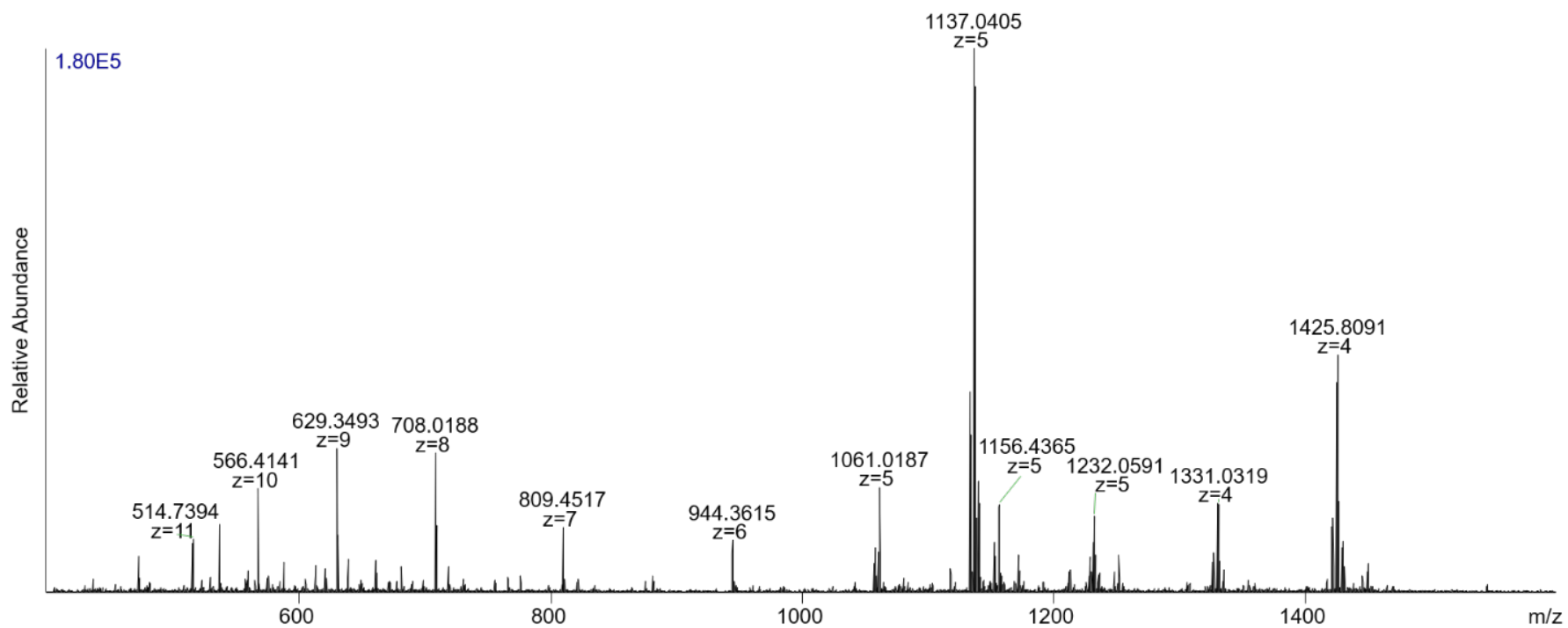


**Figure 5.2.** Mass spectrum of dp27-7-Ser from fraction 50, averaged from 42.9-43.1 min, demonstrating the observed charge state distribution and  $\text{NH}_4^+$ -H exchange.

Furthermore, there appear to be isomeric components for a few glycosaminoglycan species that we are able to separate and observe as different peaks. Most of the species appear to produce a single peak in the electropherogram, but this is not true for all species. Fraction 50 shows two species that identify as dp25-6-Ser based on accurate mass measurement. The extracted ion electropherogram (XIE) for  $m/z$  1041.62 is displayed in Figure 5.3A. There are two different peaks, P1 and P2, that correspond to the same monoisotopic  $m/z$  values,  $m/z$  1041.2203 and 1041.2201 (Figure 5.3B and C). Based on these  $m/z$  values with a 5 charge state, this oligosaccharide has molecular weight of 5211.13 which is within 5 ppm error for dp25-6-Ser. These peaks could correspond to isomers with sulfate groups on different residues or positions. In order to determine how these isomers differ, tandem mass analysis is necessary. Unfortunately, the intensity for the first peak is too small for informative MS/MS analysis. This is a representative example, but this trend followed for several isomeric peaks within most of the fractions. A more concentrated sample would need to be used to determine the structures of the isomeric components.



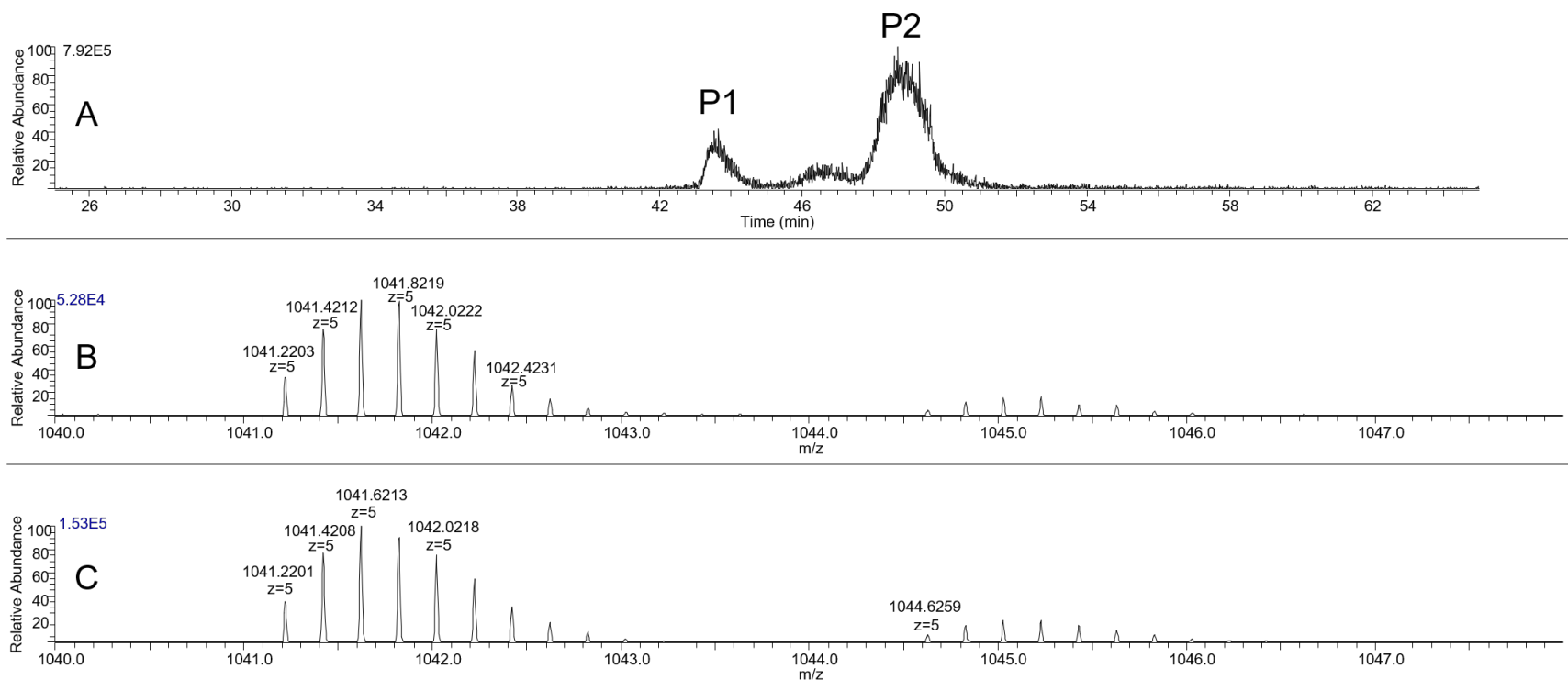


**Figure 5.3.** A) Extracted ion electropherogram (XIE) of dp25-6-Ser, m/z 1041.22, showing two peaks. Mass spectra of the two peaks correspond to P1 from 43.35-43.85 minutes (B), and P2 from 48.3-49.0 minutes. Both species have the same monoisotopic m/z value and charge resulting in a similar composition.

### *Low Energy Collisional Activation MS/MS Analysis*

Although the degree of ionization is lower producing abundant lower charge states, the number of sulfate modifications on these glycans is also low. The majority of the sulfate modifications are ionized for the most of the glycosaminoglycan chains. Therefore, low energy collisional activation, such as collision induced dissociation (CID) and higher energy collision induced dissociation (HCD) can be used to perform MS/MS analysis for adequate sequence coverage and minimal sulfo degradation.

By combining CID and HCD experiments with CZE-MS, the most abundant GAG chains were assigned. Ten glycosaminoglycans were sequenced based on the glycosidic fragment ions (Supplemental Information). An example HCD mass spectrum of dp27-5-Ser is displayed in Figure 5.4. The molecular ion is  $[M-5H]^{5-}$  which indicates that all five of the sulfate groups are ionized. Higher charge states are not abundant enough for MS/MS activation. For the lower charge states, the most intense fragment ions are a result of sulfate loss from the precursor ion. Previous work on sulfated GAGs has shown that collisional activation mainly produces sulfate loss and glycosidic cleavages for precursor ions that are not fully ionized [52]. However, since all sulfate groups are ionized, informative fragment ions are also produced with high abundance. With collisional activation of the four and five charge states, glycosidic cleavages are the only product ions observed for these GAG chains. Fragment ions are split between b- and y-type ions, but some c-type product ions are also observed. Z-type ions were not detected, and neither were cross ring fragments. The inset structure shows the annotations following the Domon-Costello nomenclature. On this structure, only the product ions without sulfate loss are displayed. The full list of fragment ions is displayed in a table found in the supplemental material.

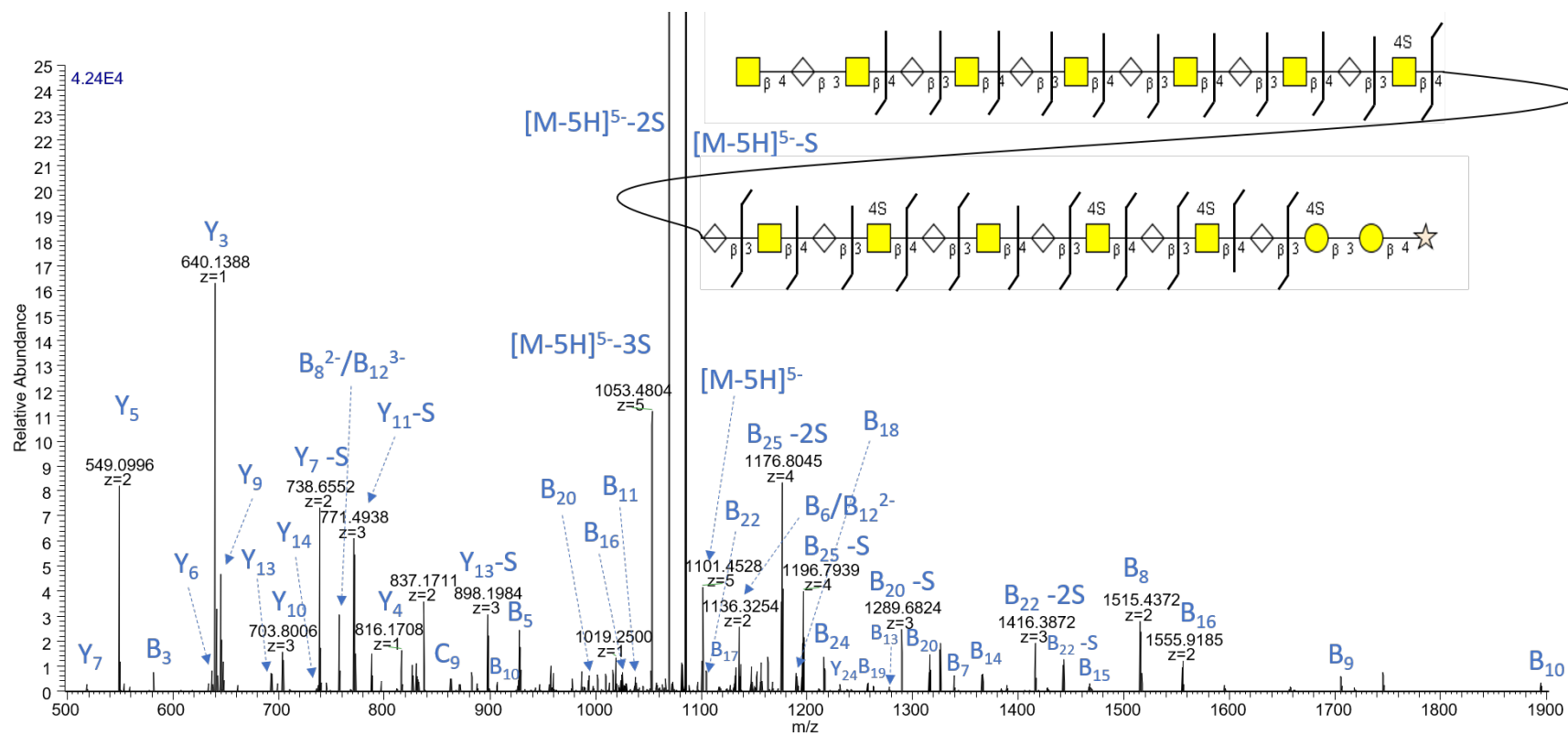


**Figure 5.4.** HCD-MS/MS mass spectrum of molecular ion  $[M-5H]^{5-}$  of dp27-5-Ser with annotated fragment ions. The inset structure shows the annotations following the Domon-Costello nomenclature without sulfate loss.

Based on the previous work completed by enzymatic analysis and direct injection of these glycosaminoglycan fractions on high resolution mass spectrometers, the released chains have consistent structure and sulfation motifs [5]. Therefore, the specific location of each sulfate modification within a residue is already known. Using enzymes, it was determined that the chains are only modified in 4-*O*-position on N-acetylgalactosamine residues. Furthermore, the sulfates were consistently found on the reducing end of the chain with specific patterns. With these results in mind, chain sequences can be resolved based purely on the glycosidic cleavages provided they span the entire molecule. The y-ions are clustered around the reducing end of the chains and the b-ions cover most of the chain including the non-reducing side. The other nine most abundant glycosaminoglycan chains were also structurally analyzed. The product ions for the remaining structures follow this trend and can be found in the supplemental material.

## CONCLUSIONS

Online capillary zone electrophoresis combined with mass spectrometry is a valuable tool for separating glycosaminoglycan mixtures prior to structural characterization. The results described in this study focus on using the CZE-MS/MS platform to analyze complex biological mixtures. Glycosaminoglycan chains released from the proteoglycan bikunin were separated using online CZE combined with low energy collisional activation to sequence the carbohydrates. The sequences obtained in this report align with published literature including the presence of both odd and even chains with a varied number of sulfate modifications. CZE-MS/MS results indicate the presence of higher sulfation levels up to 11 sulfates present on several chains. Interestingly, the presence of isomers was indicated based on multiple peaks containing the same accurate mass measurement corresponding to a single composition. This had

not been reported previously which is most likely a result of the low abundance of these species and the inability to separate isomers using direct injection. Future work will focus on analyzing a more concentrated sample that has enough abundance to perform tandem mass analysis on the lower abundance isomeric species. Overall, this work provides a step forward towards the characterization of large sulfated glycosaminoglycan mixtures from their natural sources in a single online experiment.

## **ACKNOWLEDGEMENTS**

The authors gratefully acknowledge generous financial support from the National Institutes of Health, grants R21HL136271, U01CA231074, and P41GM103390. The authors are grateful for the fractions of bikunin that were provided by Prof. Robert J. Linhardt.

## REFERENCES

1. Carr, S. A.; Annan, R. S., Overview of peptide and protein analysis by mass spectrometry. *Current protocols in molecular biology* **1997**, 38 (1), 10.21. 1-10.21. 27.
2. Varki, A., Biological roles of glycans. *Glycobiology* **2017**, 27 (1), 3-49.
3. Varki, A.; Cummings, R. D.; Esko, J. D.; Freeze, H. H.; Stanley, P.; Bertozzi, C. R.; Hart, G. W.; Etzler, M. E., *Essentials of Glycobiology*. NY, 2009; Vol. 2.
4. Chi, L.; Wolff, J. J.; Laremore, T. N.; Restaino, O. F.; Xie, J.; Schiraldi, C.; Toida, T.; Amster, I. J.; Linhardt, R. J., Structural Analysis of Bikunin Glycosaminoglycan. *Journal of the American Chemical Society* **2008**, 130 (8), 2617-2625.
5. Ly, M.; Leach, F. E., 3rd; Laremore, T. N.; Toida, T.; Amster, I. J.; Linhardt, R. J., The proteoglycan bikunin has a defined sequence. *Nat. Chem. Biol.* **2011**, 7 (11), 827-33.
6. Yu, Y.; Duan, J.; Leach, F. E.; Toida, T.; Higashi, K.; Zhang, H.; Zhang, F.; Amster, I. J.; Linhardt, R. J., Sequencing the Dermatan Sulfate Chain of Decorin. *Journal of the American Chemical Society* **2017**, 139 (46), 16986-16995.
7. Wolff, J. J.; Laremore, T. N.; Busch, A. M.; Linhardt, R. J.; Amster, I. J., Electron detachment dissociation of dermatan sulfate oligosaccharides. *J Am Soc Mass Spectrom* **2008**, 19 (2), 294-304.
8. Wolff, J. J.; Amster, I. J.; Chi, L.; Linhardt, R. J., Electron detachment dissociation of glycosaminoglycan tetrasaccharides. *J Am Soc Mass Spectrom* **2007**, 18 (2), 234-44.
9. Leach, F. E., 3rd; Wolff, J. J.; Xiao, Z.; Ly, M.; Laremore, T. N.; Arungundram, S.; Al-Mafraji, K.; Venot, A.; Boons, G. J.; Linhardt, R. J.; Amster, I. J., Negative electron transfer dissociation Fourier transform mass spectrometry of glycosaminoglycan carbohydrates. *Eur. J. Mass Spectrom.* **2011**, 17 (2), 167-76.

10. Laremore, T. N.; Leach, F. E.; Solakyildirim, K.; Amster, I. J.; Linhardt, R. J., Glycosaminoglycan characterization by electrospray ionization mass spectrometry including Fourier transform mass spectrometry. *Methods Enzymol.* **2010**, *478*, 79-108.
11. Bielik, A. M.; Zaia, J., Multistage tandem mass spectrometry of chondroitin sulfate and dermatan sulfate. *Int J Mass Spectrom* **2011**, *305* (2-3), 131-137.
12. Zaia, J., Compositional analysis of glycosaminoglycans by electrospray mass spectrometry. *Anal. Chem.* **2001**, *73* (2), 233-239.
13. Zaia, J., Tandem mass spectrometry of sulfated heparin-like glycosaminoglycan oligosaccharides. *Analytical chemistry* **2003**, *75* (10), 2445.
14. Li, G.; Steppich, J.; Wang, Z.; Sun, Y.; Xue, C.; Linhardt, R. J.; Li, L., Bottom-Up Low Molecular Weight Heparin Analysis Using Liquid Chromatography-Fourier Transform Mass Spectrometry for Extensive Characterization. *Analytical Chemistry* **2014**, *86* (13), 6626-6632.
15. Pomin, V. H.; Sharp, J. S.; Li, X.; Wang, L.; Prestegard, J. H., Characterization of Glycosaminoglycans by <sup>15</sup>N NMR Spectroscopy and in Vivo Isotopic Labeling. *Analytical Chemistry* **2010**, *82* (10), 4078-4088.
16. Langeslay, D. J.; Beecher, C. N.; Naggi, A.; Guerrini, M.; Torri, G.; Larive, C. K., Characterizing the Microstructure of Heparin and Heparan Sulfate Using N-Sulfoglucosamine <sup>1</sup>H and <sup>15</sup>N NMR Chemical Shift Analysis. *Analytical Chemistry* **2013**, *85* (2), 1247-1255.
17. Pomin, V. H., NMR chemical shifts in structural biology of glycosaminoglycans. *Analytical chemistry* **2013**, *86* (1), 65-94.
18. Staples, G. O.; Zaia, J., Analysis of Glycosaminoglycans Using Mass Spectrometry. *Curr Proteomics* **2011**, *8* (4), 325-336.

19. Zaia, J., Glycosaminoglycan glycomics using mass spectrometry. *Mol Cell Proteomics* **2013**, *12* (4), 885-92.
20. Zhou, W.; Håkansson, K., Structural Characterization of Carbohydrates by Fourier Transform Tandem Mass Spectrometry. *Current proteomics* **2011**, *8* (4), 297-308.
21. Kailemia, M. J.; Ruhaak, L. R.; Lebrilla, C. B.; Amster, I. J., Oligosaccharide Analysis by Mass Spectrometry: A Review of Recent Developments. *Analytical Chemistry* **2014**, *86* (1), 196-212.
22. Zaia, J.; McClellan, J. E.; Costello, C. E., Tandem Mass Spectrometric Determination of the 4S/6S Sulfation Sequence in Chondroitin Sulfate Oligosaccharides. *Analytical Chemistry* **2001**, *73* (24), 6030-6039.
23. Zamfir, A.; Seidler, D. G.; Kresse, H.; Peter-Katalinić, J., Structural characterization of chondroitin/dermatan sulfate oligosaccharides from bovine aorta by capillary electrophoresis and electrospray ionization quadrupole time-of-flight tandem mass spectrometry. *Rapid Communications in Mass Spectrometry* **2002**, *16* (21), 2015-2024.
24. Desaire, H.; Sirich, T. L.; Leary, J. A., Evidence of Block and Randomly Sequenced Chondroitin Polysaccharides: Sequential Enzymatic Digestion and Quantification Using Ion Trap Tandem Mass Spectrometry. *Analytical Chemistry* **2001**, *73* (15), 3513-3520.
25. Leach, F. E.; Xiao, Z.; Laremore, T. N.; Linhardt, R. J.; Amster, I. J., Electron detachment dissociation and infrared multiphoton dissociation of heparin tetrasaccharides. *International Journal of Mass Spectrometry* **2011**, *308* (2), 253-259.
26. Oh, H. B.; Leach, F. E.; Arungundram, S.; Al-Mafraji, K.; Venot, A.; Boons, G.-J.; Amster, I. J., Multivariate Analysis of Electron Detachment Dissociation and Infrared Multiphoton Dissociation Mass Spectra of Heparan Sulfate Tetrasaccharides Differing Only in



Hexuronic acid Stereochemistry. *Journal of The American Society for Mass Spectrometry* **2011**, 22 (3), 582-590.

27. Wolff, J. J.; Laremore, T. N.; Busch, A. M.; Linhardt, R. J.; Amster, I. J., Influence of charge state and sodium cationization on the electron detachment dissociation and infrared multiphoton dissociation of glycosaminoglycan oligosaccharides. *Journal of the American Society for Mass Spectrometry* **2008**, 19 (6), 790-798.

28. Wolff, J. J.; Laremore, T. N.; Leach, F. E.; Linhardt, R. J.; Amster, I. J., Electron Capture Dissociation, Electron Detachment Dissociation and Infrared Multiphoton Dissociation of Sucrose Octasulfate. *European Journal of Mass Spectrometry* **2009**, 15 (2), 275-281.

29. Klein, D.; Leach, F. I.; Amster, I.; Brodbelt, J., Structural Characterization of Glycosaminoglycan Carbohydrates using Ultraviolet Photodissociation. *Anal. Chem.* **2019**.

30. Ly, T.; Julian, R. R., Ultraviolet photodissociation: developments towards applications for mass-spectrometry-based proteomics. *Angewandte Chemie International Edition* **2009**, 48 (39), 7130-7137.

31. Racaud, A.; Antoine, R.; Dugourd, P.; Lemoine, J., Photoinduced dissociation of heparin-derived oligosaccharides controlled by charge location. *Journal of the American Society for Mass Spectrometry* **2010**, 21 (12), 2077-2084.

32. Leach, F. E.; Ly, M.; Laremore, T. N.; Wolff, J. J.; Perlow, J.; Linhardt, R. J.; Amster, I. J., Hexuronic Acid Stereochemistry Determination in Chondroitin Sulfate Glycosaminoglycan Oligosaccharides by Electron Detachment Dissociation. *Journal of The American Society for Mass Spectrometry* **2012**, 23 (9), 1488-1497.

33. Agyekum, I.; Zong, C.; Boons, G.-J.; Amster, I. J., Single Stage Tandem Mass Spectrometry Assignment of the C-5 Uronic Acid Stereochemistry in Heparan Sulfate

Tetrasaccharides using Electron Detachment Dissociation. *Journal of The American Society for Mass Spectrometry* **2017**, 1-10.

34. Agyekum, I.; Patel, A. B.; Zong, C.; Boons, G.-J.; Amster, I. J., Assignment of hexuronic acid stereochemistry in synthetic heparan sulfate tetrasaccharides with 2-O-sulfo uronic acids using electron detachment dissociation. *International Journal of Mass Spectrometry* **2015**, 390 (Supplement C), 163-169.

35. Zaia, J., On-line separations combined with MS for analysis of glycosaminoglycans. *Mass Spectrometry Reviews* **2009**, 28 (2), 254-272.

36. Volpi, N.; Galeotti, F.; Yang, B.; Linhardt, R. J., Analysis of glycosaminoglycan-derived, precolumn, 2-aminoacridone-labeled disaccharides with LC-fluorescence and LC-MS detection. *Nat. Protoc.* **2014**, 9 (3), 541-558.

37. Huang, Y.; Shi, X.; Yu, X.; Leymarie, N.; Staples, G. O.; Yin, H.; Killeen, K.; Zaia, J., Improved liquid chromatography-MS/MS of heparan sulfate oligosaccharides via chip-based pulsed makeup flow. *Anal Chem* **2011**, 83 (21), 8222-9.

38. Huang, R.; Liu, J.; Sharp, J. S., An approach for separation and complete structural sequencing of heparin/heparan sulfate-like oligosaccharides. *Anal Chem* **2013**, 85 (12), 5787-95.

39. Lemmnitzer, K.; Riemer, T.; Groessl, M.; Süß, R.; Knochenmuss, R.; Schiller, J., Comparison of ion mobility-mass spectrometry and pulsed-field gradient nuclear magnetic resonance spectroscopy for the differentiation of chondroitin sulfate isomers. *Analytical Methods* **2016**, 8 (48), 8483-8491.

40. Gill, V. L.; Aich, U.; Rao, S.; Pohl, C.; Zaia, J., Disaccharide Analysis of Glycosaminoglycans Using Hydrophilic Interaction Chromatography and Mass Spectrometry. *Analytical Chemistry* **2013**, 85 (2), 1138-1145.

41. Li, L.; Zhang, F.; Zaia, J.; Linhardt, R. J., Top-Down Approach for the Direct Characterization of Low Molecular Weight Heparins Using LC-FT-MS. *Analytical Chemistry* **2012**, *84* (20), 8822-8829.
42. Antia, I. U.; Mathew, K.; Yagnik, D. R.; Hills, F. A.; Shah, A. J., Analysis of procainamide-derivatised heparan sulphate disaccharides in biological samples using hydrophilic interaction liquid chromatography mass spectrometry. *Analytical and Bioanalytical Chemistry* **2018**, *410* (1), 131-143.
43. Sanderson, P.; Stickney, M.; Leach, F. E.; Xia, Q.; Yu, Y.; Zhang, F.; Linhardt, R. J.; Amster, I. J., Heparin/heparan sulfate analysis by covalently modified reverse polarity capillary zone electrophoresis-mass spectrometry. *Journal of Chromatography A* **2018**, *1545*, 75-83.
44. Stickney, M.; Sanderson, P.; Leach III, F. E.; Zhang, F.; Linhardt, R. J.; Amster, I. J., Online capillary zone electrophoresis negative electron transfer dissociation tandem mass spectrometry of glycosaminoglycan mixtures. *International Journal of Mass Spectrometry* **2019**, *445*, 116209.
45. Ha, X.; Sanderson, P.; Nesheiwat, S.; Lin, L.; Yu, Y.; Zhang, F.; Amster, I. J.; Linhardt, R. J., Structural Analysis of Urinary Glycosaminoglycans from Healthy Human Subjects. *Glycobiology* **2019**.
46. Ly, M.; Wang, Z.; Laremore, T. N.; Zhang, F.; Zhong, W.; Pu, D.; Zagorevski, D. V.; Dordick, J. S.; Linhardt, R. J., Analysis of E. coli K5 capsular polysaccharide heparosan. *Analytical and bioanalytical chemistry* **2011**, *399* (2), 737-745.
47. Lin, L.; Liu, X.; Zhang, F.; Chi, L.; Amster, I. J.; Leach, F. E.; Xia, Q.; Linhardt, R. J., Analysis of heparin oligosaccharides by capillary electrophoresis–negative-ion electrospray ionization mass spectrometry. *Analytical and Bioanalytical Chemistry* **2017**, *409* (2), 411-420.

48. Sun, L.; Zhu, G.; Zhang, Z.; Mou, S.; Dovichi, N. J., Third-generation electrokinetically pumped sheath-flow nanospray interface with improved stability and sensitivity for automated capillary zone electrophoresis–mass spectrometry analysis of complex proteome digests. *J. Proteome Res.* **2015**, *14* (5), 2312-2321.
49. Ceroni, A.; Maass, K.; Geyer, H.; Geyer, R.; Dell, A.; Haslam, S. M., GlycoWorkbench: a tool for the computer-assisted annotation of mass spectra of glycans. *Journal of proteome research* **2008**, *7* (4), 1650-1659.
50. Duan, J.; Jonathan Amster, I., An Automated, High-Throughput Method for Interpreting the Tandem Mass Spectra of Glycosaminoglycans. *Journal of The American Society for Mass Spectrometry* **2018**, *29* (9), 1802-1811.
51. Domon, B.; Costello, C. E., A systematic nomenclature for carbohydrate fragmentations in FAB-MS/MS spectra of glycoconjugates. *Glycoconjugate Journal* **1988**, *5* (4), 397-409.
52. Kailemia, M. J.; Li, L.; Xu, Y.; Liu, J.; Linhardt, R. J.; Amster, I. J., Structurally Informative Tandem Mass Spectrometry of Highly Sulfated Natural and Chemoenzymatically Synthesized Heparin and Heparan Sulfate Glycosaminoglycans. *Molecular & Cellular Proteomics* **2013**, *12* (4), 979-990.

## CHAPTER 6

### CONCLUSIONS

Glycans are known to play vital roles in a multitude of biological systems [1].

Glycosaminoglycans (GAGs) are a subset of linear polysaccharides with a variety of sulfate modification patterns that influence their biological function. Several biological processes, such as developmental and disease functions, are impacted by GAGs within the body through protein-binding interactions [2-4]. Structural characterization is crucial to grasp how modification patterns dictate binding interactions, but it is difficult to analyze natural sources of sulfated GAGs. The biosynthesis of GAG chains is a non-template process, facilitated by a number of enzymatic steps that do not go to completion and results in highly heterogeneous and complex mixtures [5]. Thus, methods to separate these mixtures are a critical element prior to structural analysis.

Online capillary zone electrophoresis coupled to high resolution mass spectrometry (CZE-MS) excels at separating sulfated glycosaminoglycans from disaccharides up to sugars containing 50 residues based on the results presented in this dissertation. To improve the reproducibility and decrease migration times of sulfated GAGs, efforts focused on implementing different capillary coatings to be used for reverse polarity separations [6]. Using neutral and cation coated capillaries with the CZE-MS/MS platform, structurally similar sulfated GAG oligosaccharides and complex mixtures were separated and analyzed.

In **Chapter 3**, standard mixtures containing positional isomers and stereoisomers were examined to demonstrate the effectiveness of the CZE-MS platform for separating closely-

related GAG structures. Upon achieving baseline resolution for tetrasaccharide epimers, complex mixtures of sulfated GAGs were examined as models for a variety of different applications that require separation prior to structure analysis. A pharmaceutical low molecular weight heparin (LMWH) mixture was first analyzed to determine the limit of detection based on composition and concentration. Although the LMWH mixture was not fully resolved, the mass spectra were significantly simplified and would facilitate tandem mass spectrometry of the various components in this mixture in a high throughput method.

In order to fully comprehend the manner in which glycans interact with proteins, it is essential to know the structure of the carbohydrate. To provide more avenues for sequence coverage and characterization, tandem mass spectrometry experiments were incorporated with the CZE-MS platform. Since tandem MS will be completed with online separation, fast methods for ion activation, such as collision induced dissociation/higher energy collision induced dissociation (CID/HCD) and negative electron transfer dissociation (NETD), are necessary. NETD has been proven to produce the most analytically useful fragments for highly sulfated GAGs compared to CID/HCD [7-9]. On the other hand, low energy collision activation can be beneficial for analysis of lightly-sulfated glycosaminoglycans [10-15]. Both are potential options for sequence analysis in a high throughput manner.

As mentioned previously, this methodology is primarily being developed to solve biological problems. Glycan-protein interactions are important in a variety of systems and can be explored using protein binding assays. Another method to analyze the role sulfated glycans play in biological systems is through extraction. Two different biological applications were analyzed to demonstrate the utility of this platform. Sulfated GAGs were extracted from natural sources,

urine and plasma, and analyzed using capillary zone electrophoresis mass spectrometry with no sample preparation.

**Chapter 4** discusses the application of the CZE-MS and MS/MS platform to examine GAGs present in the urine of healthy human subjects. While others have examined enzymatically digested GAGs in human urine, very little is known about the structures of intact GAGs in such samples. Urinary GAGs were collected and purified from males and females prior to being analyzed [16]. A wide variety of both heparan sulfate (HS) and chondroitin/dermatan sulfate (CS/DS) were detected. Molecular weight analysis suggested the presence of intact GAGs as well as GAG oligosaccharides with the majority of urinary GAGs being oligosaccharides of chain sizes from dp 2-20. The CZE-MS/MS analysis of urinary GAG oligosaccharides from two samples of urine collected from a healthy young adult male and female gave similar profiles having the same 10 most abundant GAG oligosaccharides. With these experiments, GAG chains ranging from dp3-9 could be sequenced including positional isomer hexamers. Interestingly, four of these oligosaccharides contain  $\Delta$ UA residues at their non-reducing end suggesting they might originate from dietary sources. This was the first biological application of the CZE-MS/MS platform for sulfated GAG oligosaccharides.

A second application of the CZE-MS/MS platform focused on larger sulfated oligosaccharides, as described in **Chapter 5**. Glycosaminoglycan chains were released from the proteoglycan bikunin and separated using online CZE combined with low energy collisional activation. Bikunin is plasma proteinase inhibitor with a single chondroitin sulfate (CS) chain covalently attached [17]. In this study, fractions containing a collection of bikunin CS GAG chains of similar size with varying sulfation levels were analyzed. Previous work was reported for these fractions with direct infusion mass spectrometry as the primary tool for analysis [18].

Using capillary zone electrophoresis tandem mass spectrometry, it is possible to simplify the mixture for tandem mass analysis and investigate for potential isomers. The glycosaminoglycan chains ranged from dp20 up to dp57 with four to eleven sulfates with the top 10 most abundant species undergoing collisional activation to provide structural analysis. The sequences obtained from the CZE-MS/MS experiments align with the published literature in which a common motif was observed with most of the sulfate modifications occurring on the reducing end.

Additionally, the presence of isomers was indicated based on multiple peaks containing the same accurate mass measurement corresponding to a single composition. This had not been reported previously which was most likely a result of the low abundance of these species and the inability to separate isomers using direct injection. Unfortunately, the isomeric species were too low in abundance to perform informative tandem mass analysis for sequence coverage. Future work will focus on analyzing a more concentrated sample that is adequate for MS/MS analysis on the lower abundance isomeric species. Overall, this work provides a step forward towards the characterization of large sulfated glycosaminoglycan mixtures from their natural sources in a single online experiment.

Collectively, this work represents separation of glycosaminoglycan standards, and two different applications spanning a wide variety of chain lengths and types of sulfated glycosaminoglycans. Nevertheless, the ultimate goal is to analyze protein-GAG interactions as these play a key role in both human health and disease. Protein binding assays can isolate GAG oligosaccharides which interact with targeted proteins. Using a unified platform for online CZE separations combined with tandem mass analysis, heterogeneous mixtures of highly interacting oligosaccharides can be structurally characterized to determine the pattern of modification that confers specificity in binding. Future applications of this approach will focus on pull down



isolations to analyze known GAG-protein binding interactions. Antithrombin III (ATIII) is a common binding protein that interacts with heparin in anticoagulation pathways and is a good model system. With successful application of the ATIII and Arixtra system, different GAG-protein binding interactions can be analyzed using a protein binding assay followed by CZE-MS/MS analysis of the sulfated oligosaccharides.

## REFERENCES

1. Varki, A., Biological roles of glycans. *Glycobiology* 2017, 27 (1), 3-49.
2. Afratis, N.; Gialeli, C.; Nikitovic, D.; Tsegenidis, T.; Karousou, E.; Theocharis, A. D.; Pavão, M. S.; Tzanakakis, G. N.; Karamanos, N. K., Glycosaminoglycans: key players in cancer cell biology and treatment. *FEBS Journal* 2012, 279 (7), 1177-1197.
3. Barbucci, R.; Magnani, A.; Lamponi, S.; Albanese, A., Chemistry and biology of glycosaminoglycans in blood coagulation. *Polym. Adv. Technol.* 1996, 7 (8), 675-685.
4. Sasisekharan, R.; Shriver, Z.; Venkataraman, G.; Narayanasami, U., Roles of heparan-sulphate glycosaminoglycans in cancer. *Nat. Rev. Cancer* 2002, 2 (7), 521.
5. Varki, A.; Cummings, R.; Esko, J.; Freeze, H.; Hart, G.; Marth, J., *Essentials of glycobiology*. Cold Spring Harbor Laboratory Press, New York 1998, (3rd edition).
6. Sanderson, P.; Stickney, M.; Leach, F. E.; Xia, Q.; Yu, Y.; Zhang, F.; Linhardt, R. J.; Amster, I. J., Heparin/heparan sulfate analysis by covalently modified reverse polarity capillary zone electrophoresis-mass spectrometry. *Journal of Chromatography A* 2018, 1545, 75-83.
7. Wolff, J. J.; Leach, F. E.; Laremore, T. N.; Kaplan, D. A.; Easterling, M. L.; Linhardt, R. J.; Amster, I. J., Negative electron transfer dissociation of glycosaminoglycans. *Analytical chemistry* 2010, 82 (9), 3460-3466.
8. Leach, F. E.; Wolff, J. J.; Xiao, Z.; Ly, M.; Laremore, T. N.; Arungundram, S.; Al-Mafraji, K.; Venot, A.; Boons, G.-J.; Linhardt, R. J.; Amster, I. J., Negative electron transfer dissociation Fourier transform mass spectrometry of glycosaminoglycan carbohydrates. *European Journal of Mass Spectrometry* (Chichester, England) 2011, 17 (2), 167-176.
9. Leach, F. E.; Riley, N. M.; Westphall, M. S.; Coon, J. J.; Amster, I. J., Negative Electron Transfer Dissociation Sequencing of Increasingly Sulfated Glycosaminoglycan

Oligosaccharides on an Orbitrap Mass Spectrometer. *Journal of The American Society for Mass Spectrometry* 2017, 28 (9), 1844-1854.

10. Zaia, J.; Costello, C. E., Compositional Analysis of Glycosaminoglycans by Electrospray Mass Spectrometry. *Analytical Chemistry* 2001, 73 (2), 233-239.

11. Zaia, J.; Costello, C. E., Tandem Mass Spectrometry of Sulfated Heparin-Like Glycosaminoglycan Oligosaccharides. *Analytical Chemistry* 2003, 75 (10), 2445-2455.

12. Zaia, J.; McClellan, J. E.; Costello, C. E., Tandem Mass Spectrometric Determination of the 4S/6S Sulfation Sequence in Chondroitin Sulfate Oligosaccharides. *Analytical Chemistry* 2001, 73 (24), 6030-6039.

13. Kailemia, M. J.; Patel, A. B.; Johnson, D. T.; Li, L.; Linhardt, R. J.; Amster, I. J., Differentiating Chondroitin Sulfate Glycosaminoglycans Using Collision-Induced Dissociation; Uronic Acid Cross-Ring Diagnostic Fragments in a Single Stage of Tandem Mass Spectrometry. *European Journal of Mass Spectrometry* 2015, 21 (3), 275-285.

14. Kailemia, M. J.; Li, L.; Xu, Y.; Liu, J.; Linhardt, R. J.; Amster, I. J., Structurally Informative Tandem Mass Spectrometry of Highly Sulfated Natural and Chemoenzymatically Synthesized Heparin and Heparan Sulfate Glycosaminoglycans. *Molecular & Cellular Proteomics* 2013, 12 (4), 979-990.

15. Kailemia, M. J.; Li, L.; Ly, M.; Linhardt, R. J.; Amster, I. J., Complete Mass Spectral Characterization of a Synthetic Ultralow-Molecular-Weight Heparin Using Collision-Induced Dissociation. *Analytical Chemistry* 2012, 84 (13), 5475-5478.

16. Ha, X.; Sanderson, P.; Nesheiwat, S.; Lin, L.; Yu, Y.; Zhang, F.; Amster, I. J.; Linhardt, R. J., Structural Analysis of Urinary Glycosaminoglycans from Healthy Human Subjects. *Glycobiology* 2019.

17. Varki, A.; Cummings, R. D.; Esko, J. D.; Freeze, H. H.; Stanley, P.; Bertozzi, C. R.; Hart, G. W.; Etzler, M. E., Essentials of Glycobiology. NY, 2009; Vol. 2.
18. Ly, M.; Leach, F. E., 3rd; Laremore, T. N.; Toida, T.; Amster, I. J.; Linhardt, R. J., The proteoglycan bikunin has a defined sequence. Nat. Chem. Biol. 2011, 7 (11), 827-33.

## APPENDIX A

### SUPPLEMENTAL DATA FOR CHAPTER 3

**Table A1. GAG oligomer compositions identified by CE-MS of Enoxaparin**

Neutral Mass	Composition	Error (ppm)
753.01	dp3_3S	2.74
771.02	dp3_3S	3.06
832.96	dp3_4S	1.25
836.01	dp3_4S	3.37
850.97	dp3_4S	2.77
854.94	dp3_4S_Na	1.03
915.97	dp3_5S	2.39
937.95	dp3_5S_Na	2.90
994.03	dp4_4S	1.87
995.92	dp3_6S	2.27
1012.95	dp3_6S_NH3	-1.50
1055.98	dp4_5S (-H2O)	1.50
1073.99	dp4_5S	1.71
1092.00	dp4_5S	2.42
1095.97	dp4_5S_Na	2.50
1153.94	dp4_6S	1.84
1170.97	dp4_6S_NH3	-1.06
1171.95	dp4_6S	0.60
1251.91	dp4_7S	1.93
1268.94	dp4_7S_NH3	-1.02
1329.98	dp5_6S	1.37
1347.00	dp5_6S_NH3	-0.77
1347.99	dp5_6S	1.76
1375.04	dp5_6S_Nac	2.41
1409.93	dp5_7S	2.09
1412.98	dp5_7S	2.04
1426.96	dp5_7S_NH3	0.04
1427.95	dp5_7S	2.55
1443.99	dp5_7S_NH3	-2.71
1453.10	dp6_5S_Nac	2.86
1491.05	dp6_6S	2.25
1492.94	dp5_8S	2.88
1533.06	dp6_6S_Nac	2.22

1571.00	dp6_7S	-0.09
1572.90	dp5_9S	2.78
1588.03	dp6_7S_NH3	-1.28
1589.01	dp6_7S	2.56
1589.92	dp5_9S_NH3	0.29
1606.95	dp5_9S_2NH3	-2.08
1613.01	dp6_7S_Nac	2.14
1630.04	dp6_7S_Nac_NH3	-2.05
1647.06	dp6_7S_Nac_2NH3	-5.25
1650.96	dp6_8S	1.12
1667.99	dp6_8S_NH3	-0.16
1668.97	dp6_8S	1.72
1685.01	dp6_8S_2NH3	-3.06
1730.92	dp6_9S	1.94
1747.94	dp6_9S_NH3	-0.11
1748.93	dp6_9S	2.20
1764.97	dp6_9S_2NH3	-2.22
1765.96	dp6_9S_NH3	0.06
1782.98	dp6_9S_2NH3	-1.31
1826.99	dp7_8S	2.02
1906.95	dp7_9S	2.07
1923.98	dp7_9S_NH3	0.11
1950.12	dp8_7S_Nac	1.96
1986.91	dp7_10S	3.30
1988.06	dp8_8S	1.01
2003.93	dp7_10S_NH3	-0.14
2020.96	dp7_10S_2NH3	-1.44
2030.07	dp8_8S_Nac	0.73
2050.01	dp7_9S_3Nac_NH3	-0.19
2067.04	dp7_9S_3Nac_2NH3	-1.54
2127.06	dp8_9S_Nac_NH3	0.45
2144.08	dp8_9S_Nac_2NH3	-2.32
2147.98	dp8_10S	2.20
2165.00	dp8_10S_NH3	0.28
2182.03	dp8_10S_2NH3	-2.27
2207.01	dp8_10S_Nac_NH3	0.46
2224.04	dp8_10S_Nac_2NH3	-0.23
2227.93	dp8_11S	1.69
2244.96	dp8_11S_NH3	0.70
2261.99	dp8_11S_2NH3	-0.54
2307.89	dp8_12S	1.30
2325.90	dp8_12S	3.40

2341.94	dp8_12S_2NH3	-2.45
2377.99	dp8_10S_2Na	1.42
2775.04	dp9_12S_5NAc_2Na_2NH3	0.44
2804.91	dp10_14S	2.77
2839.95	dp10_14S_NH3	3.15
2855.00	dp9_13S_5NAc_2Na_2NH3	0.45
2971.99	dp10_13S_4NAc_2Na_NH3	1.03
3301.92	dp12_16S	2.21

**APPENDIX B**  
**SUPPLEMENTAL DATA FOR CHAPTER 4**

**Table B.1.** Urine samples collected from healthy human donors.

<b>Age (y)</b>	<b>Race</b>	<b>Label</b>
23	Caucasian	Male 1* (M1*)
25	Caucasian	Male 2* (M2*)
24	Caucasian	Male 3* (M3*)
24	Caucasian	Female 1* (F1*)
23	Caucasian	Female 2* (F2*)
23	Caucasian	Female 3* (F3*)
35	Caucasian	Male 1 (M1)
39	Caucasian	Male 2 (M2)
39	Hispanic	Male 3 (M3)
45	Caucasian	Female 1 (F1)
38	Caucasian	Female 2 (F2)
35	Caucasian	Female 3 (F3)



**Table B.2.** Total GAG concentration in urine samples.

	Total GAGs (µg/mL)			Normalized Total GAGs (µg/mL)	
	MRM	Carbozole	Creatinine	MRM	Carbozole
<b>M1</b>	24	2	12.65	19	2
<b>M2</b>	29	46	5.2	55	88
<b>M3</b>	3	8	3.6	7	23
<b>F1</b>	19	39	5.89	33	65
<b>F2</b>	2	(-26)	2.6	7	(-100)
<b>F3</b>	33	171	14.37	23	119
<b>M1*</b>	40	195	15.82	25	123
<b>M2*</b>	21	303	4.79	44	633
<b>M3*</b>	44	118	13.01	34	91
<b>F1*</b>	4.7	13	2.23	21	59
<b>F2*</b>	48.99	125.2	6.83	72	183
<b>F3*</b>	31.65	48.1	13.48	23	36

**Table B.3.** Creatinine normalized HS and CS disaccharide composition of urinary GAGs

<b>HS (μg/mL)</b>								
	<b>TriS</b>	<b>NS6S</b>	<b>NS2S</b>	<b>NS</b>	<b>2S6S</b>	<b>6S</b>	<b>2S</b>	<b>0S</b>
<b>M1</b>	0.12	0.17	0.26	0.81	0.00	0.39	0.03	6.13
<b>M2</b>	0.07	0.19	0.28	0.78	0.00	0.28	0.02	17.61
<b>M3</b>	0.01	1.41	0.93	3.29	0.01	0.88	0.00	21.24
<b>F1</b>	0.00	0.16	0.14	0.37	0.00	0.16	0.00	16.14
<b>F2</b>	0.01	2.66	1.59	5.29	0.02	1.39	0.01	27.49
<b>F3</b>	0.25	0.18	0.92	1.90	0.00	0.71	0.05	2.94
<b>M1*</b>	0.11	0.11	0.41	1.15	0.00	0.53	0.03	3.97
<b>M2*</b>	0.26	0.49	1.00	3.16	0.00	1.65	0.21	14.11
<b>M3*</b>	0.21	0.22	0.55	1.48	0.00	0.58	0.05	4.60
<b>F1*</b>	0.18	1.81	3.06	6.47	0.00	2.64	0.12	30.57
<b>F2*</b>	0.35	0.43	1.12	2.75	0.00	1.26	0.08	8.64
<b>F3*</b>	0.14	0.29	0.63	1.22	0.00	0.53	0.04	4.57
<b>CS (μg/mL)</b>								
	<b>TriS</b>	<b>2S4S</b>	<b>2S6S</b>	<b>4S6S</b>	<b>4S</b>	<b>6S</b>	<b>2S</b>	<b>0S</b>
<b>M1</b>	0.00	0.41	0.34	0.61	5.52	0.64	0.12	0.26
<b>M2</b>	0.01	2.14	0.83	4.01	10.17	0.54	0.49	1.04
<b>M3</b>	0.03	0.13	0.54	0.63	20.63	3.19	0.01	2.62
<b>F1</b>	0.03	1.47	0.50	2.60	10.30	1.07	0.11	0.89
<b>F2</b>	2.28	0.73	0.10	0.12	27.36	5.07	1.52	1.29
<b>F3</b>	0.01	0.78	0.48	1.23	3.37	0.63	0.14	0.32
<b>M1*</b>	0.01	0.26	0.08	0.52	3.74	1.06	0.04	0.62
<b>M2*</b>	0.02	0.34	0.63	1.35	12.69	2.81	0.17	2.86
<b>M3*</b>	0.00	0.30	0.15	0.57	4.10	1.51	0.07	0.99
<b>F1*</b>	0.02	0.92	0.85	1.45	25.36	13.96	0.17	2.11
<b>F2*</b>	0.00	1.01	0.33	1.03	9.45	2.30	0.29	0.23
<b>F3*</b>	0.00	0.31	0.17	0.41	4.88	1.38	0.04	0.22

**Table B.4.** Composition and isomer components

Degree of Polymerization	Molecular Weight	Structure Notation*	Number of Isomers*	
			Male	Female
2	417.057	[1,0,1,0,1]	1	-
2	477.078	[0,1,1,1,1]	1	-
2	497.014	[1,0,1,0,2]	1	-
2	576.968	[1,0,1,0,3]	0	0
2	594.976	[0,1,1,1,3]	2	-
3	676.091	[0,1,2,0,2]	1	-
3	718.101	[0,1,2,1,2]	2	-
3	753.001	[1,1,1,0,3]	2	-
3	756.048	[0,1,2,0,3]	3	-
3	798.059	[0,1,2,1,3]	1	-
3	817.994	[1,0,2,0,4]	2	-
3	832.958	[1,1,1,0,4]	2	-
3	835.996	[0,1,2,0,4]	3	1
3	850.968	[0,2,1,0,4]	2	-
3	878.015	[0,1,2,1,4]	3	-
3	915.962	[0,1,2,0,5]	1	1
3	995.916	[0,1,2,0,6]	1	-
4	834.113	[1,1,2,0,2]	1	-
4	936.145	[0,2,2,2,2]	3	-
4	974.092	[0,2,2,1,3]	4	-
4	994.024	[1,1,2,0,4]	4	1
4	1012.038	[0,2,2,0,4]	4	-
4	1016.100	[0,2,2,2,3]	-	3
4	1036.039	[1,1,2,1,4]	3	-
4	1054.049	[0,2,2,1,4]	4	-
4	1073.981	[1,1,2,0,5]	3	3
4	1091.992	[0,2,2,0,5]	3	-
4	1096.060	[0,2,2,2,4]	1	1
4	1115.995	[1,1,2,1,5]	1	-
4	1153.938	[1,1,2,0,6]	1	1
4	1171.949	[0,2,2,0,6]	2	2
5	1212.068	[1,2,2,1,4]	1	-
5	1219.179	[0,2,3,3,3]	5	4
5	1250.016	[1,2,2,0,5]	1	-
5	1257.137	[0,2,3,2,4]	2	-
5	1295.072	[0,2,3,1,5]	6	-

5	1299.136	[0,2,3,3,4]	3	6
5	1315.008	[1,1,3,0,6]	2	-
5	1329.972	[1,2,2,0,6]	1	-
5	1333.018	[0,2,3,0,6]	5	-
5	1375.029	[0,2,3,1,6]	3	3
5	1379.093	[0,2,3,3,5]	1	2
5	1394.966	[1,1,3,0,7]	1	2
5	1412.973	[0,2,3,0,7]	3	4
5	1454.002	[0,3,2,2,6]	0	-
5	1492.931	[0,2,3,0,8]	1	1
5	1511.960	[0,3,2,2,7]	1	-
5	1572.892	[0,2,3,0,9]	1	-
6	1377.200	[1,2,3,3,3]	-	3
6	1395.213	[0,3,3,3,3]	4	-
6	1453.091	[1,2,3,1,5]	0	-
6	1475.170	[0,3,3,3,4]	-	4
6	1491.042	[1,2,3,0,6]	2	-
6	1533.048	[1,2,3,1,6]	0	-
6	1552.984	[0,3,3,0,6]	0	-
6	1555.130	[0,3,3,3,5]	-	1
6	1570.995	[1,2,3,0,7]	0	-
6	1613.006	[1,2,3,1,7]	0	0
6	1631.020	[0,3,3,1,7]	1	-
6	1632.945	[0,3,3,0,7]	0	-
6	1635.080	[0,3,3,3,6]	-	1
6	1650.952	[1,2,3,0,8]	0	3
6	1668.965	[0,3,3,0,8]	2	-
6	1730.912	[1,2,3,0,9]	1	-
6	1748.920	[0,3,3,0,9]	2	-
7	1572.160	[1,2,4,0,5]	-	1
7	1598.293	[0,3,4,4,3]	4	3
7	1678.244	[0,3,4,4,4]	5	3
7	1716.204	[0,3,4,3,5]	3	-
7	1758.204	[0,3,4,4,5]	3	0
7	1838.161	[0,3,4,4,6]	2	3
7	1891.980	[1,2,4,0,9]	2	-
7	2103.956	[1,2,4,4,9]	0	-
8	1752.248	[1,3,4,2,4]	0	-
8	1774.325	[0,4,4,4,3]	3	-
8	1854.281	[0,4,4,4,4]	3	-

8	1934.238	[0,4,4,4,5]	1	-
8	2012.056	[0,4,4,1,7]	0	-
8	2030.066	[1,3,4,1,8]	2	-
8	2110.023	[1,3,4,1,9]	1	-
8	2138.011	[1,3,4,2,8]	1	-
9	1791.358	[1,3,5,1,3]	2	-
9	1871.307	[1,3,5,1,4]	2	-
9	1977.395	[0,4,5,5,3]	5	-
9	2057.360	[0,4,5,5,4]	2	-
9	2137.315	[0,4,5,5,5]	3	3
9	2175.272	[0,4,5,4,6]	3	-

\*Structure Notation: [ $\Delta$ HexA, HexA, HexN, Ac, SO<sub>3</sub>]

¥ Dash (-) indicates not present in sample; 0 indicates only one species detected for that molecular weight

**APPENDIX C**  
**SUPPLEMENTAL DATA FOR CHAPTER 5**

**Table C.1.** Glycosaminoglycan compositions in fraction 50.

Fraction 50				
dp	Number of Sulfate Modifications			
20	4			
21	4	5		
22	4			
23	4	5	6	
24	3	4	5	6
25	4	5	6	7
26	4	5	6	7
27	5	6	7	8
28	6	7	8	
29	7	8	9	
30	5			
31	6	8		
33	6			
35	6			
37	5			

**Table C.2.** Glycosaminoglycan compositions in fraction 55.

Fraction 55					
dp	Number of Sulfate Modifications				
21	3	4			
22					
23	3	4	5		
24	4	5	6		
25	3	4	5	6	7
26	3	4	5	6	7
27	4	5	6	7	8
28	4	5	6	7	8
29	4	5	6	7	8
30	6	7	8	9	
31	4	7	8	9	
32	7	9			
33					
34	6	8			

**Table C.3.** Glycosaminoglycan compositions in fraction 63.

Fraction 63						
dp	Number of Sulfate Modifications					
23	2	3	4			
24						
25	2	3	4	5	6	
26						
27	2	3	4	5	6	7
28	7					
29	3	4	5	6	7	8
30	5	6	7	8		
31	4	5	6	7	8	
32	5	6	7			
33	5	6	7	8	9	
34	6	7	8	9		
35	7	8	9			
36	8	9				
37	7					

**Table C.4.** Glycosaminoglycan compositions in fraction 72.

Fraction 72						
dp	Number of Sulfate Modifications					
27	3	4	5			
28						
29	2	3	4	5	6	
30	4	5	6			
31	3	4	5	6	7	
32	4	5	6	7		
33	3	4	5	6	7	8
34	4	5	6	7		
35	4	5	6	7	8	
36	5	6	7			
37	6	7	8			
38	6	7	8			
39	7					

**Table C.5.** Glycosaminoglycan compositions in fraction 92.

Fraction 92							
dp	Number of Sulfate Modifications						
35	2	3	4	5			
36	6						
37	3	4	5	6	8		
38	5	6	7				
39	3	4	5	6	7	9	
40	5	6	7	8	9		
41	3	4	5	6	7	8	9
42	5	6	7	8			
43	4	5	7	8	9		
44	3	5	6	8			
45	7	8	9				
46	6						



**Table C.6.** Glycosaminoglycan compositions in fraction 101.

Fraction 101							
dp	Number of Sulfate Modifications						
39	5						
40							
41	5	6					
42	6	8	9				
43	5	6	7	8	9		
44	5	6	7	8	9	10	11
45	5	6	7	8	9		
46	6	7	8	9	10		
47	5	6	7	8	10		
48	6	8	9	10	11		
49	6	7	8	9			
50	10						

**Table C.7.** Glycosaminoglycan compositions in fraction 117.

Fraction 117			
dp	Number of Sulfate Modifications		
43	5	6	
44			
45	5	6	
46			
47	5	6	7
48	7	8	9
49	5	6	7
50	7	8	9
51	5	6	
52	7	9	
53	5	6	7
54	8	9	
55	5	6	7
56			
57	6		

**Table C.8.** Glycosaminoglycan compositions in all fractions.

<b>GAG Length (dp)</b>	<b>Number of Sulfate Modifications</b>							
20	4							
21	3	4	5					
22	4							
23	2	3	4	5	6			
24	3	4	5	6				
25	2	3	4	5	6	7		
26	3	4	5	6	7			
27	2	3	4	5	6	7	8	
28	4	5	6	7	8			
29	2	3	4	5	6	7	8	9
30	4	5	6	7	8	9		
31	3	4	5	6	7	8	9	
32	4	5	6	7	9			
33	3	4	5	6	7	8	9	
34	4	5	6	7	8	9		
35	2	3	4	5	6	7	8	9
36	5	6	7	8	9			
37	3	4	5	6	7	8		
38	5	6	7	8				
39	3	4	5	6	7	9		
40	5	6	7	8	9			
41	3	4	5	6	7	8	9	
42	5	6	7	8	9			
43	4	5	6	7	8	9		
44	3	5	6	7	8	9	10	11
45	5	6	7	8	9			
46	6	7	8	9	10			
47	5	6	7	8	10			
48	6	7	8	9	10	11		
49	5	6	7	8	9			
50	7	8	9	10				
51	5	6						
52	7	9						
53	5	6	7					
54	8	9						
55	5	6	7					
56								
57	6							

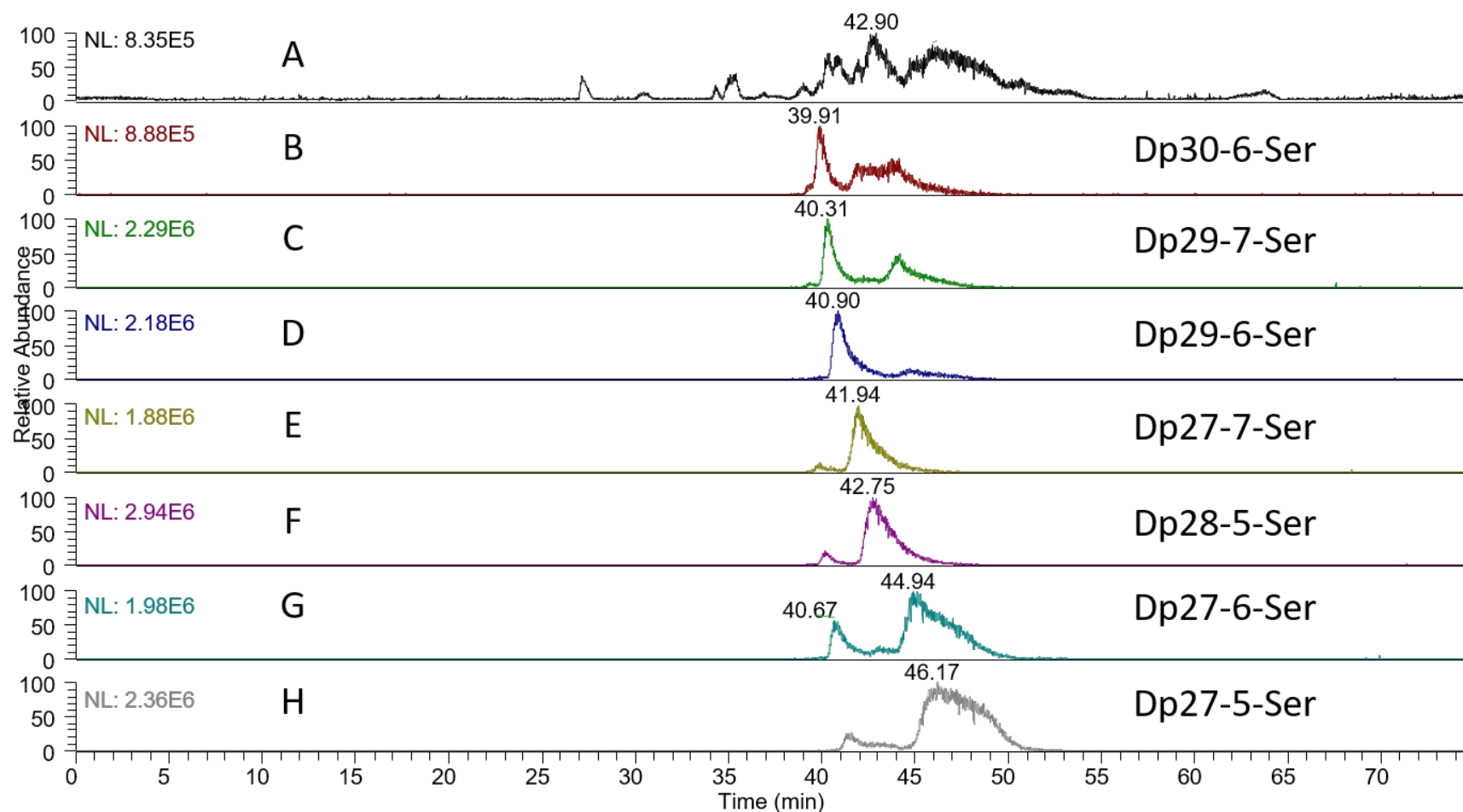


**Figure C.1.** Base peak (A, BPE) and extraction ion electropherograms (B-E, XIE) of the seven most abundant glycosaminoglycans in fraction 55: B) dp30-6-Ser, C) dp29-7-Ser, D) dp29-6-Ser, E) dp27-7-Ser, F) dp28-5-Ser, G) dp27-6-Ser, and H) dp27-5-Ser.

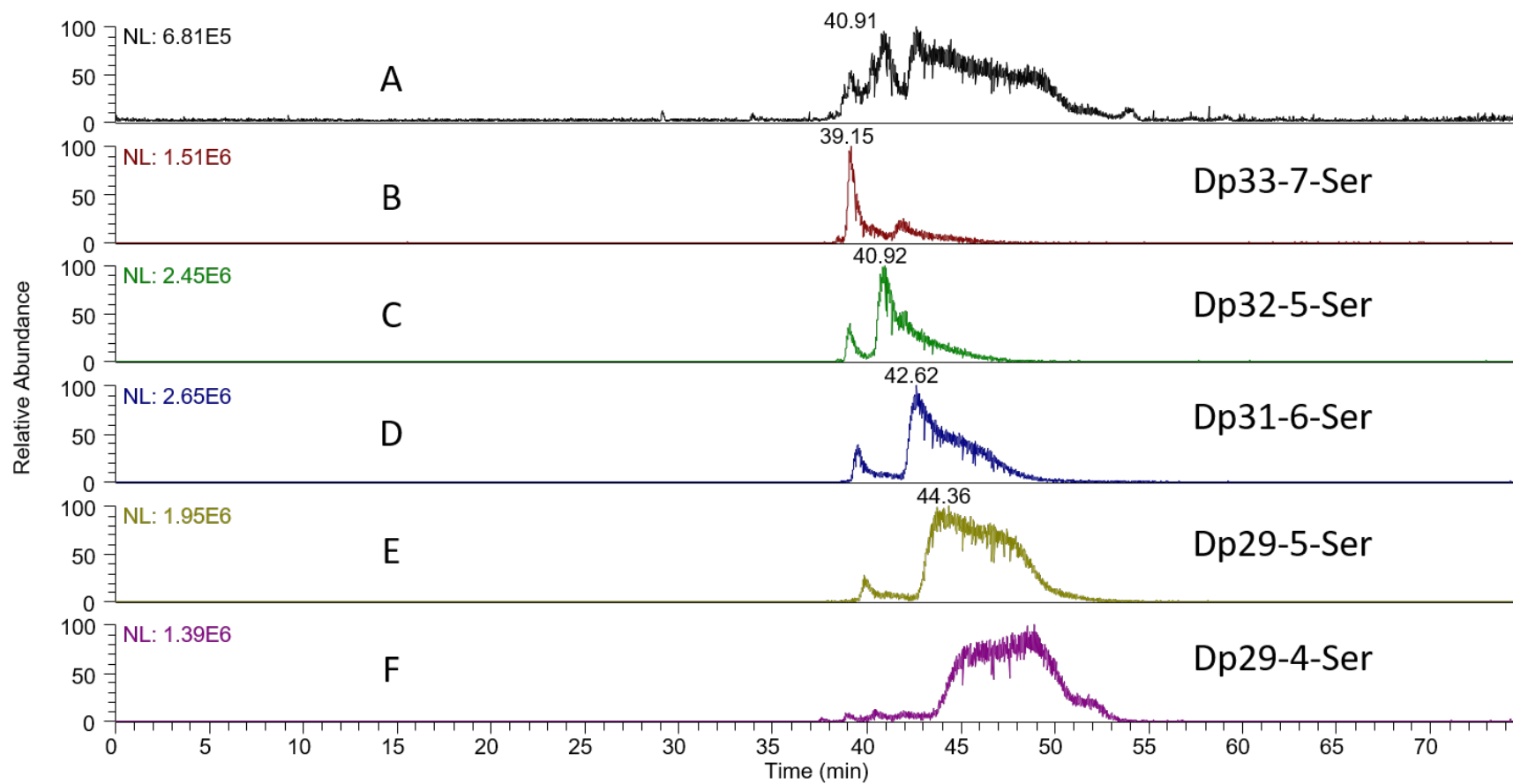


**Figure C.2.** Base peak (A, BPE) and extraction ion electropherograms (B-F, XIE) of the five most abundant glycosaminoglycans in fraction 63: B) dp33-7-Ser, C) dp32-5-Ser, D) dp31-6-Ser, E) dp29-5-Ser, and F) dp29-4-Ser.

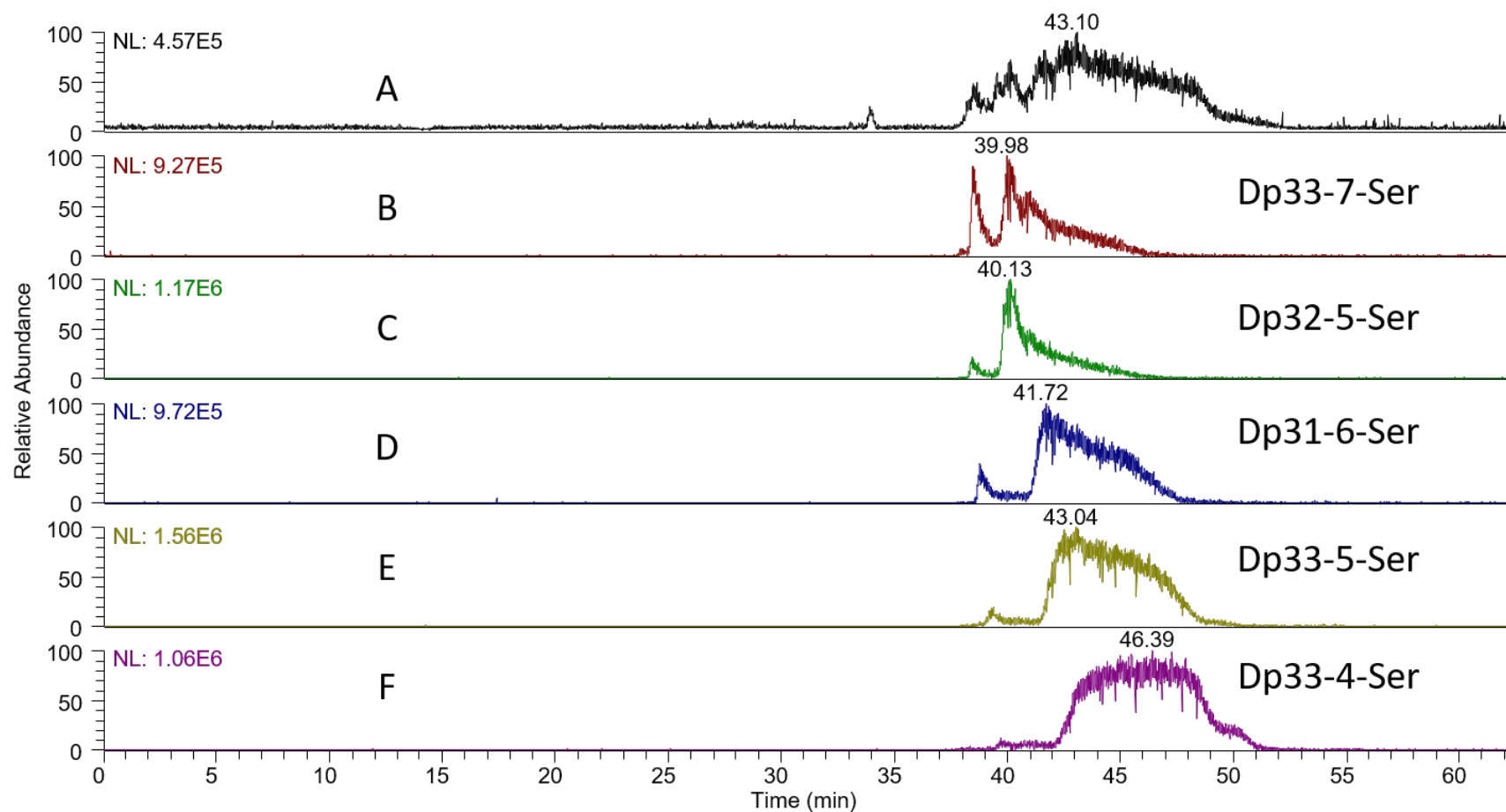


**Figure C.3.** Base peak (A, BPE) and extraction ion electropherograms (B-F, XIE) of the five most abundant glycosaminoglycans in fraction 72: B) dp33-7-Ser, C) dp32-5-Ser, D) dp31-6-Ser, E) dp33-5-Ser, and F) dp33-4-Ser.

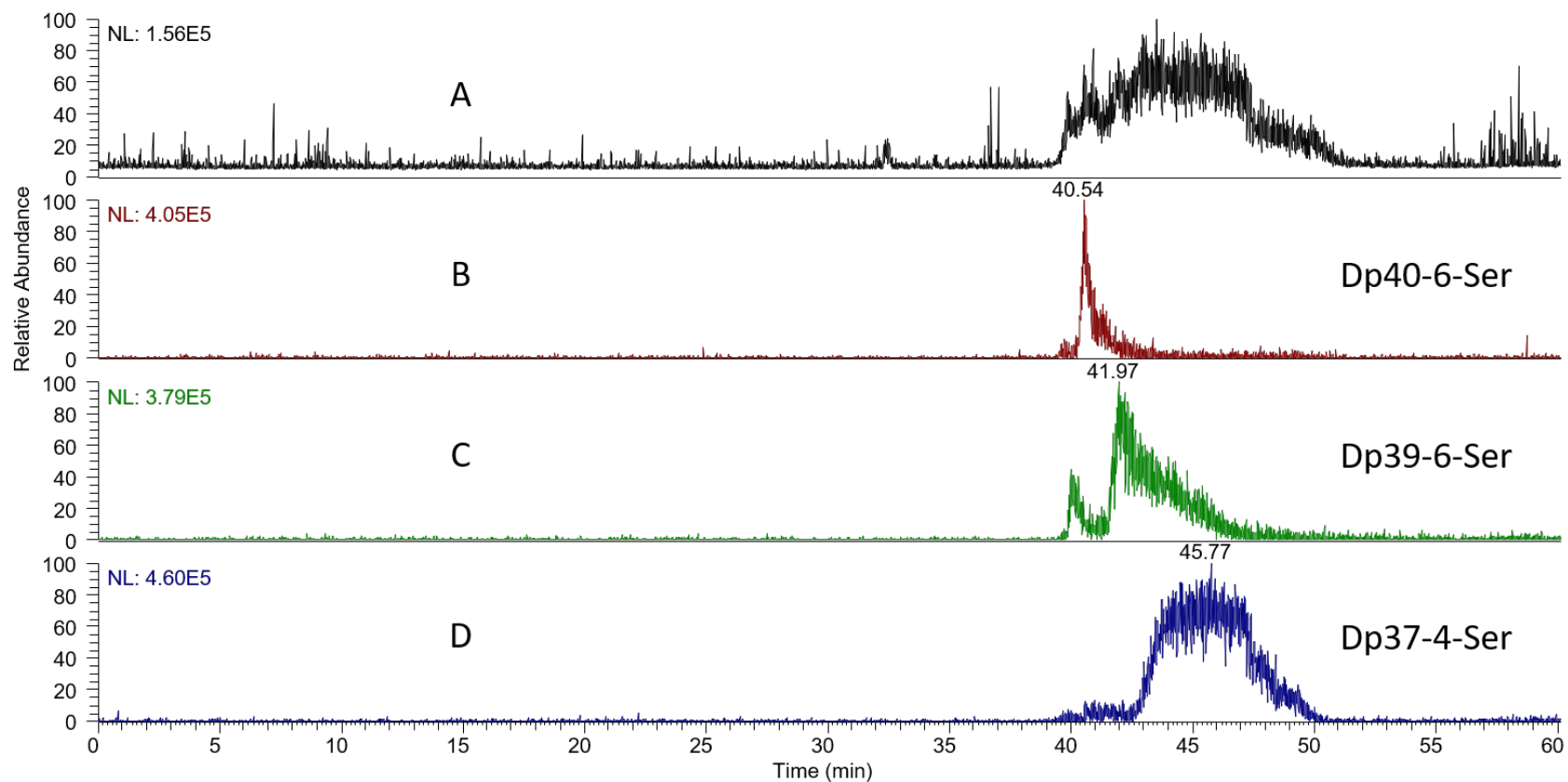


**Figure C.4.** Base peak (A, BPE) and extraction ion electropherograms (B-D, XIE) of the three most abundant glycosaminoglycans in fraction 92: B) dp40-6-Ser, C) dp39-6-Ser, and D) dp37-4-Ser.

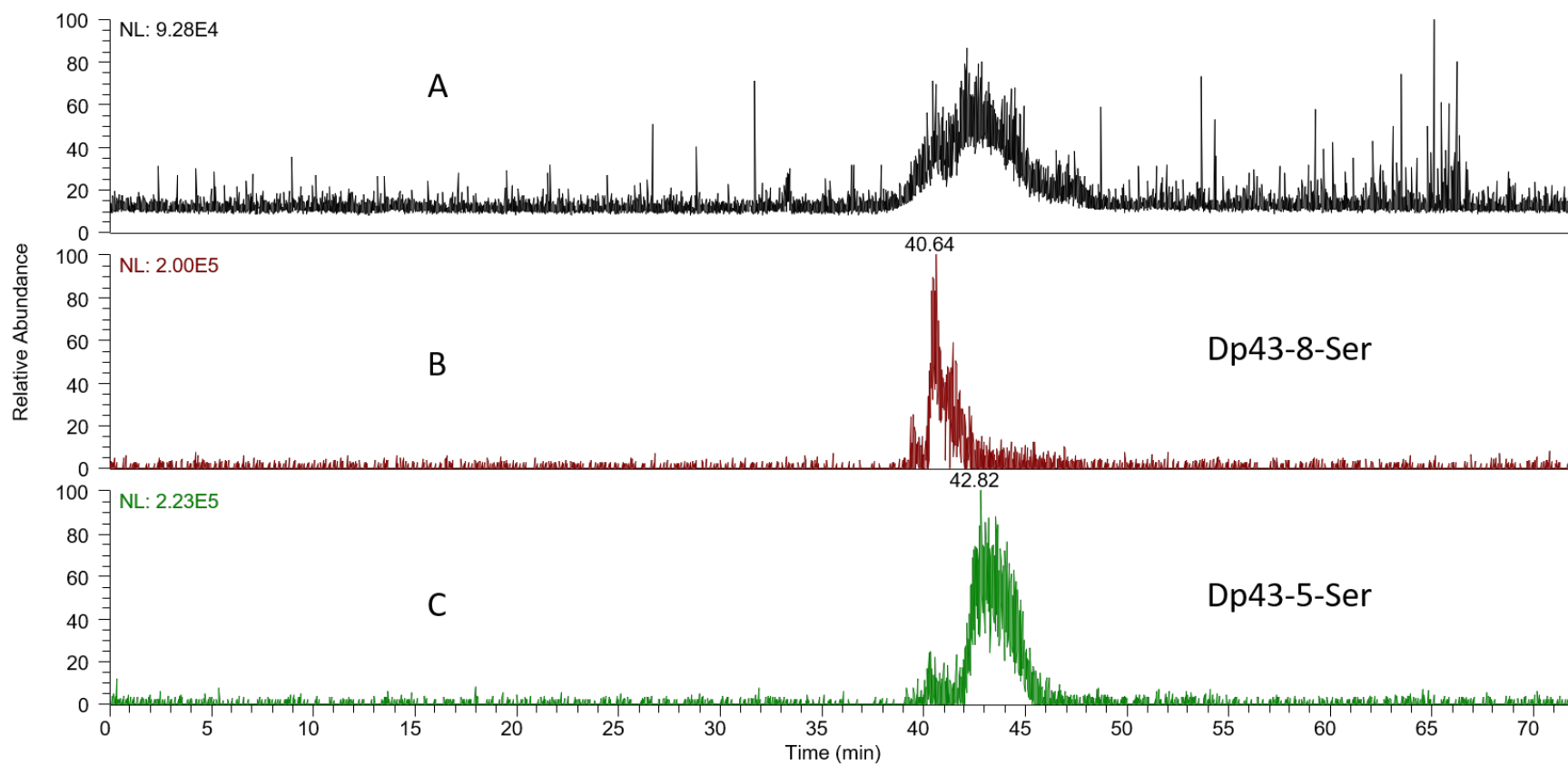


**Figure C.5.** Base peak (A, BPE) and extraction ion electropherograms (B & C, XIE) of the two most abundant glycosaminoglycans in fraction 101: B) dp43-8-Ser and C) dp43-5-Ser.

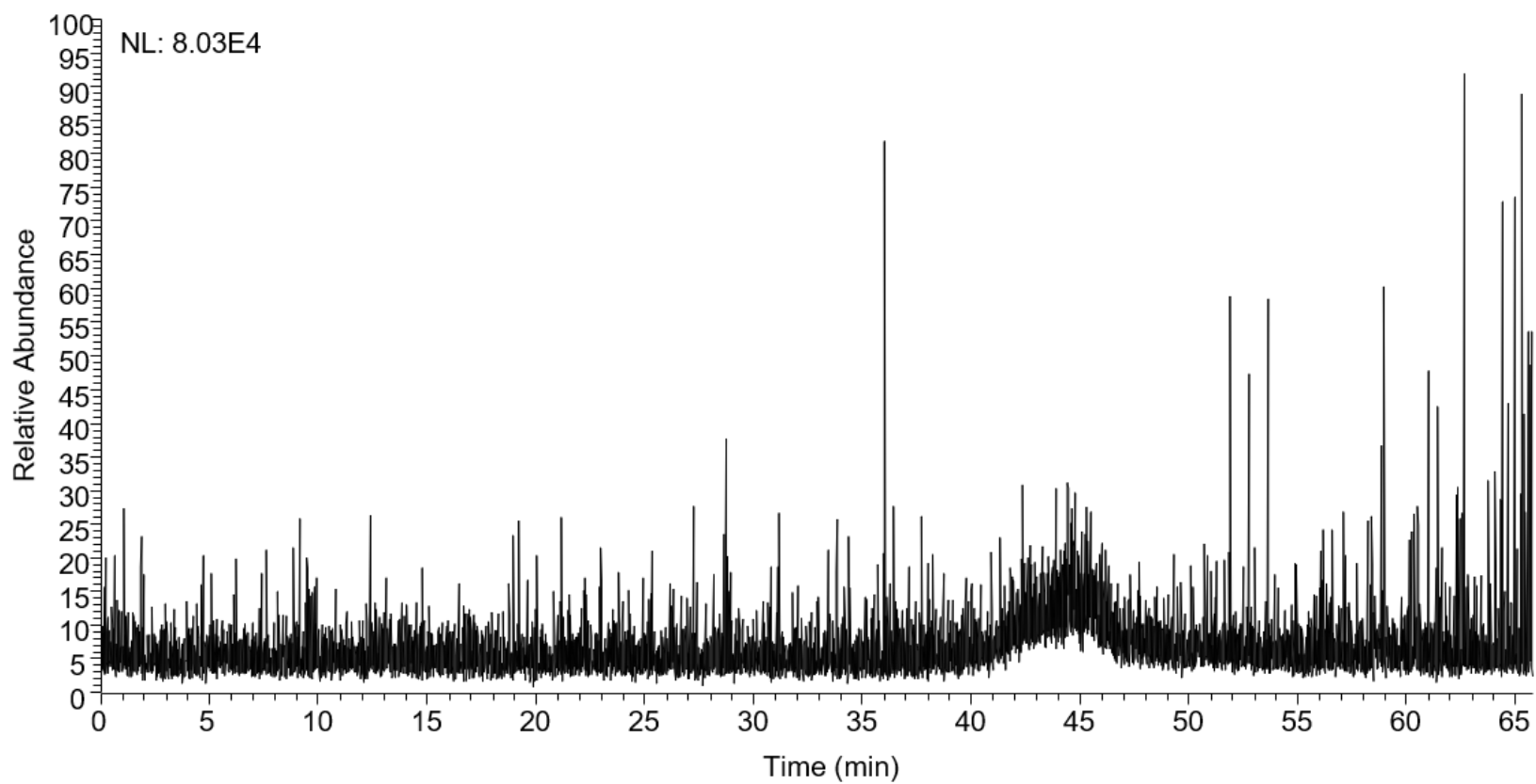


**Figure C.6.** Base peak electropherograms (BPE) of the glycosaminoglycans in fraction 117.



**Table C.9.** Assignment of HCD fragment ions of  $m/z$  1281.7931<sup>4+</sup> from dp25-5-Ser in fraction 50 with sulfo modifications on residues 11, 15, 19, 21, and 23.

Mass to charge	Relative Intensity (%)	Fragment Type	Accuracy PPM	Theoretical Ion $m/z$	Charge
549.1002	13.88	Y5	1.46	549.1010	2
581.1830	0.13	B3	0.96	581.1836	1
637.1158	0.53	Y6	1.96	637.1170	2
640.1394	28.05	Y3	2.51	640.1410	1
703.8013	0.16	Y10	1.26	703.8022	3
738.6553	8.15	Y7-S	1.94	738.6567	2
757.2148	4.05	B8	1.12	757.2156	2
757.2148	4.05	B4	1.12	757.2156	1
771.4941	0.71	Y11-S	1.57	771.4953	3
816.1713	5.35	Y4	2.20	816.1731	1
826.6712	6.23	Y8-S	1.91	826.6728	2
830.1711	0.65	Y12-S	1.89	830.1727	3
897.8639	1.09	Y13-S	2.11	897.8658	3
928.2107	3.37	Y9-S	1.90	928.2125	2
956.5412	0.38	Y14-S	2.05	956.5432	3
960.2942	0.67	B5	0.85	960.2950	1
1016.2266	5.26	Y10-S	1.88	1016.2285	2
1019.2498	0.67	Y5-S	2.62	1019.2525	1
1024.2339	0.57	Y15-2S	2.33	1024.2363	3
1082.9109	0.44	Y16-2S	2.54	1082.9136	3
1116.2536	0.29	Y22-S	2.34	1116.2562	4
1117.7658	0.53	Y11-2S	2.14	1117.7682	2
1136.3253	1.29	B6	1.59	1136.3271	1
1142.5303	0.16	Z23-2S	3.42	1142.5342	4
1147.0364	0.20	Y23-2S	0.40	1147.0369	4
1150.6053	0.41	Y17-2S	1.28	1150.6068	3
1162.5184	0.14	Z23-S	4.31	1162.5234	4
1167.0249	0.32	Y23-S	0.99	1167.0261	4
1195.2822	0.36	Y6-S	1.97	1195.2846	1
1201.8271	0.11	[M-4H]2- -4S	7.66	1201.8363	4
1205.7821	0.13	Y12-2S	1.77	1205.7842	2
1209.2829	0.84	Y18-2S	1.02	1209.2841	3
1211.0348	0.18	Y24-S	-0.60	1211.0341	4
1221.8237	8.99	[M-4H]2- -3S	1.49	1221.8255	4
1241.8129	36.56	[M-4H]2- -2S	1.46	1241.8147	4
1250.3269	0.12	Y19-3S	-1.53	1250.3250	3
1257.3237	0.18	B19-S	0.85	1257.3248	3

1261.8023	32.31	[M-4H]2- -S	1.29	1261.8039	4
1276.9737	0.26	Y19-2S	2.78	1276.9773	3
1283.9763	0.07	B19	0.87	1283.9770	3
1316.0003	0.25	B20-S	1.39	1316.0021	3
1335.6534	0.24	Y20-2S	0.91	1335.6546	3
1339.4073	0.17	B7	-0.61	1339.4065	1
1342.6569	0.21	B20	-0.73	1342.6544	3
1383.6935	0.21	B21-2S	1.27	1383.6953	3
1403.3452	0.15	Y21-2S	1.81	1403.3477	3
1410.3477	0.69	B21-S	-0.12	1410.3475	3
1442.3725	1.05	B22-2S	0.08	1442.3726	3
1462.0227	0.11	Y22-2S	1.65	1462.0251	3
1467.3998	0.69	B15-S	0.77	1467.4009	2
1469.0237	1.16	B22-S	0.81	1469.0249	3
1555.4176	0.44	B16-S	-0.40	1555.4170	2
1595.3973	0.18	B16	-1.20	1595.3954	2
1696.9403	0.19	B17	-3.08	1696.9351	2
1974.5111	0.23	B20-S	-2.16	1974.5068	2

**Table C.10.** Assignment of HCD fragment ions of  $m/z$  1101.0518<sup>5-</sup> from dp27-5-Ser in fraction 55 with sulfo modifications on residues 13, 17, 21, 23, and 25.

Mass to charge	Relative Intensity	Type	Accuracy PPM	Theoretical Ion $m/z$	Charge
518.7532	0.29	Y7	2.19	518.7543	3
549.0999	11.11	Y5	2.01	549.1010	2
581.1823	1.32	B3	2.16	581.1836	1
618.4707	0.15	Y9-S	2.99	618.4726	3
637.1153	0.99	Y6	2.74	637.1170	2
640.1392	26.21	Y3	2.83	640.1410	1
645.1234	6.05	Y9	2.20	645.1248	3
646.1246	0.65	Y15	-4.67	646.1216	5
693.1349	0.71	Y13	2.64	693.1367	4
698.6763	0.79	Y7-2S	2.90	698.6783	2
703.8005	1.64	Y10	2.39	703.8022	3
736.2140	0.19	Y4-S	3.10	736.2163	1
737.1427	0.09	Y14	2.79	737.1448	4
738.6552	10.69	Y7-S	2.08	738.6567	2
744.8412	0.95	Y11-2S	2.47	744.8430	3
757.2147	5.22	B4	1.25	757.2156	1
767.9238	0.10	Y15-2S	2.07	767.9254	4
771.4937	8.27	Y11-S	2.09	771.4953	3
787.9127	0.99	Y15-S	2.41	787.9146	4
811.9311	0.10	Y16-2S	2.85	811.9334	4
816.1711	2.07	Y4	2.45	816.1731	1
826.6706	1.28	Y8-S	2.63	826.6728	2
830.1703	1.08	Y14-S	2.86	830.1727	3
831.9205	0.20	Y16-S	2.55	831.9226	4
862.7012	0.34	Y17-2S	2.39	862.7033	4
867.7585	0.12	C9	2.44	867.7606	2
871.2112	0.66	Y13-2S	2.67	871.2135	3
882.6904	0.32	Y17-S	2.34	882.6925	4
888.2318	0.84	Y9-2S	2.54	888.2341	2
897.8645	3.27	Y13-S	1.44	897.8658	3
906.7090	0.24	Y18-2S	2.51	906.7113	4
926.6990	0.13	Y18-S	1.60	926.7005	4
928.2108	3.75	Y9-S	1.79	928.2125	2
939.2927	0.25	Y5-2S	3.15	939.2957	1
942.7394	0.11	B19	2.50	942.7418	4
946.7693	0.78	B10	2.19	946.7714	2
946.7693	0.78	B20-2S	2.19	946.7714	4
956.5413	0.17	Y14-S	1.94	956.5432	3

957.4790	0.72	Y19-2S	2.22	957.4811	4
960.2931	1.30	B5	2.00	960.2950	1
976.2474	0.10	Y10-2S	2.77	976.2501	2
977.4663	0.15	Y19-S	4.12	977.4703	4
986.7480	1.50	B20	1.81	986.7498	4
989.6441	0.24	Z25-2S	4.15	989.6482	5
993.2482	0.21	Y25-2S	2.13	993.2503	5
997.5816	0.28	Y15-3S	2.42	997.5840	3
1001.4870	0.34	Y20-2S	2.14	1001.4891	4
1009.2419	0.11	Y25-S	-0.22	1009.2417	5
1016.2260	1.02	Y10-S	2.47	1016.2285	2
1019.2501	2.23	Y5-S	2.32	1019.2525	1
1024.2342	0.55	Y15-2S	2.03	1024.2363	3
1024.8527	0.22	Z26-2S	1.88	1024.8546	5
1025.2512	0.95	C26-2S	6.20	1025.2576	5
1028.4534	0.07	Y26-2S	3.24	1028.4567	5
1032.2673	0.08	Y21-3S	2.41	1032.2698	4
1036.6069	0.23	B16	1.92	1036.6089	3
1037.0880	0.14	[M-5H]5- -4S	1.82	1037.0899	5
1041.2487	0.13	C26-S	0.21	1041.2489	5
1048.3096	0.15	B11	1.39	1048.3111	2
1052.2605	0.73	Y21-2S	-1.44	1052.2590	4
1053.0797	5.32	[M-5H]5- -3S	1.47	1053.0812	5
1057.5076	0.09	B21	1.16	1057.5088	4
1069.0714	28.08	[M-5H]5- -2S	1.13	1069.0726	5
1072.2457	0.08	Y21-S	2.32	1072.2482	4
1076.2735	0.08	Y22-3S	4.00	1076.2778	4
1081.5255	0.81	B22-S	1.99	1081.5276	4
1085.0614	9.24	[M-5H]5- -S	2.37	1085.0640	5
1096.2649	0.13	Y22-2S	1.92	1096.2670	4
1101.0630	0.41	[M-5H]5-	-6.96	1101.0553	5
1101.5163	0.11	B22	0.50	1101.5169	4
1104.3000	0.62	B17-S	1.82	1104.3020	3
1117.7663	0.44	Y11-2S	1.69	1117.7682	2
1123.9523	0.18	Y17-3S	1.96	1123.9545	3
1127.0460	0.15	Y23-3S	1.46	1127.0476	4
1130.9517	0.10	B17	2.29	1130.9543	3
1132.2950	0.44	B23-2S	2.20	1132.2975	4
1136.3259	4.51	B12	1.06	1136.3271	2
1136.3259	4.51	B6	1.06	1136.3271	1
1136.3259	4.51	B18-2S	1.06	1136.3271	3
1147.0349	0.37	Y23-2S	1.70	1147.0369	4
1150.6052	0.09	Y17-2S	1.36	1150.6068	3
1152.2847	0.17	B23-S	1.73	1152.2867	4

1156.3143	0.96	B24-3S	1.74	1156.3163	4
1162.9777	1.56	B18-S	1.44	1162.9794	3
1176.3040	5.37	B24-2S	1.29	1176.3055	4
1189.6301	0.48	B18	1.30	1189.6316	3
1191.0422	0.07	B24-2S	2.25	1191.0449	4
1195.2816	0.75	Y6-S	2.47	1195.2846	1
1196.2914	1.86	B24-S	2.77	1196.2947	4
1216.2819	1.85	B24	1.66	1216.2839	4
1230.6714	0.16	B19-S	0.89	1230.6725	3
1237.8658	0.18	B13-S	0.80	1237.8668	2
1257.3234	0.10	B19	1.09	1257.3248	3
1262.6956	0.30	B20-2S	1.58	1262.6976	3
1277.8437	0.15	B13	1.17	1277.8452	2
1289.3484	2.41	B20-S	1.14	1289.3499	3
1316.0007	0.77	B20	1.09	1316.0021	3
1325.8814	2.58	B14-S	1.08	1325.8828	2
1339.4060	1.00	B7	0.36	1339.4065	1
1365.8603	0.86	B14	0.69	1365.8612	2
1389.0675	0.19	B22-3S	0.42	1389.0681	3
1398.3618	0.09	Y7-S	1.52	1398.3639	1
1415.7204	1.32	B22-2S	-0.04	1415.7204	3
1427.4243	0.16	B15-S	-1.25	1427.4225	2
1442.3729	0.39	B22-S	-0.19	1442.3726	3
1467.4025	0.14	B15	-1.07	1467.4009	2
1515.4383	4.67	B8	0.18	1515.4386	1
1515.4383	4.67	B16-S	0.18	1515.4386	2
1555.4183	1.20	B16	-0.85	1555.4170	2
1595.3973	0.35	B24-S	-1.20	1595.3954	3
1656.9614	0.08	B17-S	-2.86	1656.9567	2
1704.9976	0.71	B18-2S	-1.94	1704.9943	2
1718.5196	0.24	B9	-0.97	1718.5179	1
1744.9745	0.39	B18-S	-1.03	1744.9727	2
1894.5530	0.70	B10	-1.57	1894.5500	1
1894.5530	0.70	B20-2S	-1.57	1894.5500	2

**Table C.11.** Assignment of HCD fragment ions of  $m/z$  1117.0426<sup>5-</sup> from dp27-6-Ser in fraction 55 with sulfo modifications on residues 9, 13, 17, 21, 23, and 25.

Mass to charge	Relative Intensity	Type	Accuracy PPM	Theoretical Ion $m/z$	Charge
518.7527	0.30	Y7	3.15	518.7543	3
549.0994	29.03	Y5	2.92	549.1010	2
581.1816	1.10	B3	3.37	581.1836	1
637.1145	1.74	Y6	4.00	637.1170	2
640.1385	44.88	Y3	3.92	640.1410	1
645.1224	7.25	Y9	3.75	645.1248	3
693.1341	0.53	Y13	3.80	693.1367	4
703.7988	1.38	Y10	4.81	703.8022	3
738.6546	17.95	Y7-S	2.89	738.6567	2
757.2132	8.51	B4	3.23	757.2156	1
771.4930	15.49	Y11-S	2.99	771.4953	3
787.9118	2.53	Y15-S	3.55	787.9146	4
816.1695	5.48	Y4	4.41	816.1731	1
826.6691	2.41	Y8-S	4.45	826.6728	2
830.1704	3.67	Y12-S	2.74	830.1727	3
882.6898	0.86	Y17-S	3.02	882.6925	4
897.8626	8.44	Y13-S	3.56	897.8658	3
926.6977	0.32	Y18-S	3.00	926.7005	4
928.2088	3.48	Y9-S	3.95	928.2125	2
960.2925	1.63	B5	2.62	960.2950	1
1001.4844	0.34	Y20-3S	4.74	1001.4891	4
1009.2347	0.32	Y25-2S	6.92	1009.2417	5
1016.2224	0.56	Y10-S	6.01	1016.2285	2
1019.2490	3.65	Y6-S	3.40	1019.2525	1
1025.2318	0.56	Y25-S	1.21	1025.2330	5
1052.2594	0.44	Y21-3S	-0.39	1052.2590	4
1053.0786	1.04	[M-5H]5- -4S	2.52	1053.0812	5
1069.0704	27.11	[M-5H]5- -3S	2.07	1069.0726	5
1072.2448	0.69	Y21-2S	3.16	1072.2482	4
1085.0605	25.48	[M-5H]5- -2S	3.20	1085.0640	5
1096.2649	0.30	Y22-3S	1.92	1096.2670	4
1101.0550	7.95	[M-5H]5- -S	0.31	1101.0553	5
1116.8073	1.06	C23-4S	3.25	1116.8109	4
1117.7647	1.40	Y11-2S	3.13	1117.7682	2
1136.3241	6.49	B6	2.64	1136.3271	1
1136.3241	6.49	B12-S	2.64	1136.3271	2
1176.3038	2.14	B12	1.46	1176.3055	2
1176.3038	2.14	B24-3S	1.46	1176.3055	4

1196.2906	3.39	B24-2S	3.44	1196.2947	4
1216.2815	4.64	B18	1.99	1216.2839	3
1216.2815	4.64	B24-S	1.99	1216.2839	4
1289.3468	0.35	B20-2S	2.38	1289.3499	3
1316.0018	1.49	B20-S	0.25	1316.0021	3
1325.8814	3.22	B14-2S	1.08	1325.8828	2
1339.4093	0.34	B7	-2.11	1339.4065	1
1365.8571	0.74	B14-S	3.03	1365.8612	2
1415.7211	0.51	B22-3S	-0.53	1415.7204	3
1442.3728	0.78	B22-2S	-0.12	1442.3726	3
1467.3980	0.31	B15-S	2.00	1467.4009	2
1469.0190	0.40	B22-S	4.01	1469.0249	3
1515.4385	3.93	B8	0.04	1515.4386	1
1515.4385	3.93	B24-S	0.04	1515.4386	2
1555.4162	2.46	B16-S	0.50	1555.4170	2

**Table C.12.** Assignment of HCD fragment ions of  $m/z$  1136.2589<sup>5-</sup> from dp28-5-Ser in fraction 55 with sulfo modifications on residues 13, 17, 21, 23 and 25.

Mass to charge	Relative Intensity	Type	Accuracy PPM	Theoretical Ion $m/z$	Charge
549.0996	12.34	Y5	2.56	549.1010	2
554.1353	4.25	B3	1.75	554.1363	1
637.1147	1.41	Y6	3.68	637.1170	2
640.1388	21.68	Y3	3.45	640.1410	1
645.1231	5.60	Y9	2.67	645.1248	3
703.7998	1.44	Y10	3.39	703.8022	3
738.6552	8.20	Y7-S	2.08	738.6567	2
744.8403	0.35	Y11-2S	3.68	744.8430	3
757.2141	2.93	B4	2.04	757.2156	1
771.4937	7.47	Y11-S	2.09	771.4953	3
787.9123	0.82	Y15-S	2.91	787.9146	4
816.1705	2.47	Y4	3.18	816.1731	1
826.6698	1.40	Y8-S	3.60	826.6728	2
830.1700	1.30	Y12-S	3.22	830.1727	3
882.6892	0.35	Y17-S	3.70	882.6925	4
897.8640	3.34	Y13-S	2.00	897.8658	3
928.2103	3.17	Y9-S	2.33	928.2125	2
933.2460	2.88	B5	1.86	933.2477	1
956.5408	0.36	Y14-S	2.47	956.5432	3
957.4784	0.40	Y19-2S	2.84	957.4811	4
977.4672	0.39	Y19-S	3.20	977.4703	4
986.7472	0.78	B20	2.62	986.7498	4
1016.2250	1.19	Y10-S	3.45	1016.2285	2
1019.2493	1.56	Y6-S	3.11	1019.2525	1
1024.2329	0.59	Y15-2S	3.30	1024.2363	3
1052.2562	0.45	Y21-3S	2.65	1052.2590	4
1088.2858	3.61	[M-5H]5- -3S	1.71	1088.2877	5
1096.2673	0.59	Y22-2S	-0.26	1096.2670	4
1104.2776	24.88	[M-5H]5- -2S	1.29	1104.2790	5
1116.2535	0.51	Y22-S	2.43	1116.2562	4
1120.2685	12.95	[M-5H]5- -S	1.69	1120.2704	5
1136.2688	1.71	[M-5H]5-	-6.20	1136.2618	5
1136.3252	48.32	B6	1.68	1136.3271	1
1136.3252	48.32	B12	1.68	1136.3271	2
1136.3252	48.32	B18-2S	1.68	1136.3271	3
1162.9773	0.47	B18-S	1.79	1162.9794	3
1176.3026	1.05	B24-2S	2.48	1176.3055	4
1195.2816	0.38	Y6-S	2.47	1195.2846	1



1196.2906	0.36	B24-S	3.44	1196.2947	4
1216.2817	1.46	B24	1.82	1216.2839	4
1220.3115	3.03	B25-2S	1.67	1220.3135	4
1221.6539	0.77	B19-S	2.32	1221.6567	3
1224.3407	0.65	B13	2.00	1224.3431	2
1240.3006	1.68	B25-S	1.72	1240.3027	4
1312.3570	1.72	B7	1.67	1312.3592	1
1348.0254	1.09	B21-S	1.35	1348.0272	3
1374.6774	0.49	B21	1.53	1374.6795	3
1413.8991	1.62	B15-S	-0.16	1413.8989	2
1453.8765	0.39	B15	0.54	1453.8773	2
1474.3977	0.77	B23-2S	0.01	1474.3977	3
1501.0507	0.48	B23-S	-0.48	1501.0500	3
1515.4376	1.67	B8	0.64	1515.4386	1
1515.4376	1.67	B16-S	0.64	1515.4386	2
1603.4552	1.74	B17-S	-0.37	1603.4546	2
1643.4345	0.67	B17	-0.90	1643.4330	2
1691.4721	0.66	B9	-0.86	1691.4707	1
1894.5528	0.12	B10	-0.37	1894.5500	1

**Table C.13.** Assignment of HCD fragment ions of  $m/z$  1192.8642<sup>5-</sup> from dp29-6-Ser in fraction 55 with sulfo modifications on residues 11, 15, 19, 23, 25, and 27.

Mass to charge	Relative Intensity	Type	Accuracy PPM	Theoretical Ion $m/z$	Charge
549.0995	16.30	Y5	2.74	549.1010	2
637.1145	1.58	Y6	4.00	637.1170	2
640.1387	25.55	Y3	3.61	640.1410	1
645.1225	4.78	Y9	3.60	645.1248	3
703.7994	4.54	Y10	3.96	703.8022	3
738.6548	8.88	Y7-S	2.62	738.6567	2
757.2127	2.32	B8	3.89	757.2156	2
757.2127	2.32	B4	3.89	757.2156	1
771.4931	8.48	Y11-S	2.86	771.4953	3
797.1918	0.34	B16	2.82	797.1941	4
816.1701	5.56	Y4	3.67	816.1731	1
826.6694	3.74	Y8-S	4.09	826.6728	2
830.1694	2.04	Y12-S	3.94	830.1727	3
897.8625	3.91	Y13-S	3.67	897.8658	3
926.6961	0.27	Y18-S	4.73	926.7005	4
928.2101	6.63	Y9-S	2.55	928.2125	2
956.5392	0.78	Y14-S	4.14	956.5432	3
957.4760	0.49	Y19-2S	5.35	957.4811	4
986.7475	1.22	B20-S	2.31	986.7498	4
1001.4870	0.45	Y20-3S	2.14	1001.4891	4
1016.2248	3.13	Y10-S	3.65	1016.2285	2
1019.2484	3.53	Y6-S	3.99	1019.2525	1
1024.2325	1.09	Y15-2S	3.69	1024.2363	3
1052.2558	0.45	Y21-3S	3.03	1052.2590	4
1072.2445	0.92	Y21-2S	3.44	1072.2482	4
1082.9104	0.29	Y16-2S	3.00	1082.9136	3
1088.2863	1.14	B11	2.91	1088.2895	2
1116.2509	0.36	Y22-2S	4.76	1116.2562	4
1117.7636	0.80	Y11-2S	4.11	1117.7682	2
1128.8997	0.53	[M-5H]5- -4S	3.40	1128.9035	5
1136.3253	1.13	B6	1.59	1136.3271	1
1144.8923	11.46	[M-5H]5- -3S	2.27	1144.8949	5
1147.0327	0.30	Y23-3S	3.62	1147.0369	4
1150.6038	0.52	Y17-2S	2.58	1150.6068	3
1152.2795	0.58	B23-S	6.24	1152.2867	4
1160.8843	27.79	[M-5H]5- -2S	1.69	1160.8863	5
1176.3021	3.52	B12	2.90	1176.3055	2
1176.3021	3.52	B24-2S	2.90	1176.3055	4

1176.8744	14.97	[M-5H]5- -S	2.74	1176.8776	5
1195.2807	0.69	Y6-S	3.23	1195.2846	1
1196.2894	1.05	B24-S	4.44	1196.2947	4
1216.2808	4.51	B24	2.56	1216.2839	4
1247.0625	0.62	B25-2S	1.65	1247.0646	4
1257.3216	0.98	B19-S	2.52	1257.3248	3
1271.0801	0.85	B25-S	2.58	1271.0834	4
1277.8444	0.37	B13	0.63	1277.8452	3
1289.3487	0.50	B20-2S	0.90	1289.3499	2
1291.0699	2.67	B26-2S	2.08	1291.0726	4
1311.0564	0.43	B26-S	4.11	1311.0618	4
1316.0032	0.99	B20-S	-0.81	1316.0021	3
1339.4011	0.24	B7	4.01	1339.4065	1
1365.8606	1.30	B14	0.47	1365.8612	2
1415.7222	0.32	B22-2S	-1.31	1415.7204	3
1442.3702	0.38	B22-S	1.68	1442.3726	3
1515.4379	1.81	B24-4S	0.44	1515.4386	1
1542.0882	0.22	B24-3S	1.71	1542.0908	3
1555.4164	2.17	B16-S	0.37	1555.4170	2
1568.7424	0.60	B24-2S	0.45	1568.7431	3
1595.3947	2.53	B16	0.43	1595.3954	2
1595.3947	2.53	B24-S	0.43	1595.3954	3
1744.9733	2.58	B18-S	-0.34	1744.9727	2
1886.5005	0.23	B19-S	-5.14	1886.4908	2
1894.5512	0.25	B10	-0.62	1894.5500	1
1974.5097	0.29	B20-S	-1.45	1974.5068	2

**Table C.14.** Assignment of HCD fragment ions of  $m/z$  1261.7994<sup>4+</sup> from dp25-4-Ser in fraction 55 with sulfo modifications on residues 15, 19, 21, and 23.

Mass to charge	Relative Intensity	Type	Accuracy PPM	Theoretical Ion $m/z$	Charge
549.0997	16.75	Y5	2.37	549.1010	2
581.1821	2.53	B3	2.51	581.1836	1
637.1150	1.78	Y6	3.21	637.1170	2
640.1391	41.92	Y3	2.98	640.1410	1
698.6755	0.77	Y7-2S	4.05	698.6783	2
736.2130	6.86	Y4-S	4.46	736.2163	1
738.6550	25.45	Y7-S	2.35	738.6567	2
757.2145	15.76	B12	1.51	757.2156	1
771.4928	3.38	Y11-S	3.25	771.4953	3
816.1696	7.77	Y4	4.28	816.1731	1
826.6701	8.72	Y8-S	3.24	826.6728	2
830.1706	0.36	Y12-S	2.50	830.1727	3
888.2310	3.26	Y9-2S	3.44	888.2341	2
897.8624	4.42	Y13-S	3.78	897.8658	3
928.2108	20.62	Y9-S	1.79	928.2125	2
939.2920	6.76	Y5-2S	3.89	939.2957	1
946.7690	0.29	B10	2.51	946.7714	2
956.5420	0.50	Y14-S	1.21	956.5432	3
960.2918	3.23	B5	3.35	960.2950	1
976.2482	0.40	Y10-2S	1.95	976.2501	2
997.5809	0.79	Y15-2S	3.12	997.5840	3
1016.2256	4.53	Y10-S	2.86	1016.2285	2
1019.2505	18.04	Y5-S	1.93	1019.2525	1
1024.2329	0.88	Y15-S	3.30	1024.2363	3
1077.7861	0.70	Y11-3S	3.42	1077.7898	2
1082.9104	0.29	Y16-S	3.00	1082.9136	3
1104.2997	0.44	B17	2.10	1104.3020	3
1117.7656	7.00	Y11-2S	2.32	1117.7682	2
1123.9511	0.98	Y17-2S	3.02	1123.9545	3
1136.3250	12.69	B12	1.85	1136.3271	2
1136.3250	12.69	B6	1.85	1136.3271	1
1162.9764	0.53	B18	2.56	1162.9794	3
1195.2815	6.01	Y6-S	2.56	1195.2846	1
1201.8334	8.06	[M-4H]4- -3S	2.42	1201.8363	4
1205.7827	0.41	Y12-2S	1.28	1205.7842	2
1221.8233	37.02	[M-4H]4- -2S	1.81	1221.8255	4
1230.6688	0.41	B19-S	3.01	1230.6725	3
1237.8671	0.27	B13	-0.25	1237.8668	2

1241.8123	24.92	[M-4H]4- -S	1.95	1241.8147	4
1250.3193	0.50	Y19-2S	4.55	1250.3250	3
1257.3218	0.47	B19	2.36	1257.3248	3
1261.8050	0.31	[M-4H]4-	-0.85	1261.8039	4
1289.3479	2.37	B19-S	1.52	1289.3499	3
1307.3203	0.46	Y13-2S	2.77	1307.3239	2
1316.0022	1.63	B20	-0.05	1316.0021	3
1325.8815	5.89	B14	1.01	1325.8828	2
1339.4052	2.42	B7	0.95	1339.4065	1
1357.0428	0.37	B21-2S	0.14	1357.0430	3
1383.6941	0.53	B21-S	0.84	1383.6953	3
1398.3626	1.54	Y7-2S	0.95	1398.3639	1
1415.7187	1.42	B22-2S	1.17	1415.7204	3
1427.4248	0.55	B15-S	-1.60	1427.4225	2
1442.3700	1.01	B22-S	1.82	1442.3726	3
1467.4004	0.96	B15	0.36	1467.4009	2
1515.4386	12.90	B8	-0.02	1515.4386	1
1515.4386	12.90	B16-S	-0.02	1515.4386	2
1555.4183	2.62	B16	-0.85	1555.4170	2
1574.3917	0.23	Y8-2S	2.74	1574.3960	1
1656.9548	0.26	B17	1.12	1656.9567	2
1704.9960	1.18	B18-S	-1.00	1704.9943	2
1718.5181	0.43	B9	-0.09	1718.5179	1
1744.9754	1.95	B18	-1.55	1744.9727	2
1894.5525	2.36	B10	-1.31	1894.5500	1

**Table C.15.** Assignment of HCD fragment ions of m/z 1152.2501<sup>5-</sup> from dp28-6-Ser in fraction 55 with sulfo modifications on residues 10, 14, 18, 22, 24, and 26.

Mass to charge	Relative Intensity	Type	Accuracy PPM	Theoretical Ion m/z	Charge
549.1002	30.92	Y5	1.46	549.1010	2
554.1361	3.76	B3	0.31	554.1363	1
637.1159	0.45	Y6	1.80	637.1170	2
640.1394	58.98	Y3	2.51	640.1410	1
645.1241	5.15	Y9	1.12	645.1248	3
693.1361	0.22	Y13	0.91	693.1367	4
703.8011	0.56	Y10	1.54	703.8022	3
738.6555	19.52	Y7-S	1.67	738.6567	2
744.8410	0.32	Y11-2S	2.74	744.8430	3
757.2151	3.05	B4	0.72	757.2156	1
757.2151	3.05	B8	0.72	757.2156	2
771.4940	15.31	Y11-S	1.70	771.4953	3
787.9135	2.52	Y15-S	1.39	787.9146	4
816.1712	3.04	Y4	2.32	816.1731	1
826.6713	1.72	Y8-S	1.79	826.6728	2
830.1711	1.67	Y12-S	1.89	830.1727	3
831.9203	0.34	Y16-S	2.79	831.9226	4
882.6909	1.04	Y17-S	1.77	882.6925	4
897.8644	6.17	Y13-S	1.55	897.8658	3
928.2108	1.45	Y9-S	1.79	928.2125	2
933.2465	2.85	B5	1.32	933.2477	1
956.5421	0.77	Y14-S	1.11	956.5432	3
957.4780	0.65	Y19-2S	3.26	957.4811	4
1016.2267	0.52	Y10-S	1.78	1016.2285	2
1019.2501	0.51	Y6-S	2.32	1019.2525	1
1021.4787	0.62	Y20-2S	-0.34	1021.4783	4
1024.2344	0.65	Y15-2S	1.84	1024.2363	3
1028.4545	0.25	Y26-3S	2.18	1028.4567	5
1052.2586	0.27	Y21-3S	0.37	1052.2590	4
1072.2435	0.63	Y21-2S	4.38	1072.2482	4
1088.2854	2.61	[M-5H]5- -4S	2.08	1088.2877	5
1096.2659	0.40	Y22-3S	1.01	1096.2670	4
1104.2774	30.52	[M-5H]5- -3S	1.48	1104.2790	5
1116.2537	0.51	Y22-2S	2.25	1116.2562	4
1120.2688	20.93	[M-5H]5- -2S	1.42	1120.2704	5
1136.2602	5.46	[M-5H]5- -S	1.37	1136.2618	5
1136.3251	1.49	B6	1.76	1136.3271	1
1147.0353	0.55	Y23-3S	1.35	1147.0369	4

1176.3032	0.35	B12	1.97	1176.3055	2
1176.3032	0.35	B24-3S	1.97	1176.3055	4
1189.6307	0.32	B18-S	0.80	1189.6316	3
1191.0412	0.22	Y24-3S	3.09	1191.0449	4
1196.2929	0.28	B24-2S	1.52	1196.2947	4
1200.3241	0.32	B25-4S	0.19	1200.3243	4
1216.2828	2.15	B18	0.92	1216.2839	3
1216.2828	2.15	B24-S	0.92	1216.2839	4
1221.6533	0.25	B19-2S	2.82	1221.6567	3
1224.3407	0.24	B13-S	2.00	1224.3431	2
1240.3005	2.22	B25-2S	1.80	1240.3027	4
1248.3075	0.35	B19-S	1.21	1248.3090	3
1260.2901	0.94	B25-S	1.46	1260.2919	4
1261.8023	0.30	Y25-2S	1.29	1261.8039	4
1312.3590	0.87	B7	0.15	1312.3592	1
1348.0244	0.72	B21-2S	2.10	1348.0272	3
1365.8599	0.45	B14-S	0.98	1365.8612	2
1374.6776	0.56	B21-S	1.38	1374.6795	3
1413.8976	1.27	B15-2S	0.90	1413.8989	2
1474.3942	0.27	B23-3S	2.38	1474.3977	3
1501.0445	0.46	B23-2S	3.65	1501.0500	3
1515.4375	0.95	B8	0.70	1515.4386	1
1527.7023	0.22	B24-S	-0.03	1527.7023	3
1595.3992	0.34	B16	-2.39	1595.3954	2
1643.4324	0.53	B17-S	0.38	1643.4330	2

**Table C.16.** Assignment of HCD fragment ions of  $m/z$  1176.8715<sup>5-</sup> from dp29-5-Ser in fraction 63 with sulfo modifications on residues 15, 19, 23, 25 and 27.

Mass to charge	Relative Intensity	Type	Accuracy PPM	Theoretical Ion $m/z$	Charge
549.0999	16.55	Y5	2.01	549.1010	2
581.1821	1.61	B3	2.51	581.1836	1
637.1151	2.08	Y6	3.06	637.1170	2
640.1391	32.97	Y3	2.98	640.1410	1
645.1233	6.96	Y9	2.36	645.1248	3
698.6764	0.49	Y7-2S	2.76	698.6783	2
703.8001	1.45	Y10	2.96	703.8022	3
736.2135	0.32	Y4-S	3.78	736.2163	1
738.6551	10.42	Y7-S	2.21	738.6567	2
744.8407	0.73	Y11-2S	3.14	744.8430	3
757.2146	6.60	B8	1.38	757.2156	2
757.2146	6.60	B4	1.38	757.2156	1
771.4935	9.58	Y11-S	2.34	771.4953	3
787.9121	0.33	Y15-S	3.17	787.9146	4
816.1708	3.44	Y4	2.81	816.1731	1
826.6703	1.91	Y8-S	3.00	826.6728	2
830.1701	1.19	Y12-S	3.10	830.1727	3
862.7007	0.22	Y17-2S	2.97	862.7033	4
871.2107	0.55	Y13-2S	3.24	871.2135	3
882.6896	0.28	Y17-S	3.24	882.6925	4
888.2315	0.94	Y9-2S	2.88	888.2341	2
897.8641	4.26	Y13-S	1.89	897.8658	3
906.7085	0.20	Y18-2S	3.07	906.7113	4
926.6974	0.21	Y18-S	3.33	926.7005	4
928.2107	5.60	Y9-S	1.90	928.2125	2
939.2922	0.28	Y5-2S	3.68	939.2957	1
946.7692	0.29	B10	2.30	946.7714	2
956.5414	0.22	Y14-S	1.84	956.5432	3
957.4782	0.57	Y19-2S	3.05	957.4811	4
960.2928	1.35	B5	2.31	960.2950	1
977.4685	0.22	Y19-S	1.87	977.4703	4
997.5812	0.39	Y15-3S	2.82	997.5840	3
1001.4868	0.32	Y20-2S	2.34	1001.4891	4
1016.2257	1.45	Y10-S	2.76	1016.2285	2
1019.2500	3.34	Y5-S	2.42	1019.2525	1
1024.2340	0.78	Y15-2S	2.23	1024.2363	3
1048.3092	0.17	B11	1.78	1048.3111	2
1052.2567	0.58	Y21-2S	2.17	1052.2590	4



1085.0839	0.17	C28-3S	4.23	1085.0885	5
1101.0757	1.33	C28-2S	3.77	1101.0799	5
1112.9094	0.21	[M-5H]5- -4S	2.50	1112.9122	5
1117.0652	0.24	C28-S	5.38	1117.0712	5
1117.7658	0.52	Y11-2S	2.14	1117.7682	2
1123.9523	0.21	Y17-3S	1.96	1123.9545	3
1128.9018	5.40	[M-5H]5- -3S	1.54	1128.9035	5
1132.2943	0.19	B23-S	2.82	1132.2975	4
1133.0478	0.55	C28	13.04	1133.0626	5
1136.3269	5.45	B12	0.18	1136.3271	2
1136.3269	5.45	B6	0.18	1136.3271	1
1144.8931	21.68	[M-5H]5- -2S	1.58	1144.8949	5
1147.0345	0.16	Y23-2S	2.05	1147.0369	4
1150.6052	0.15	Y17-2S	1.36	1150.6068	3
1156.8154	0.51	Z12-3S	-12.84	1156.8005	2
1160.8838	6.37	[M-5H]5- -S	2.12	1160.8863	5
1176.3036	2.22	B24 -S	1.63	1176.3055	4
1176.8794	0.32	[M-5H]5-	-1.50	1176.8776	5
1195.2818	0.76	Y6-S	2.31	1195.2846	1
1196.2876	0.25	B24	5.95	1196.2947	4
1196.7944	0.33	Z12-2S	-12.90	1196.7790	2
1227.0739	0.18	B25-2S	1.19	1227.0754	4
1230.6708	0.28	B19-S	1.38	1230.6725	3
1231.0049	1.05	Y24	14.93	1231.0233	4
1241.8126	0.17	Y25-2S	1.71	1241.8147	4
1251.0920	0.72	B26-3S	1.74	1251.0942	4
1271.0818	3.05	B26-2S	1.24	1271.0834	4
1289.3481	1.46	B20-S	1.37	1289.3499	3
1291.0717	0.62	B26-S	0.68	1291.0726	4
1316.0008	0.15	B20	1.01	1316.0021	3
1325.8813	1.44	B14	1.16	1325.8828	2
1339.4054	0.92	B7	0.80	1339.4065	1
1389.0676	0.17	B22-2S	0.34	1389.0681	3
1415.7200	1.30	B22-S	0.25	1415.7204	3
1442.3734	0.22	B22	-0.54	1442.3726	3
1515.4381	5.51	B8	0.31	1515.4386	1
1515.4381	5.51	B16-S	0.31	1515.4386	2
1515.4381	5.51	B24-3S	0.31	1515.4386	3
1542.0915	0.73	B24-2S	-0.43	1542.0908	3
1555.4182	0.29	B16	-0.79	1555.4170	2
1568.7476	0.26	B24-S	-2.86	1568.7431	3
1595.3976	0.27	B24	-1.39	1595.3954	3
1704.9961	2.82	B18-S	-1.06	1704.9943	2
1718.5190	0.34	B9	-0.62	1718.5179	1

1744.9748	0.43	B18	-1.20	1744.9727	2
1894.5542	1.74	B10	-2.20	1894.5500	1
1894.5542	1.74	B20-2S	-2.20	1894.5500	2

**Table C.17.** Assignment of HCD fragment ions of  $m/z$  1160.8817<sup>5-</sup> from dp29-4-Ser in fraction 63 with sulfo modifications on residues 19, 23, 25, and 27.

Mass to charge	Relative Intensity	Type	Accuracy PPM	Theoretical Ion $m/z$	Charge
549.0997	20.01	Y5	2.37	549.1010	2
581.1820	2.13	B3	2.68	581.1836	1
637.1149	1.45	Y6	3.37	637.1170	2
640.1390	41.10	Y3	3.14	640.1410	1
645.1232	10.11	Y9	2.51	645.1248	3
698.6758	2.00	Y7-2S	3.62	698.6783	2
703.8004	0.45	Y10	2.54	703.8022	3
736.2130	3.00	Y4-S	4.46	736.2163	1
738.6547	16.23	Y7-S	2.75	738.6567	2
744.8407	0.97	Y11-2S	3.14	744.8430	3
757.2144	10.01	B4	1.64	757.2156	1
771.4934	8.04	Y11-S	2.47	771.4953	3
816.1698	3.53	Y4	4.04	816.1731	1
826.6703	3.14	Y8-S	3.00	826.6728	2
862.7016	0.25	Y17-S	1.92	862.7033	4
867.7585	0.43	C9	2.44	867.7606	2
871.2109	1.01	Y13-2S	3.01	871.2135	3
888.2307	2.45	Y9-2S	3.78	888.2341	2
897.8629	2.91	Y13-S	3.23	897.8658	3
928.2104	8.22	Y9-S	2.22	928.2125	2
939.2923	3.69	Y5-2S	3.57	939.2957	1
946.7689	1.43	B10	2.61	946.7714	2
957.4775	0.42	Y19-S	3.78	957.4811	4
960.2928	1.19	B5	2.31	960.2950	1
997.5810	0.95	Y15-2S	3.02	997.5840	3
1016.2260	0.51	Y10-S	2.47	1016.2285	2
1017.5268	0.15	B21	3.56	1017.5304	4
1019.2500	10.13	Y5-S	2.42	1019.2525	1
1020.2525	3.39	C26-S	14.56	1020.2674	5
1024.2329	0.51	Y15-S	3.30	1024.2363	3
1048.3087	0.55	B11	2.25	1048.3111	2
1052.2564	0.19	Y21-S	2.46	1052.2590	4
1057.3159	0.48	C11	0.42	1057.3163	2
1069.0673	0.22	Y27-S	4.97	1069.0726	5
1077.7861	0.23	Y11-3S	3.42	1077.7898	2
1085.0833	1.04	C28-2S	4.78	1085.0885	5
1101.0743	1.06	C28-S	5.04	1101.0799	5
1112.3044	0.46	B23-S	3.49	1112.3083	4

1112.9087	2.02	[M-5H]5- -3S	3.13	1112.9122	5
1117.7652	0.80	Y11-2S	2.68	1117.7682	2
1123.9519	0.79	Y17-2S	2.31	1123.9545	3
1128.9015	26.18	[M-5H]5- -2S	1.81	1128.9035	5
1132.2955	0.60	B23	1.76	1132.2975	4
1136.3263	9.46	B18	0.71	1136.3271	3
1136.3263	9.46	B12	0.71	1136.3271	2
1136.3263	9.46	B6	0.71	1136.3271	1
1144.8928	31.02	[M-5H]5- -S	1.84	1144.8949	5
1156.3137	1.35	B24-S	2.26	1156.3163	4
1156.8144	3.06	Z12-3S	-11.97	1156.8005	2
1160.8829	0.44	[M-5H]5-	2.90	1160.8863	5
1176.3033	4.23	B24	1.88	1176.3055	4
1195.2811	2.46	Y6-S	2.89	1195.2846	1
1196.7940	0.40	Z12-2S	-12.57	1196.7790	2
1207.0828	0.18	B25-2S	2.78	1207.0862	4
1221.8224	0.43	Y25-2S	2.55	1221.8255	4
1227.0719	0.59	B25-S	2.82	1227.0754	4
1230.6691	0.19	B19	2.76	1230.6725	3
1237.8648	0.42	B13	1.61	1237.8668	2
1241.8106	0.15	Y25-S	3.32	1241.8147	4
1251.0923	3.13	B26-2S	1.50	1251.0942	4
1262.6950	1.90	B20-S	2.05	1262.6976	3
1271.0812	4.68	B26-S	1.71	1271.0834	4
1289.3477	2.15	B20	1.68	1289.3499	3
1325.8820	3.44	B14	0.63	1325.8828	2
1339.4076	0.71	B7	-0.84	1339.4065	1
1357.0432	0.52	B21	-0.16	1357.0430	3
1389.0667	1.64	B22-S	0.99	1389.0681	3
1398.3642	0.27	Y7-2S	-0.19	1398.3639	1
1415.7191	3.35	B22	0.88	1415.7204	3
1427.4199	0.22	B15	1.84	1427.4225	2
1515.4378	7.98	B16	0.51	1515.4386	2
1515.4378	7.98	B8	0.51	1515.4386	1
1515.4378	7.98	B24-2S	0.51	1515.4386	3
1542.0902	1.68	B24-S	0.41	1542.0908	3
1704.9977	3.03	B18	-2.00	1704.9943	2
1718.5233	0.28	B9	-3.12	1718.5179	1
1894.5533	3.96	B10	-1.73	1894.5500	1
1894.5533	3.96	B20-S	-1.73	1894.5500	2

**Table C.18.** Assignment of HCD fragment ions of  $m/z$  1287.9028<sup>5-</sup> from dp32-5-Ser in fraction 63 with sulfo modifications on residues 18, 22, 26, 28, and 30.

Mass to charge	Relative Intensity	Type	Accuracy PPM	Theoretical Ion $m/z$	Charge
549.1006	17.70	Y5	0.73	549.1010	2
554.1364	5.53	B3	-0.23	554.1363	1
637.1166	1.96	Y6	0.70	637.1170	2
640.1400	30.13	Y3	1.58	640.1410	1
645.1244	4.64	Y9	0.65	645.1248	3
703.8009	0.33	Y10	1.83	703.8022	3
738.6558	11.02	Y7-S	1.26	738.6567	2
757.2152	2.11	B16	0.59	757.2156	4
757.2152	2.11	B12	0.59	757.2156	3
757.2152	2.11	B8	0.59	757.2156	2
757.2152	2.11	B4	0.59	757.2156	1
757.2152	2.11	B20-S	0.59	757.2156	5
771.4944	9.47	Y11-S	1.18	771.4953	3
816.1714	5.07	Y4	2.08	816.1731	1
826.6716	3.01	Y8-S	1.42	826.6728	2
830.1715	0.45	Y12-S	1.41	830.1727	3
897.8646	1.51	Y13-S	1.33	897.8658	3
928.2107	2.93	Y9-S	1.90	928.2125	2
933.2466	2.62	B5	1.21	933.2477	1
1016.2271	0.41	Y10-S	1.39	1016.2285	2
1019.2496	0.65	Y5-S	2.81	1019.2525	1
1021.4748	0.25	Y20-S	3.47	1021.4783	4
1024.2339	0.28	Y15-2S	2.33	1024.2363	3
1052.2585	0.29	Y21-2S	0.46	1052.2590	4
1072.2436	0.24	Y21-S	4.28	1072.2482	4
1117.7621	0.26	Y11-2S	5.45	1117.7682	2
1136.3258	1.21	B6	1.15	1136.3271	1
1147.0389	0.13	Y23-2S	-1.78	1147.0369	4
1150.6048	0.14	Y17-2S	1.71	1150.6068	3
1167.0236	0.15	Y23-S	2.11	1167.0261	4
1176.3032	0.43	B24	1.97	1176.3055	4
1176.4960	0.13	Z30-2S	2.73	1176.4992	5
1196.0968	0.09	Y30-S	-3.44	1196.0927	5
1211.0312	0.10	Y24-S	2.38	1211.0341	4
1224.3414	2.19	B13	1.43	1224.3431	2
1236.7239	0.19	Y31-S	-12.40	1236.7086	5
1237.3114	0.42	Y25-2S	0.55	1237.3121	4
1239.9312	8.34	[M-5H]5- -3S	0.85	1239.9323	5

1241.8148	0.14	Y25-2S	-0.07	1241.8147	4
1250.3225	0.24	Y19-3S	1.99	1250.3250	3
1252.7169	0.19	Y31	-13.55	1252.6999	5
1255.9241	22.29	[M-5H]5- -2S	-0.39	1255.9236	5
1271.9144	16.46	[M-5H]5- -S	0.45	1271.9150	5
1287.9070	0.23	[M-5H]5-	-0.51	1287.9063	5
1312.3568	0.86	B7	1.82	1312.3592	1
1365.8619	0.28	B28-2S	-0.48	1365.8612	4
1385.8505	0.14	B28-S	-0.04	1385.8504	4
1386.3512	1.88	Z14-2S	-11.91	1386.3347	2
1389.8836	0.25	B29-3S	-2.55	1389.8801	4
1405.8399	0.11	B28	-0.18	1405.8396	4
1409.8674	1.44	B29-2S	1.32	1409.8693	4
1411.3725	0.97	Y29-3S	6.20	1411.3812	4
1413.8951	0.22	B15	2.67	1413.8989	2
1415.7181	0.13	B22-S	1.59	1415.7204	3
1429.8571	1.03	B29-S	0.96	1429.8585	4
1431.3606	1.24	Y29-2S	6.88	1431.3704	4
1474.3996	0.13	B23-S	-1.28	1474.3977	3
1515.4368	1.04	B16	1.17	1515.4386	2
1515.4368	1.04	B8	1.17	1515.4386	1
1600.7654	0.42	B25-S	1.75	1600.7682	3
1691.4713	0.43	B9	-0.38	1691.4707	1
1753.7907	0.27	B27-S	0.15	1753.7910	3
1894.5521	0.14	B10	-1.09	1894.5500	1
1982.5693	0.40	B21-S	-1.63	1982.5661	2

**Table C.19.** Assignment of HCD fragment ions of  $m/z$  1252.8956<sup>5-</sup> from dp31-5-Ser in fraction 63 with sulfo modifications on residues 17, 21, 25, 27, and 29.

Mass to charge	Relative Intensity	Type	Accuracy PPM	Theoretical Ion $m/z$	Charge
549.0998	15.71	Y5	2.19	549.1010	2
581.1822	1.28	B3	2.33	581.1836	1
637.1151	2.85	Y6	3.06	637.1170	2
640.1391	25.68	Y3	2.98	640.1410	1
645.1233	5.97	Y9	2.36	645.1248	3
698.6759	0.12	Y7-2S	3.47	698.6783	2
703.7998	1.42	Y10	3.39	703.8022	3
738.6551	9.57	Y7-S	2.21	738.6567	2
744.8400	0.14	Y11-2S	4.08	744.8430	3
757.2145	5.14	B8	1.51	757.2156	2
757.2145	5.14	B4	1.51	757.2156	1
771.4935	8.37	Y11-S	2.34	771.4953	3
816.1708	4.16	Y4	2.81	816.1731	1
826.6703	3.02	Y8-S	3.00	826.6728	2
830.1701	1.55	Y12-S	3.10	830.1727	3
871.2113	0.14	Y13-2S	2.55	871.2135	3
882.6891	0.12	Y17-S	3.81	882.6925	4
888.2316	0.24	Y9-2S	2.77	888.2341	2
897.8637	3.39	Y13-S	2.33	897.8658	3
926.6972	0.17	Y18-S	3.54	926.7005	4
928.2106	4.68	Y9-S	2.01	928.2125	2
956.5405	0.42	Y14-S	2.78	956.5432	3
957.4787	0.34	Y19-2S	2.53	957.4811	4
960.2929	1.32	B5	2.20	960.2950	1
977.4671	0.28	Y19-S	3.30	977.4703	4
997.5823	0.18	Y15-2S	1.72	997.5840	3
1001.4869	0.31	Y20-2S	2.24	1001.4891	4
1016.2257	1.17	Y10-S	2.76	1016.2285	2
1019.2492	2.65	Y5-S	3.21	1019.2525	1
1021.4757	0.33	Y20-S	2.59	1021.4783	4
1024.2339	1.24	Y15-2S	2.33	1024.2363	3
1025.2355	0.30	Y25	-2.39	1025.2330	5
1048.3074	0.43	B11	-1.84	1048.3111	2
1052.2561	0.65	Y21-2S	2.74	1052.2590	4
1072.2453	0.47	Y21-S	2.70	1072.2482	4
1082.9126	0.17	Y16-2S	0.97	1082.9136	3
1088.2862	0.13	Y28-3S	1.35	1088.2877	5
1096.2643	0.14	Y22-2S	2.47	1096.2670	4

1116.2544	0.20	Y22-S	1.62	1116.2562	4
1117.7657	0.52	Y11-2S	2.23	1117.7682	2
1123.9518	0.13	Y17-3S	2.40	1123.9545	3
1132.2935	0.69	B21	2.36	1132.2975	4
1136.3251	4.14	B6	1.76	1136.3271	1
1136.3251	4.14	B12	1.76	1136.3271	2
1144.8906	0.21	Y29-2S	3.76	1144.8949	5
1147.0345	0.47	Y23-2S	2.05	1147.0369	4
1150.6051	0.39	Y17-2S	1.45	1150.6068	3
1160.8884	0.16	Y29-S	-1.84	1160.8863	5
1167.0233	0.47	Y23-S	2.36	1167.0261	4
1176.3035	0.61	B24	1.71	1176.3055	4
1188.7324	0.18	[M-5H]5- -4S	1.74	1188.7345	5
1195.2832	0.67	Y6-S	1.14	1195.2846	1
1204.7244	8.68	[M-5H]5- -3S	1.19	1204.7258	5
1211.0310	0.15	Y24-S	2.54	1211.0341	4
1220.7155	26.60	[M-5H]5- -2S	1.39	1220.7172	5
1236.7064	17.05	[M-5H]5- -S	1.75	1236.7086	5
1241.8122	0.18	Y25-2S	2.03	1241.8147	4
1247.3146	0.27	B25	-1.84	1247.0646	4
1252.6978	0.93	[M-5H]5-	1.69	1252.6999	5
1261.8016	0.21	Y25-S	1.84	1261.8039	4
1271.0806	0.35	B26-S	2.19	1271.0834	4
1276.9792	0.11	Y19-2S	-1.52	1276.9773	3
1289.3500	0.41	B20	1.45	1289.3499	3
1291.0703	0.94	B26	2.05	1291.0726	4
1321.8517	0.27	B27-2S	1.15	1321.8532	4
1325.8816	0.83	B14	0.93	1325.8828	2
1325.8816	0.83	B28-4S	0.93	1325.8828	4
1336.5920	0.27	Y27-2S	0.44	1336.5926	4
1339.4056	0.97	B7	0.66	1339.4065	1
1341.8413	0.21	B27-S	0.84	1341.8424	4
1345.8700	0.40	B28-3S	1.52	1345.8720	4
1356.5826	0.21	Y27-S	-0.60	1356.5818	4
1361.8393	0.09	B27	0.30	1361.8316	4
1365.8600	3.64	B28-2S	0.91	1365.8612	4
1385.8498	1.52	B28-S	0.47	1385.8504	4
1389.0721	0.11	B22-2S	-2.89	1389.0681	3
1405.8402	0.13	B28	-0.39	1405.8396	4
1415.7200	0.69	B22-S	0.25	1415.7204	3
1427.4221	0.13	B15	0.30	1427.4225	2
1442.3688	0.65	B22	0.25	1442.3726	3
1510.0611	0.86	B23	-0.39	1510.0657	3
1515.4388	3.91	B8	-0.15	1515.4386	1



1515.4388	3.91	B16	-0.15	1515.4386	2
1542.0923	0.87	B24-2S	-0.95	1542.0908	3
1568.7460	0.26	B24	-1.84	1568.7431	3
1668.4623	0.29	B26-2S	-0.58	1668.4613	3
1695.1168	0.66	B26-S	-1.89	1695.1136	3
1704.9965	1.18	B18-S	-1.29	1704.9943	2
1718.5184	0.30	B9	-0.27	1718.5179	1
1721.1112	0.53	B26	-2.89	1721.7659	3
1744.9747	0.22	B18	-1.14	1744.9727	2
1846.5054	0.28	B19	0.47	1846.5124	2
1894.5519	3.59	B10	-0.99	1894.5500	1
1894.5519	3.59	B20-S	-0.99	1894.5500	2
1934.5284	0.92	B20	-0.91	1934.5284	2